

**DYNAMIC RESISTIVITY BEHAVIOR OF TIN OXIDE BASED
MULTILAYER THIN FILMS UNDER REDUCING CONDITIONS**

**A THESIS SUBMITTED TO
THE GRADUATE SCHOOL OF NATURAL AND APPLIED SCIENCES OF
MIDDLE EAST TECHNICAL UNIVERSITY**

BY

BAŐAK KURBANOĐLU

**IN PARTIAL FULLFILLMENT OF THE REQUIREMENTS
FOR
THE DEGREE OF MASTER OF SCIENCE
IN
CHEMICAL ENGINEERING**

JANUARY 2006

Approval of the Graduate School of Natural and Applied Sciences

Prof. Dr. Canan Özgen
Director

I certify that this thesis satisfies all the requirements as a thesis for degree of Master of Science.

Prof. Dr. Nurcan Baç
Head of Department

This is to certify that we have read this thesis and that in our opinion it is fully adequate, in scope and quality, as a thesis and for the degree of Master of Science.

Assoc. Prof. Dr. Gürkan Karakaş
Supervisor

Examining Committee Members

Prof. Dr. Timur Doğu (METU, CHE) _____

Assoc. Prof. Dr. Gürkan Karakaş (METU, CHE) _____

Prof. Dr. Ufuk Bakır (METU, CHE) _____

Prof. Dr. Suna Balcı (Gazi Univ.,CHE) _____

Dr. Yusuf Uludağ (METU, CHE) _____

I hereby declare that all information in this document has been obtained and presented in accordance with academic rules and ethical conduct. I also declare that, as required by these rules and conduct, I have fully cited and referenced all material and results that are not original to this work.

Name, Last name :

Signature :

ABSTRACT

DYNAMIC RESISTIVITY BEHAVIOR OF TIN OXIDE BASED MULTILAYER THIN FILMS UNDER REDUCING CONDITIONS

Kurbanoglu, Bařak

M.Sc., Department of Chemical Engineering

Supervisor: Assoc. Prof. Dr. Grkan Karakař

January 2006, 123 pages

Effects of urban air pollution on health and environment have lead researchers to find economic air quality monitoring regulations. Since tin dioxide (SnO_2) was demonstrated as a gas sensing device in 1962, tin oxide based thin film sensors have been widely studied due to their high sensitivity and fast response. The main advantages of using tin oxide sensors are their low cost, small size and low power consumption for mobile system applications. But, in order SnO_2 based sensors to meet low concentration of gases they should be highly upgraded in sensitivity, selectivity and stability.

This study was focused on the capacity of dopants in the SnO_2 layer to increase the sensitivity of the sensor in detecting carbon monoxide. 1 wt. % Pd promoted and 0.1 wt. % Na-1 % Pd promoted SnO_2 multilayer thin films were produced by sol-gel technique followed by spin coating route on soda-lime glass substrates.

The EDX and SEM studies showed the surface composition and the surface structure is homogeneous throughout the films. The film thickness was

determined app. 450 nm from the SEM image of the cross-section, after coating 8 layers. The experiments conducted at several temperatures namely 150, 175 and 200°C, in oxygen free and 1% oxygen containing atmospheres showed that the responses at higher temperatures in the presence of oxygen were much sharper with respect to others. Besides, Na promoted test sensors showed larger responses with shorter response time in oxygen free atmospheres at relatively lower temperatures. The results showed that the sensor signal is not directly correlated with the carbon dioxide production in oxygen free atmospheres.

Keywords: Chemical gas sensors, Pd/SnO₂ thin films, alkali metal promotion, CO sensing

ÖZ

KALAY OKSİT BAZLI ÇOK KATLI İNCE FİLMLEİN İNDİRGEYİCİ ORTAMLARDA DİRENÇ TEPKİLERİ

Kurbanoglu, Başak

Yüksek Lisans, Kimya Mühendisliği Bölümü

Tez Yöneticisi: Doç. Dr. Gürkan Karakaş

Ocak 2006, 123 sayfa

Yerleşim bölgelerindeki hava kirliliğinin insan sağlığı üzerindeki etkileri araştırmacıları ekonomik hava kirliliği ölçüm yöntemleri bulmaya yönlendirmiştir. 1962 yılında kalay oksitin gaz algılayıcı bir cihaz olarak tanıtılmasıyla birlikte, kalay oksit bazlı ince kaplamalar gösterdikleri yüksek seçicilik ve algı hızları nedeniyle sıkça gaz sensörü olarak kullanılmışlardır. Kalay oksit bazlı sensörlerin en belirgin avantajı düşük maliyetleri, küçük boyutları ve mobil ölçümlere uyumu sağlayan düşük güç gereksinimleridir. Fakat SnO₂ bazlı sensörlerin düşük konsantrasyonlu gazlara olan tepkilerinin güçlendirilmesi için algı, seçicilik ve kararlılık açısından geliştirilmeleri gerekmektedir.

Bu çalışmada, SnO₂ tabakasına uygulanan katkı konsantrasyonunun CO gazına gösterilen algıyı ne derece etkilediğini araştırılmaktadır. Ağırlık olarak %1 Pd ve %0.1 Na + %1 Pd katkıları ile güçlendirilmiş SnO₂ katalizörler sol-jel tekniği ile üretilerek, döndürerek kaplama yöntemi ile cam substratlar üzerine uygulanmıştır.

EDX ve SEM çalışmaları sonucunda yüzey konsantrasyonunun ve yüzey yapısının homojen olduğu belirlenmiştir. SEM kesit fotoğrafı göz önüne

alınarak 8 kaplama uygulaması sonucunda film kalınlığı 450 nm. olarak belirlenmiştir. Deneyler 150, 175 ve 200°C'de oksijensiz ve %1 oksijen içeren atmosferlerde tekrar edilmiş ve oksijen içeren atmosferde yüksek sıcaklıklara çıkıldığında diğer koşullarıkilere göre daha belirgin tepkiler gözlemlenmiştir. Bunun yanında, Na katkısı ile güçlendirilmiş test sensörleri oksijensiz ortamda, düşük sıcaklıklarda, daha hızlı ve daha fazla tepki vermiştir. Sonuçlar oksijensiz atmosferde sensör sinyallerinin karbon dioksit üretimi ile doğrudan bağlantılı olmadığını göstermiştir.

Anahtar Kelimeler: Kimyasal gaz sensörleri, Pd/SnO₂ ince kaplamalar, alkali metal katkısı, CO algılama

*To The Ones Who Supported Me
All Through My Life*

ACKNOWLEDGEMENTS

I would like to use this opportunity to express my gratitude to my supervisor Assoc. Prof. Dr. Gürkan Karakaş and my senior Mrs. Burcu Mirkelamođlu for their guidance and support throughout the study. I am very thankful to Mrs. Burcu Mirkelamođlu for her existence whenever and wherever needed. I should also express my appreciation to Mr. Nevzat Bekçi, Mr. İsa Çađlar and the rest of the workshop staff for their technical support and their friendship.

I would like to thank my family, who showed me issues can not be obstacle when there is love, for their support and being beside me whenever I needed, even from kilometers away.

Finally; I want to say that never can I share such great time and nowhere can I find such great friends like Burcu Mirkelamođlu, Özge Ođuzer, Işıl Işık, Berker Fıçıcılar, Sinan Ok, Ceylan Karakaya and Onur Diri. Thank you all for being beside me.

TABLE OF CONTENTS

PLAGIARISM.....	iii
ABSTRACT.....	iv
ÖZ.....	vi
DEDICATION.....	viii
ACKNOWLEDGEMENT.....	ix
TABLE OF CONTENTS.....	xiii
LIST OF TABLES.....	ix
LIST OF FIGURES.....	xix
NOMENCLATURE.....	xx
CHAPTER	
1. INTRODUCTION.....	1
2. LITERATURE SURVEY.....	6
2.1. SENSORS.....	6
2.2. CHEMICAL SENSORS.....	7
2.3. SENSOR PERFORMANCE SPECIFICATIONS.....	9
2.3.1. SENSITIVITY	10
2.3.2. SELECTIVITY	10
2.3.3. STABILITY.....	10
2.3.4. ACCURACY.....	10
2.3.5. REPEATIBILITY.....	11
2.3.6. RESPONSE / RECOVERY TIME.....	11
2.3.7. TEMPERATURE AND PRESSURE.....	11
2.3.8. HYSTERESIS.....	12
2.4. SEMICONDUCTORS.....	12
2.5. SEMICONDUCTING OXIDE GAS SENSORS.....	16
2.5.1. OPERATION PRINCIPLE.....	17

2.6. PARAMETERS AFFECTING THE SEMICONDUCTING OXIDE	
GAS SENSOR PERFORMANCE.....	27
2.6.1. EFFECT OF TEMPERATURE.....	28
2.6.2. EFFECT OF ADDITIVES.....	30
2.6.3. EFFECT OF HUMIDIT.....	31
2.6.4. EFFECT OF FILM THICKNESS.....	33
2.6.5. EFFECT OF FILM MORPHOLOGY.....	34
2.6.6. EFFECT OF ELECTRODES.....	38
2.7. EFFECT OF ALKALI METAL PROMOTION.....	40
3. EXPERIMENTAL PROCEDURE.....	42
3.1. MATERIAL SELECTION.....	43
3.2. CATALYST SYNTHESIS BY THE SOL-GEL METHOD.....	44
3.3. SUBSTRATE PREPARATION.....	45
3.4. COATING PROCESS.....	48
3.5. DRYING.....	49
3.6. CALCINATION.....	49
3.7. ANALYSIS OF THE FILMS.....	50
3.8 SENSOR PREPARATION.....	50
3.9. EXPERIMENTAL SETUP	50
3.9.1. FEED UNIT	52
3.9.2. INJECTION VALVES	52
3.9.3. REACTION CHAMBER.....	53
3.9.4. DATA ACQUISITION UNIT.....	53
3.10. EXPERIMENTAL PROCEDURE.....	53
3.10.1. TEMPERATURE EFFECT ON THE GAS SENSING	
RESPONSES	54
3.10.2. EFFECT OF OXYGEN ON THE GAS SENSING RESPONSES...	54
4. RESULTS AND DISCUSSION.....	55
4.1. FILM CHARACTERIZATION.....	55
4.1.1. SEM ANALYSIS	56
4.1.2. EDX ANALYSIS	61

4.1.3. X-RAY DIFFRACTION ANALYSIS	62
4.2. RESPONSE ANALYSIS OF THE TEST SENSORS TO METHANE	64
4.3. RESPONSE ANALYSIS OF THE TEST SENSORS TO CARBON MONOXIDE.....	68
4.3.1. TEMPERATURE EFFECT ON THE RESISTANCE BEHAVIOR...	69
4.4. PROMOTION EFFECT ON THE RESISTANCE BEHAVIOR.....	77
4.5. OXYGEN EFFECT ON THE RESISTANCE BEHAVIOR.....	82
5. CONCLUSIONS AND FURTHER SUGGESTIONS.....	106
REFERENCES.....	108
APPENDICES	
A. SAMPLE CALCULATIONS	115
A.1. SnO ₂ Catalyst Preparation Calculations.....	115
A.2. 1 wt. % Pd /SnO ₂ Catalyst Preparation Calculations.....	117
A.3. 0.1 wt. % Na, Pd / SnO ₂ Catalyst Preparation Calculations.....	118
B. MASS FLOW CONTROLLER CALIBRATION CURVES.....	119
C. VOLUMETRIC FLOW RATE CALCULATIONS.....	121
D. EQUIVALENT RESISTANCE CALCULATIONS.....	122

LIST OF TABLES

A.1. Molecular weights of the species used in the catalyst preparation.....	115
D.1. Some of the calculated equivalent resistance values.....	123

LIST OF FIGURES

2.1. General representation of a sensor system.....	7
2.2. Schematic diagram of a typical air contamination sensor.....	8
2.3. Typical output curve of the studied sensor.....	11
2.4. Schematic energy band representations (a) conductor with two possibilities (b) a semiconductor and (c) an insulator.....	13
2.5. Schematic energy band representation of extrinsic semiconductors with (a) acceptor sites (b) donor sites.....	14
2.6. Crystal structure of tin dioxide	15
2.7. Chemical reactions at the surface of SnO ₂ with the surrounding oxygen	17
2.8. Schematic representation of two SnO ₂ neighbour grains and their induced depletion region due to negatively adsorbed oxygen species at the boundry	18
2.9. Model of inter grain potential barrier.....	20
2.10. Mechanism for the interaction of CO with the sensing layer in dry conditions.....	21
2.11. Direct chemisorption of CO on SnO ₂ (on the left), oxidation of CO (on the right)	22
2.12. Water adsorption on the surface, on the left; co-ordinated water, in the middle creation of rooted OH- group and on the right; isolated OH- group	23
2.13. Reaction of CO with isolated hydroxy groups	24
2.14. Bicarbonate formation	25

2.15. (a) Spillover (e.g. Pt-SnO ₂) and (b) Fermi level (e.g. PdO-SnO ₂) mechanisms	27
2.16. Model for the influence of film thickness on morphology	34
2.17. Schematic models for the grain size effects	36
3.1. Flow diagram of tin oxide film preparation	44
3.2. Flow Diagramm for the chemical solution deposition of the multilayer thin films	46
3.3. Schematic diagram of spin coating process	47
3.4. Process time vs. process temperature graph	48
3.5. Experimental Setup	51
3.6. General presentation of reaction chamber.....	56
4.1. SEM image (cross-sectional view) of Na-Pd/SnO ₂ film.....	58
4.2. SEM image (top view) of SnO ₂ film	58
4.3. SEM image (top view) of Pd/SnO ₂ film	59
4.4. SEM image (top view) of Na-Pd/SnO ₂ film	59
4.5. High magnification SEM image of SnO ₂ film spin coated 8 layers.....	60
4.6. EDX analysis of 450 nm thick Pd/SnO ₂ films calcined at 500°C.....	61
4.7. EDX analysis of 450 nm thick Na-Pd/SnO ₂ films calcined at 500°C	62
4.8. XRD Patterns of calcined Pd/SnO ₂ substrate.....	63
4.9. XRD Patterns of calcined Na-Pd/SnO ₂ substrate.....	63
4.10. Response of Na-Pd/SnO ₂ test sensor to pure CH ₄ injections at 200°C in He atmosphere	65
4.11. Response of Pd/SnO ₂ test sensor to pure CH ₄ injections at 200°C in He atmosphere	66
4.12. Response of Na-Pd/SnO ₂ test sensor to 5% CH ₄ step changes at 200°C in He atmosphere.....	67

4.13. Pd/SnO ₂ multilayer thin film resistance behavior in He atmosphere under 750 ppm CO injection at 100 °C	70
4.14. Pd/SnO ₂ multilayer thin film resistance behavior in He atmosphere under 750 ppm CO injection at 125 °C	71
4.15. Na-Pd/SnO ₂ multilayer thin film resistance behavior in He atmosphere under 750 ppm. CO gas injection at 150, 175 and 200 °C.....	72
4.16. Pd/SnO ₂ multilayer thin film resistance behavior in He atmosphere under 750 ppm. CO gas injection at 150, 175and 200 °C	73
4.17. Na-Pd/SnO ₂ multilayer thin film resistance behavior in 1% O ₂ + 99% He atmosphere under 750 ppm CO injection at 150, 175 and 200 °C	75
4.18. Pd/SnO ₂ multilayer thin film resistance behavior in 1% O ₂ + 99% He atmosphere under 750 ppm CO injection at 150, 175 and 200 °C.....	76
4.19. Comparison of Pd and Na-Pd/SnO ₂ multilayer thin film resistance behavior in He atmosphere under 750 ppm CO injection at 150°C	77
4.20. Comparison of Pd and Na-Pd/SnO ₂ multilayer thin film resistance behavior in He atmosphere under 750 ppm CO injection at 175°C	78
4.21. Comparison of Pd and Na-Pd/SnO ₂ multilayer thin film resistance behavior in He atmosphere under 750 ppm CO injection at 200°C	79
4.22. Comparison of Pd and Na-Pd/SnO ₂ multilayer thin film resistance behavior in 1% O ₂ + 99% He atmosphere under 750 ppm CO injection at 150°C.....	80
4.23. Comparison of Pd and Na-Pd/SnO ₂ multilayer thin film resistance behavior in 1% O ₂ + 99% He atmosphere under 750 ppm CO injection at 175°C	81
4.24. Comparison of Pd and Na-Pd/SnO ₂ multilayer thin film resistance behavior in 1% O ₂ + 99% He atmosphere under 750 ppm CO injection at 200°C	82

4.25. Comparison of Na-Pd/SnO ₂ multilayer thin film resistance behavior in oxygen free and 1% O ₂ containing He atmosphere at 150°C.....	83
4.26. Comparison of Na-Pd/SnO ₂ multilayer thin film resistance behavior in oxygen free and 1% O ₂ containing He atmosphere at 175°C	84
4.27. Comparison of Na-Pd/SnO ₂ multilayer thin film resistance behavior in oxygen free and 1% O ₂ containing He atmosphere at 200°C.....	85
4.28. Comparison of Pd/SnO ₂ multilayer thin film resistance behavior in oxygen free and 1% O ₂ containing He atmosphere at 150°C.....	86
4.29. Comparison of Pd/SnO ₂ multilayer thin film resistance behavior in oxygen free and 1% O ₂ containing He atmosphere at 175°C.....	87
4.30. Comparison of Pd/SnO ₂ multilayer thin film resistance behavior in oxygen free and 1% O ₂ containing He atmosphere at 200°C	88
4.31. Typical CO injection, CO ₂ production mass signal over the studied SnO ₂ based test sensors	89
4.32. Response of Na-Pd/SnO ₂ test sensor to CO injections at 150°C in He atmosphere	91
4.33. Response of Pd/SnO ₂ test sensor to CO injections at 150°C in He atmosphere.....	92
4.34. Response of Na-Pd/SnO ₂ test sensor to CO injections 99% He atmosphere.....	93
4.35. Response of Pd/SnO ₂ test sensor to CO injections at 150°C in 1% O ₂ + 99% He atmosphere	94
4.36. Response of Na-Pd/SnO ₂ test sensor to CO injections at 175°C in He atmosphere	96
4.37. Response of Pd/SnO ₂ test sensor to CO injections at 175°C in He atmosphere	97

4.38. Response of Na-Pd/SnO ₂ test sensor to CO injections at 175°C in 1% O ₂ + 99% He atmosphere	99
4.39. Response of Pd/SnO ₂ test sensor to CO injections at 175°C in 1% O ₂ + 99% He atmosphere	100
4.40. Response of Na-Pd/SnO ₂ test sensor to CO injections at 200°C in He atmosphere	101
4.41. Response of Pd/SnO ₂ test sensor to CO injections at 200°C in He atmosphere.....	102
4.42. Response of Na-Pd/SnO ₂ test sensor to CO injections at 200°C in 1% O ₂ + 99% He atmosphere	103
4.43. Response of Pd/SnO ₂ test sensor to CO injections at 200°C in 1% O ₂ + 99% He atmosphere	104
B.1. Mass flow controller calibration curve for 99.99 % He gas.....	119
B.2. Mass flow controller calibration curve for 1% CO and 5% O ₂ gas in Helium	120
D.1. Resistance configuration for the calculation of equivalent resistance value.....	122

NOMENCLATURE

Symbols

D	Mean crystallite size
E_c	Energy level of electrons in the conduction band
E_f	Fermi level energy of electrons
E_g	Band gap energy
E_v	Energy level of electrons in the valance band
eV_s	The height of the potential barrier
L	Depletion region thickness
M	Metal
n	Negative
p	Positive
R	Alkyl Group
R_e	Equivalent resistance
R_a	Sensor resistance in air
R_g	Sensor resistance in the testing gas
O_{ad}	Adsorbed oxygen
S	Sensitivity
T₈₀	Response time
V_o	Occupied vacant site
*	Free adsorption site
θ	Phase angle

Abbreviations

CSD	Chemical solution deposition
DRIFTS	Diffuse reflectance infrared Fourier transform spectroscopy

DMM	Digital multi meter
EDX	Energy dispersive X-ray spectrometer
MFC	Mass Flow Controller
SEM	Scanning electron microscopy
STM	Scanning Tunneling Microscope
XRD	X-ray diffraction

CHAPTER 1

INTRODUCTION

Air pollution is the presence of contaminants in the atmosphere in such quality and for such duration that it tends to be harmful to the livings. Modernisation and progress have led the air pollution getting more serious over the years. Since the organic fuels and chemicals had been a part of the day, air pollution prevention and detection have become an important issue in daily life. Recently it was decided in the European Union for every country to establish a network of air quality monitoring (AQM) stations in the main cities and to inform citizens about the air quality status on the daily basis [1]. Air pollution can also exist inside homes and other buildings, and thus; both indoor and outdoor pollution need to be controlled and / or prevented.

Every country accepts its own air pollution standard, in each industrial field, these standards are similar to each other, but only there are small variations among them. Upto the National Ambient Air Quality Standards, there are 6 main air pollutants, which can be listed as;

- Sulfur dioxide (SO_2)
- Oxides of nitrogen (NO_x)
- Ozone (O_3)
- Lead (Pb)
- Carbon Monoxide (CO)
- Particulate Matter

Among these pollutants, carbon monoxide is a colorless, odorless gas that is produced by the incomplete burning of carbon-based fuels, including

petrol, diesel and wood. It is also produced from the combustion of natural and synthetic products such as cigarettes [2].

The pollutants in air can be detected by using gas sensors. Though it is necessary to detect the pollutants in air, to date, there is no gas sensor exist 100% selective to a single gas. To achieve a good selectivity in air pollutant measurements, the air monitoring stations are based on complex equipment applying analytical techniques (e.g. Fourier Transform Infrared instrument, gas chromatograph, mass spectrometer etc.). These complex equipments are designed for laboratories or specific online applications for in-plant applications and require skilled and knowledgeable operators. In addition, they have disadvantages like high maintenance, slow response time and large size, which are impractical for work area air quality and safety. This causes two main drawbacks; the cost of the stations can reach up to several million Euros and lengthy air sampling and data processing do not allow real time dissemination of the information of the public [3]. For work area air quality monitoring, the equipment must be;

- Weather and dust proof, rugged and corrosion resistant
- Capable of being installed in hazardous areas
- Operated stable, maintained easily
- Operated by a minimally skilled person
- Suitable for multisensor systems (e.g. entire chemical plant)
- Have high sensitivity and selectivity (low cross sensitivity)
- Low sensitivity to humidity and temperature
- High reproducibility and reliability
- Short reaction and recovery time
- Easily calibrated
- Portable

Decades ago, it was discovered that atoms and molecules interacting with semiconductor surfaces influence the surface properties of semiconductors such as conductivity [4]. Since then, the sensors based on metal oxide sensitive layers are playing an important role in the detection of toxic pollutants [5].

Semiconductor is a material that has an electrical resistance between that of an electrical insulator and an electrical conductor. They are poor conductors at low temperatures, and since there are many empty sites in the conduction band for the electrons, or there are not enough electrons to fill the sites in the conduction band, a small applied potential can easily move the electrons resulting a moderate current. So, in semiconductors the number of electrons in the conduction band is usually small, and there are two ways of increasing the number of the electrons [6];

- Adding specific impurities to the semiconductor [7]
- Increasing the temperature [8]

Gas sensitive layers of the chemical gas sensors are made from different metal oxides of semiconducting nature. In 1962, tin dioxide was first demonstrated as a gas sensing device because of its semiconductive properties [9, 10]. Since then, tin oxide based thin film sensors have been widely studied due to their high sensitivity and fast response. The main advantages of using these sensors are their low cost, small size and low power consumption for mobile system applications. But, in order SnO_2 based sensors to meet low concentration of gases they should be highly upgraded in sensitivity, selectivity and stability.

Two types of particles carry electrical current in a semi-conductor, negatively charged electrons (n) and positively charged holes (p). Thus, there are two types of semiconductivities which are namely n-type and p-type semiconductivities [11]. The semiconductor based gas sensor responds to a reducing gas by an increase or a decrease in the resistance, depending on the type of the semiconductor.

Tin dioxide is an n-type semiconductor with a band gap of approximately 3.6 eV. When the SnO_2 is exposed to a reducing atmosphere, the interaction between the gas and the adsorbed oxygen result in oxidation at the surface, and in a decrease of chemisorbed oxygen concentration, and the electrons that have been trapped as negatively charged ions are released. Due to the n-type behavior of SnO_2 , the electrical conductivity increases when

in contact with a reducing gas like CO and / or CH₄, on the contrary decreases in the presence of an oxidising gas like NO₂ [7].

There are many parameters affecting the sensor response [12]. Some of them can be listed as:

- The SnO₂ based material with different dopings, crystallinity and thickness, including the details of the coating preparation [13,14]
- The geometry of the material of the test substrate [15]
- The aging and preconditioning procedure [16,17,18]
- The porosity, adsorption-desorption properties of the material [19]
- The sensing mode with external and internal modulations (partial pressures, temperatures) [20,21]
- The modulation of measurement parameters such as potential, frequency and resistance [22,23].

From the above listed parameters one can decide easily that the sensor preparation procedure strongly affects the sensor response. There are numerous methods for the preparation of the catalytic films in the literature. Some of them are can be explained as followed:

- **Sol-gel Technique**, usually consists on the precipitation of tin hydroxide from an aqueous solution where a high pH is reached by the addition of some compound, then, an annealing process is required to obtain tin oxide.
- **CVD & Spray Pyrolysis**, techniques are suitable for the direct preparation of films, and not powders as in sol-gel. They basically consist on the spraying of a tin (IV) on a suitable substrate. The spraying process is usually done in an air atmosphere, then, the substrate is heated in order to produce the tin (IV) oxide film.
- **Sputtering**, basically consists on the formation of a tin (IV) oxide film by the sputtering of a heated substrate from a evaporated metallic tin or tin (IV) oxide target in a controlled oxygen atmosphere. The temperature of the substrate (100-150 °C) is usually not as high as in CVD (400-500 °C).

- **Rheotaxial Growth and Thermal Oxidation (RGTO)**, technique is a two-step process in which the first step consists on the evaporation of metallic Sn onto substrates heated above the melting temperature of Sn. In these conditions, the evaporated Sn tends to cluster into small spherical droplets that do not touch each other. In a second step, the Sn droplets are oxidised by thermal annealing in air at temperatures of the order of 500-700 °C, thereby forming polycrystalline SnO₂ films.
- In the **Pulsed Laser Deposition**, the tin oxide film is formed by physical vapour deposition of tin oxide from tin oxide pellets that are focused with a pulsed laser in controlled atmosphere.
- **Hydrothermal Method** consists on the immersion of a substrate in an aqueous solution of tin hydroxide at temperatures above 100 °C for several hours.

The sol-gel synthesis, which was chosen as the catalyst preparation technique in this study, is the most common method among those, due to the advantages of low processing temperatures, possibility of tailoring the starting solutions, resulting better compositions and better control of the final structure [7,24]. In the current study, the coated films were dried at 100 °C, and then calcined at 500 °C. The same coating route was followed until the desired film thickness was reached. Then the investigation of the response behavior of Pd/SnO₂ and Na promoted Pd/ SnO₂ multilayer thin films to 1% CO in He gas mixture has been done under 1% oxygen containing and oxygen free atmospheres.

CHAPTER 2

LITERATURE SURVEY

2.1. SENSORS

Sensors are interface devices between various physical values and electric circuits who “understand” only a language of moving electrical charges. With a closer definition, sensors are devices receiving a signal or a stimulus and responding with an electrical signal, which is compatible with electric circuits. Generally, a sensor’s input signals (stimuli) may have almost any conceivable physical or chemical nature. For instance, light flux, temperature, pressure, vibration, displacement, position, velocity or concentration. A sensor does not function by itself, it is always a part of a larger system which may incorporate many other detectors; signal conditioners, signal processors, memory devices, data recorders and actuators.

A variation in any parameter leads to a variation in the electrical structure of the material. This change in the electrical structure can be displayed or recorded by a variety of electronic devices. In Figure 2.1, general system of a sensor can be seen. First the sensor receives a stimulus, and then the signal is modified and transmitted as an output signal [25].

A gas sensor is a transducer that detects gas molecules and which produces an electrical signal with a magnitude proportional to the concentration of the gas. Unlike other types of measurement that are relatively straight forward and deal with voltage, temperature and humidity, the measurement of gases is much more complicated. Because there are hundreds of different gases, there is a wide array of diverse applications in

which these gases are present, and each application must implement a unique set of requirements.

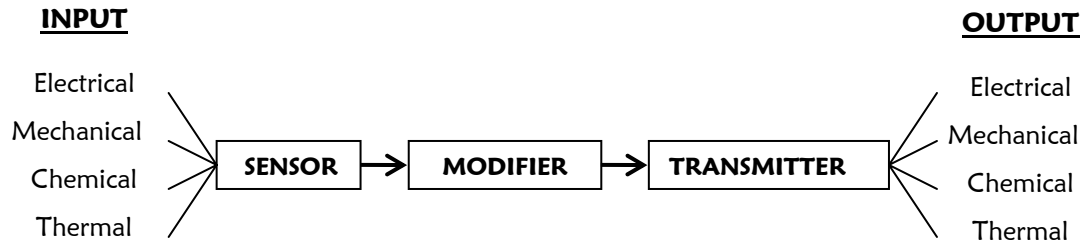


Figure 2.1. General representation of a sensor system

There are many different technologies currently available for the detection of gases, each with certain advantages and disadvantages. All these technologies are used for detection of toxic and combustible gases in the work area for human and property protection, or for process control.

2.2. CHEMICAL SENSORS

A chemical sensor is a device which produces an electrical signal in response to a chemical reaction. This type of sensors is sensitive to stimuli produced by various chemical compounds or elements. Chemical sensors are intended for recognition of presence of specific substances and their concentrations, partial pressures or activities [25].

Chemical sensors are classified into various categories according to different properties, such as the field of application, sensor material, operating mode, etc. Depending on the field of application, some of the chemical sensors can be classified as medicine, military, scientific measurement, automotive, domestic, environment, marine and space sensors. And with respect to the sensor material, the sensor categories can be listed as inorganic,

organic, conductor, insulator, semiconductor, etc. According to the sensors are divided into gas and liquid sensors. Examples are the oxygen sensor to monitor either the O_2 concentration in air or for detection of concentration of dissolved oxygen.

Depending on the operating mode, chemical sensors are divided into three as; those which measure voltage (potentiometric), those which measure electric current (amperometric), and those which rely on the measurement of conductivity and resistivity (conductometric). In all these methods special electrodes are used, where either a chemical reaction takes place or the charge transport is modulated by the reaction. A fundamental of an electrochemical sensor always requires a closed circuit, that is, an electric current must be able to flow in order to make a measurement. Since electric current flow essentially requires a closed loop, the sensor needs at least two electrodes, one of which often is called a return electrode. It should be noted that even if in the potentiometric sensors no flow of current is required for measurement; the loop still must be closed for the measurement of the voltage [25].

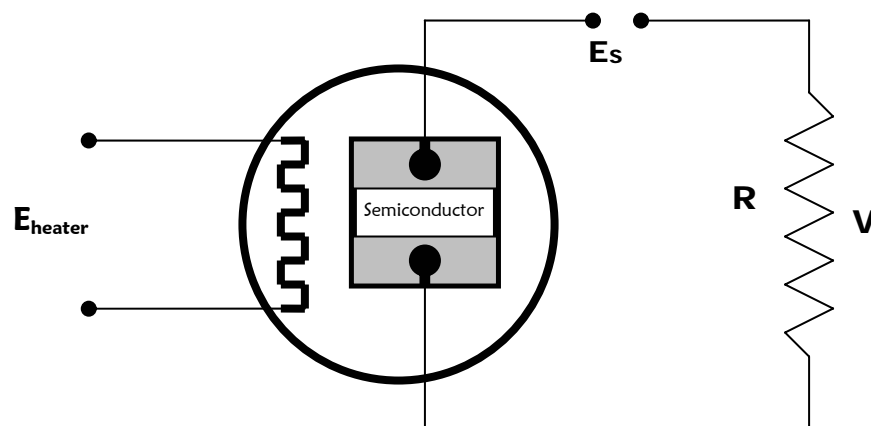


Figure 2.2. Schematic diagram of a typical air contamination sensor

In the electrochemical sensors, voltage, current, resistance, or capacitance is generally measured. In Figure 2.2 a scheme of an air

contamination sensor is represented, which is a typical solid state gas sensor also investigated in this study [28]. Often, the sensor is called an electrochemical cell, and how the cell is used mainly depends on the sensitivity, selectivity and accuracy. The electrochemical sensors are the most versatile and more developed than any other chemical sensors.

One common characteristic of these sensors is that they are not specialized to detect any one specific gas. Each sensor is sensitive to a group or family of gases. In other words, the sensor is non-specific and subject to interference by other gases much like a smoke detector in a house cannot distinguish between the smoke caused by a furniture fire and the smoke caused by food burning in the oven.

For gas monitoring applications, a proper sensor is usually selected to match the specific application requirements and circumstances, with the user interpreting and readings based on an awareness of the sensor limitations. To be aware of the limitations one needs to know the properties affecting the sensor performance.

2.3. SENSOR PERFORMANCE SPECIFICATIONS:

There are some specifications for determining the properties of sensors such as sensitivity, selectivity, stability, accuracy, repeatability, response time, interference, hysteresis, linearity and ambient conditions [26]. Ideal gas sensors should present,

- High sensitivity towards chemical compounds
- High selectivity and stability
- Low sensitivity to humidity and temperature
- High reproducibility and reliability
- Short reaction and recovery time
- Be robust and durable
- Easy calibration
- Portable

2.3.1. SENSITIVITY

Sensitivity can be defined as the ratio of conductivities changing upon the exposure of the reducing gas [14,19,32,25]. Sensitivity (S) can be expressed in terms of sensor resistance in air (R_a) and sensor resistance in the testing gas (R_g) can be expressed as [14];

$$S = ((R_a - R_g) / R_a) \times 100 \% \quad (2.1)$$

2.3.2. SELECTIVITY

Selectivity is the ability of a sensor to respond primarily to only one chemical element or compound in the presence of other species. In order to achieve some degree of selectivity, different techniques are implied, for example; a charcoal filter is used to filter out most hydrocarbons while letting only CO, H₂ and CH₄ pass through [12,19,22].

2.3.3. STABILITY

Aging and poisoning of a chemical sensor can cause some decrease in sensitivity and selectivity. However a chemical sensor is expected to maintain its structure for a long period of time [49]. In the case of tin dioxide based gas sensors, there are studies reporting that stability over more than 8 months for CO concentrations in the 50-500 ppm range had already been achieved [27].

2.3.4. ACCURACY

Being accurate is defined as, being free from mistake or error; precise and adhering closely to a standard. The accuracy can only be determined when compared to a standard [19,26].

2.3.5. REPEATABILITY

Repeatability is the ability of sensors to repeat the measurements of gas concentrations when the sensors are subjected to precisely calibrated gas samples [19,26].

2.3.6. RESPONSE / RECOVERY TIME

Response time is defined as the time it takes for a sensor to read a certain percentage of full-scale reading after being exposed to a full-scale concentration of a given gas. For example: $T_{80} = 5$ means that the sensor takes 5 seconds to reach 80 % of the full-scale reading after being exposed to a full-scale gas concentration [26].

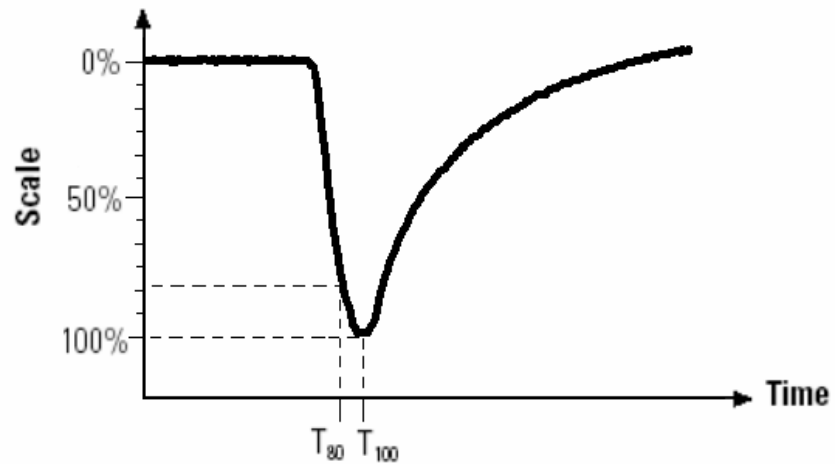


Figure 2.3. Typical output curve of the studied sensor

2.3.7. TEMPERATURE AND PRESSURE

The amount of actual water vapor in air is a function of temperature. For example at 25 °C 80% humidity means water vapor is present at a level of 3%. When the same relative humidity value considered at 48 °C water vapor is present at a level of 10%. In the presence of chemicals, combined with the changing temperature the possible water condensation and resultant corrosive mixtures can compromise the life expectancy of a sensor [26]. The ambient conditions are very important in sensors, the surface temperature of the solid state gas sensor can be set differently in order to make it more sensitive to one gas and less sensitive to other gases [19].

2.3.8. HYSTERESIS

Hysteresis is the difference in response of the sensor when calibrating from a zero level to mid-scale compared to the response when calibrating from full scale to mid-scale [26]. For instance, a 100 ppm instrument when calibrated from 0 to 50 ppm and exposed to a 50 ppm calibration gas, will indicate 50 ppm. On the other hand, when sensor is calibrated to 100 ppm gas but is exposed to 50 ppm the sensor may indicate 55 ppm. This variation of 5 ppm between the measurements is 5% full-scale hysteresis. Most infrared and photoionization sensors do not exhibit hysteresis, but many other sensors like electrochemical, solid state, and catalytic sensors do exhibit hysteresis.

2.4. SEMICONDUCTORS

Semiconductors are materials that have an electrical conductance between that of an electrical conductor and an electrical insulator. Conductors, have very low value of electrical resistivity. Their conduction band either is partially filled or overlaps the valance band so that there is no band gap (Fig. 2.4.a). Therefore, the uppermost electrons in the partially filled band or the electrons at the top of the valance band can easily move to the next higher available energy level when they gain kinetic energy from an applied electric field. Electrons can freely move with only a small applied field because there are many unoccupied states close to the occupied energy states.

In insulators, the valance electrons form strong bonds between neighbouring atoms. These bonds are difficult to break, so there are no free electrons to participate in current conduction at room temperature. Insulators have very wide bandgap and the electrons occupy all energy levels in the valance band and all energy levels in the conduction band are empty (Fig.2.4.c). Thermal energy or energy of an electrical field is insufficient to raise the uppermost electron in the valance band to the conduction band. Thus, although an insulator has many vacant states in the conduction band that can accept electrons, so few electrons actually occupy conduction band

states that the overall contribution to electrical conductivity is very small, resulting in a very high resistivity. Therefore they can not conduct current.

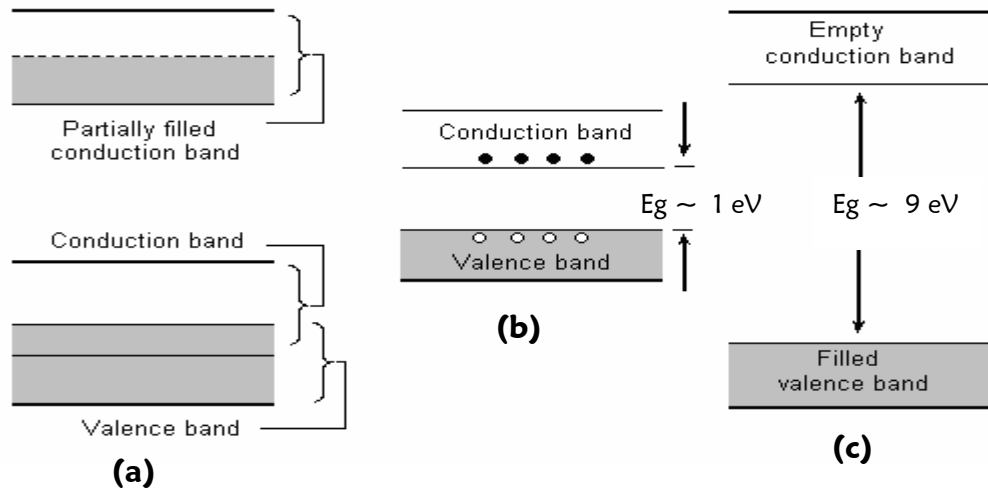


Figure 2.4. Schematic energy band representations (a) conductor with two possibilities (at the upper portion, the partially filled conduction band, and in the lower portion overlapping bands) (b) a semiconductor and (c) an insulator

Semiconductors have a much smaller energy gap on the order of 1 eV (Fig.2.4.b). At 0 K, the electrons fill the energy levels up to a certain level which is called Fermi Energy Level. At the absolute zero temperature all electrons are in the valance band, and there are no electrons in the conduction band. Thus semiconductors are poor conductors at low temperatures. The thermal energy at room temperature (298 K) is a good fraction of energy bandgap (E_g), and an applicable numbers of electrons are thermally excited from the valance band to the conduction band. Since there are many empty states in the conduction band, a small applied potential can easily move these electrons resulting a moderate current [25].

In semiconductors the number of electrons in the conduction band is usually small and with an addition of impurity atoms the conductivity of the material can be altered [28]. To introduce acceptor sites to the semiconductor,

atoms with smaller number of electrons, and to introduce donor sites, atoms with larger number of electrons can be added to the structure [62]. These types of semiconductors are called extrinsic semiconductors (Fig.2.5). When a Vth group element is doped, the semiconductor conducts with the negative charged free electrons therefore is called n-type, when a IIIrd group element is doped, the semiconductor conducts with the positive charged holes which move through the structure, therefore called p-type semiconductor [25].

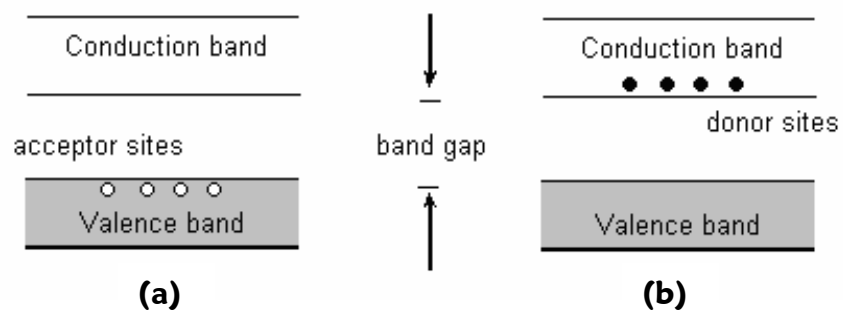
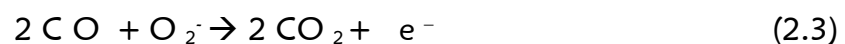
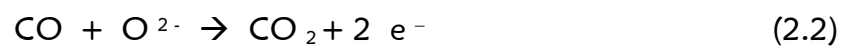


Figure 2.5. Schematic energy band representation of extrinsic semiconductors with (a) acceptor sites (b) donor sites

The semiconductor based gas sensor responds to a reducing gas by an increase or a decrease in the resistance, depending on the type of the semiconductor. The change of resistance can also be a result of the impact of the reducing gases on the surface oxygen species. For instance in the case of carbon monoxide the following reactions take place at the surface; setting the electrons free back to the conduction band,



In n-type semiconductors, ionized donors act as electron sources. The charge carrier concentration at the interface is reduced when the electrons are

drawn from the conduction band with a development of an energy barrier. As a result of the reduction in surface potential barrier height, surface adsorbed oxygen species are reduced with an increase in the conductance [28].

In the case of a p-type semiconductor, surface adsorbed oxygen species act as surface acceptor sites. The charge carrier concentration at the interface is increased when the electrons are drawn from the valance band. When the combustion reaction of carbon monoxide occurs the number of surface adsorbed oxygen species gets lower with a decrease in the charge carrier concentration, and as a result the resistance increases.

2.4.1. TIN DIOXIDE

Pure tin dioxide is a semiconductor with a band gap of approximately 3.6 eV. It has a tetragonal TiO_2 anatase type structure. The structure of tin oxide consists of a lattice of tin atoms, Sn^{+2} , Sn^{+4} and oxygen atoms, O^{2-} . The reason for the stability is that the Sn ion has two stable oxidation states. For SnO_2 (110), a layer of bridging oxygen ions are present on the perfect surface which can easily removed and resulting a compact stable surface. As Barsan and Göpel reported [12], it was proved experimentally and calculated that the removal of bridging oxygen atoms did not, but the removal of inplane oxygen ions provided additional donors (Fig. 2.6).

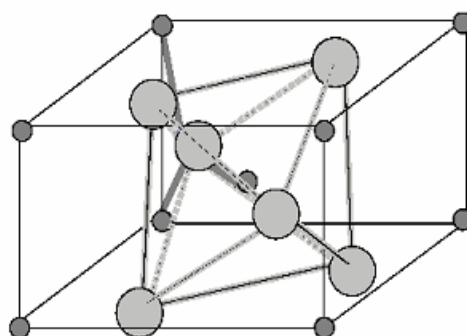


Figure 2.6. Crystal structure of tin dioxide (larger spheres are oxygen atoms)

Heating tin dioxide in a reducing atmosphere causes oxygen vacancies in the crystal structure whose concentration depends on the surface temperature and gas composition. Therefore, n-type tin oxide is usually denoted as SnO_{2-x} because of the oxygen vacancies in the structure. Loosely bound electrons of the vacancies have a high probability, in comparison to valance electrons, to reach the conduction band and thereby contribute to conductivity properties of the material [29]. Because of the natural non-stoichiometry of SnO_2 , adsorption of oxygen is easy at its surface. Consequently, electrical conductivity of tin dioxide is sensitive to oxidative and reducing atmospheres and that is the reason why it is used in gas sensor applications.

2.5. SEMICONDUCTING OXIDE GAS SENSORS

Gas sensitive layers of the chemical gas sensors are made from different metal oxides of semiconducting nature. The most widely preferred materials are oxides because of the opportunity for molecular reactions that is confined to the surface layer of the atoms but the electrical consequences of which are manifest through a considerable volume of the solid [11]. Among a list of materials, SnO_2 , In_2O_3 and WO_3 are effective metal oxides used in the developement of gas sensors for both indoor and outdoor air quality.

The best understood and mostly used prototype of oxide based sensors is SnO_2 in the bulk ceramic, thick-film or thin-film form. Basically, there are two extremes in the preparation of SnO_2 based gas sensors which are successful according to the report written by Barsan and Göpel [12] in 1999. These are thickfilms with controlled nanocrystalline sizes and thin films monolayers of nanocrystalline SnO_2 . Thin films in comparison to bulk faces have a small surface area which causes a poor sensitivity. However, thin film with high surface area has the advantage of fast recovery, lower energy input and ability to control the film morphology [30]. Therefore the recent focus sensor research has been shifted to thin films to improve their properties.

2.5.1. OPERATION PRINCIPLE

The detection of the reducing gas by the sensitive surface is a process following the diffusion, adsorption, reaction and desorption steps. The process can be summarized in seven steps [31] as;

- I. The target gas diffuse from bulk fluid to the external surface of the catalyst
- II. The species diffuse within the pores of the catalytic surface
- III. The species adsorb on the catalyst
- IV. The target gas and oxygen react on the surface
- V. The product desorbes from the surface
- VI. The product difuses through the pore mouth
- VII. Finally the product diffuses from the external surface to the bulk fluid.

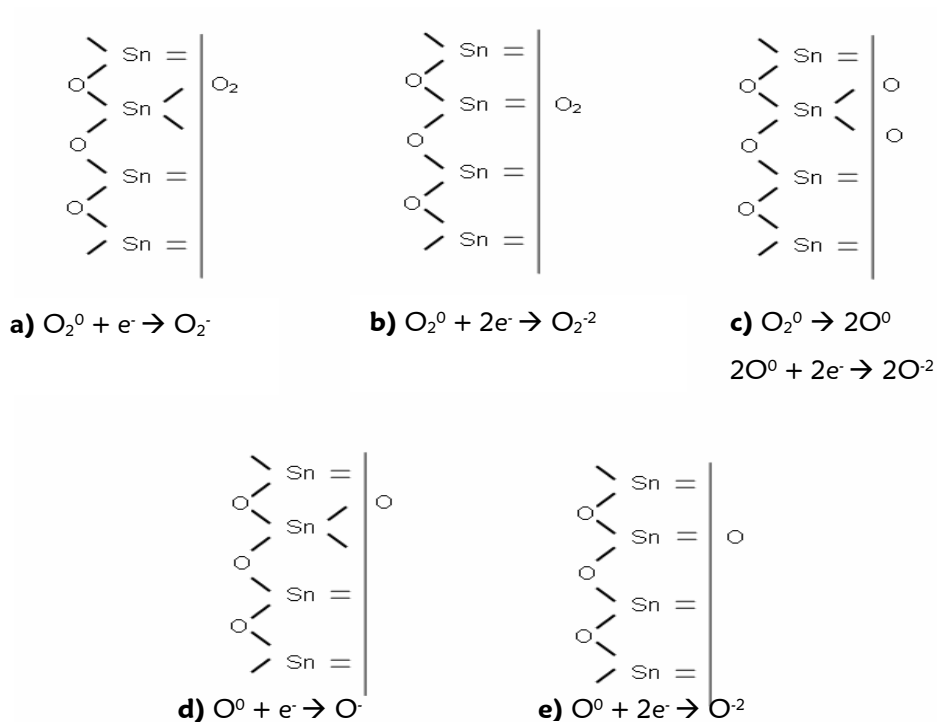


Figure 2.7. Chemical reactions at the surface of SnO_2 with the surrounding oxygen

The ideal surface of SnO_2 can adsorb oxygen and water from the atmosphere. Oxygen may be either physisorbed as uncharged molecules, or chemisorbed as charged species on its surface. The physisorbed oxygen will not affect the surface states, while the chemisorbed oxygen species act as surface acceptors, trapping electrons and reducing surface conductivity of the tin oxide. The surface is electronically and chemically modified by reacting with the different oxygen species present in the atmosphere (O^0 and / or O_2^0). Then, the oxygen on the surface is ionized into different oxygen species such as O_2^- , O^- and O^{2-} , becoming stable in isothermal processes. In Figure 2.7, the different possible oxygen ionization reactions are shown.

The electrons used for the oxygen ionization come from tin dioxide, and as a result, a depletion layer exists on and near the surface of the material, building a potential barrier in this region. This makes the surface conductivity of the SnO_2 lower than the bulk conductivity. The same process also occurs at the grain boundaries (Fig.2.8).

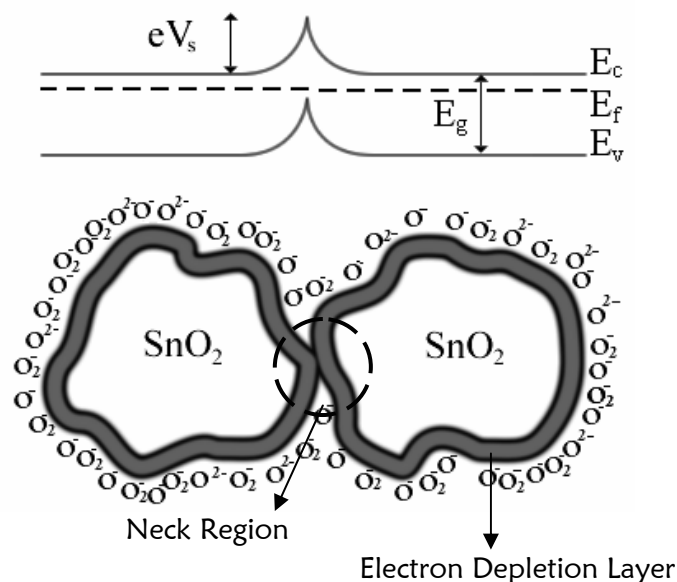
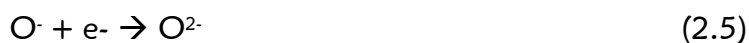


Figure 2.8. Schematic representation of two SnO_2 neighbour grains and their induced depletion region due to negatively adsorbed oxygen species at the boundry

The height of the potential barrier (eV_s) is dependent on the temperature and partial pressure of the other oxidizing and the reducing species, doping level and the exposure time. The surface density of the adsorbed oxygen species is important, because it determines the maximum amount of charge that can be trapped. Thus, the height of the potential barrier is increased by the concentration of the oxygen species present on the surface of the material. Substitution of some cations in the host semiconductor modifies the electrical properties and also alters the gas sensing properties by increasing the catalytic activity [32].

The density of the surface adsorbed oxygen species is influenced by the composition and the temperature of the ambient atmosphere. At room temperature, both O²⁻ and O⁻ species remain on the surface. With increasing temperature, O²⁻ species dissociates to O⁻ (2.4) and becomes the dominant species at temperatures above 180°C and desorbes at higher temperatures [33]. Wang et al. [34] stated that, O⁻ ion is more reactive and thus makes the material more sensitive to the presence of reducing gases.



At relatively low temperatures the surface preferentially adsorbs O₂⁻ (2.5) and the sensitivity of the material is consequently very small. Because the O₂⁻ species are highly unstable and do not play much role in determining the sensitivity. If the temperature increases too much, progressive adsorption of all oxygen ionic species previously adsorbed occurs and the sensitivity decreases.

When the SnO₂ is exposed to a reducing atmosphere, the interaction between the gas and the adsorbed oxygen result in oxidation at the surface, and in a decrease of chemisorbed oxygen concentration, and the electrons that have been trapped as negatively charged ions are released.

The contact of flammable gases with SnO₂ does not only eliminate adsorbed oxygen but also create oxygen vacancies by reacting with the lattice

oxygen as a result reducing SnO₂ [35]. These vacancies on the semiconductor oxide behave as donors. Thus, both of these cases give rise to the increase of the carrier concentration [13]. So O[•] and O₂[•] species are considered to have no direct role on CH₄ oxidation.

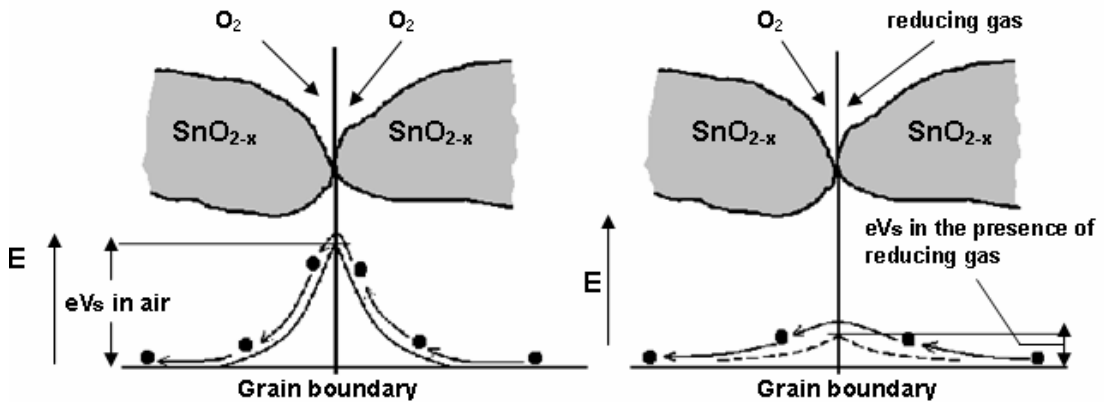
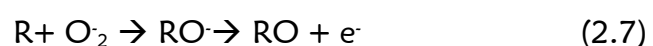
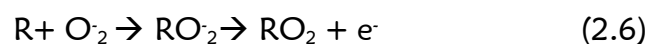


Figure 2.9. Model of inter grain potential barrier (Dark circles are electrons)

Due to the n-type behavior of SnO₂, the electrical conductivity increases when in contact with a reducing gas like CO and /or CH₄, on the contrary decreases in the presence of an oxidising gas like NO₂ [7]. For example; CO can reduce the surface of SnO₂ by taking oxygen chemisorbed and, thus, giving electrons to the bulk of the semiconductor, decreasing barrier height and increasing surface conductance (Fig.2.9). Reducing gases can react also with the lattice oxygen, but the reaction rate is much slower than the surface reaction and can be neglected [33]. The possible surface reactions can be described as follows where R represents the reducing gas;



In the report by Ertl [36], the combustion reaction of CO is described in following steps, where the symbol * represents a free adsorption site;



A power law relationship between sensor conductivity and reducing gas concentration was theoretically derived and observed by Göpel [37] that explains the conductivity was proportional with the reducing gas concentration. CO interaction with the semiconductor surface is explained in oxygen free, in limited oxygen containing and in oxygen containing atmospheres in Figure 2.10.

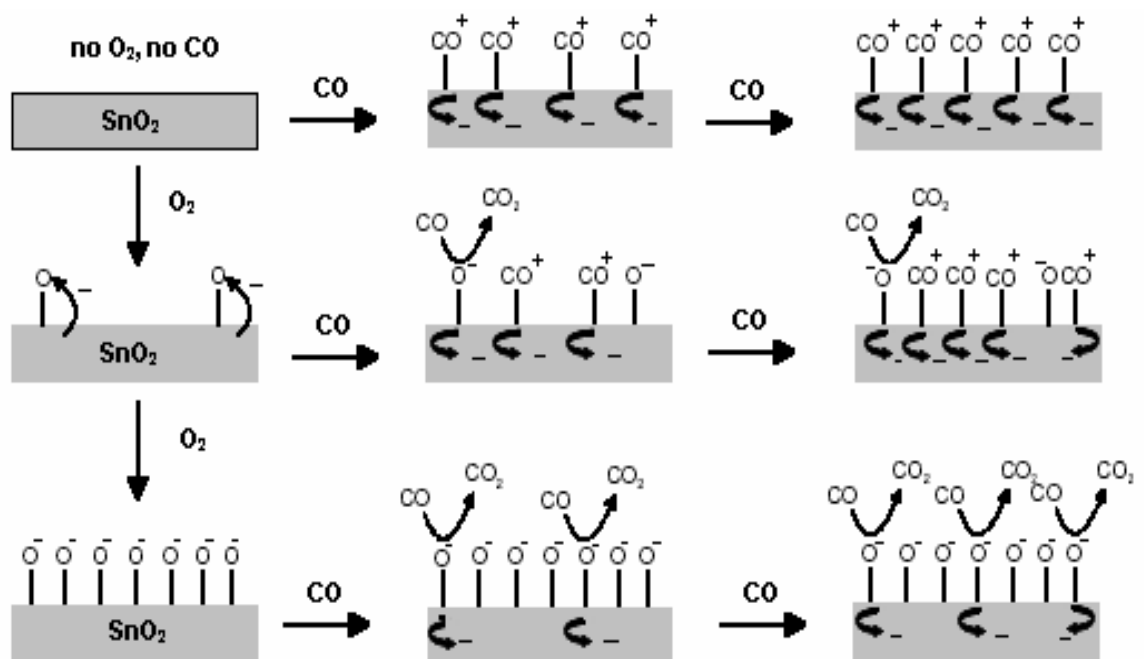


Figure 2.10. Mechanism for the interaction of CO with the sensing layer in dry conditions

At lower temperatures than 200°C, CO adsorption may occur without oxidation of the adsorbed gas and the subsequent release of electrons into the conduction band. Starke [2] et al. reported that the nanoparticles and multilayer coating have increased the surface area the adsorption of the CO molecules might have a marked affect on the conductivity of the film without an oxidation reaction taking place. They had also mentioned this behavior was supported by the fact that CO adsorbs strongly at temperatures below 200°C. And the CO signal is not related directly with the CO₂ production. A larger sensor signal is not necessarily seen in the result of consumption reaction. Schmid et al. [38] explained this result telling that in the presence of very small amount of oxygen and water, CO could adsorb on the surface of the sensitive layer and act as an electron donor. The released electron was inserted into the conduction band of the material and this resulted with an increase in the conductivity of the material. But in higher oxygen containing atmospheres the generation of CO₂ is the main reaction, though resulting with a less electrical effect then the adsorption (Fig. 2.11).

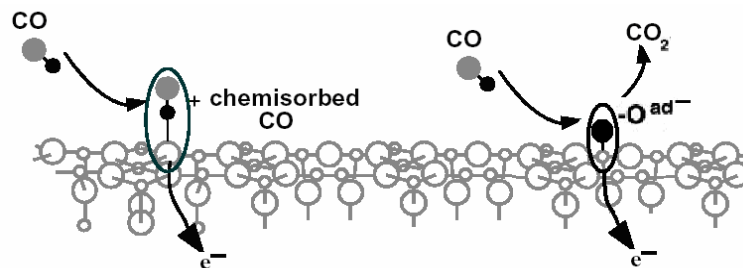


Figure 2.11. Direct chemisorption of CO on SnO₂ (on the left), oxidation of CO (on the right)

However, as mentioned, the above process explanation is valid after the removal of water molecules. Semiconductor oxide gas sensor performance is also dependent on the water vapor concentration and the responses to combustible gases are affected by the ambient atmosphere humidity. It was

investigated that the surface of tin dioxide adsorbs approximately 40 times greater quantities of water than oxygen [33]. Water can be absorbed in the form of physisorbed neutral molecules; hydrogen bonded molecules and chemisorbed reactive water molecules or as surface Sn-OH groups [33].

The H₂O molecules also interact with the semiconductor surface and lead to complex effects on the conductance evolution as a function of temperature. Adsorption of water on the surface results with the CO₂ production and protonated water, which affects the electrical response through the insertion of an electron into the conduction band (Fig. 2.13). The hydrogen atoms can also react with lattice oxygen atoms and produce oxygen vacancies as donors and surface hydroxyl groups. Thus chemisorbed water increases surface conductivity of the tin oxide.

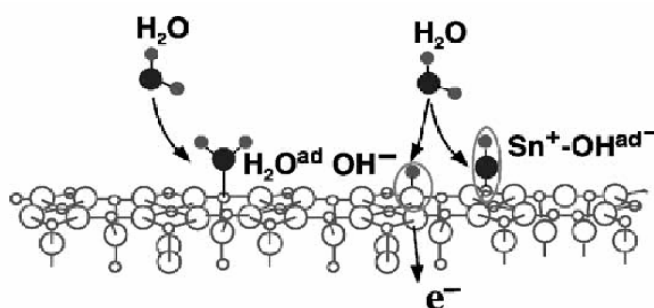


Figure 2.12. Water adsorption on the surface, on the left; co-ordinated water, in the middle creation of rooted OH⁻ group and on the right; isolated OH⁻ group

Investigations showed that on heating to 100°C only a minor water loss was observed, and the major loss occurred between the 240-450°C temperature range. Among the possibilities of adsorption, reaction with hydroxyl groups or ionosorbed oxygen, the direct adsorption results in the largest electrical effect followed by the reaction with hydroxyl groups and the reaction with ionosorbed oxygen [38].

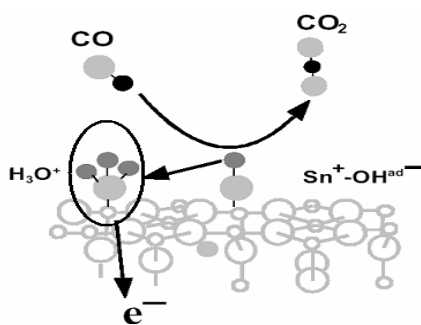
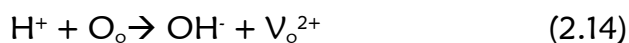
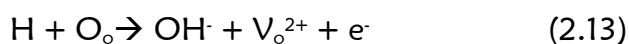


Figure 2.13. Reaction of CO with isolated hydroxy groups



Several surface species like different OH groups, coordinated and molecular water, oxygen and carbonate ions, different hydrated proton species H_3O^+ , H_5O_2^+ , H_7O_3^+ , etc. were investigated by Harbeck *et al.* [20]. CO interacts with specific OH groups, water and oxygen ions at different reaction rates, and forms covalently bound carboxylate and carbonate groups. Besides, Wurzinger *et al.* [39] suggested that large amounts of formate groups, OH groups and either carbonate or hydride groups have been detected in the DRIFT studies on CO sensing. And as Barsan and Göpel [12] reported; the CO related species are;

- Unidentate and bidentate carbonate between 150-400°C (Fig. 2.14)
- Carboxylate between 250-400°C

CO can interact with the adsorbed hydroxy groups HO_{ads} and be oxidized to formate (HCOO_{ads}) [40], but this reaction does not cause any electrical effect. Formate is stable upto 230°C on polycrystalline SnO_2 surface.

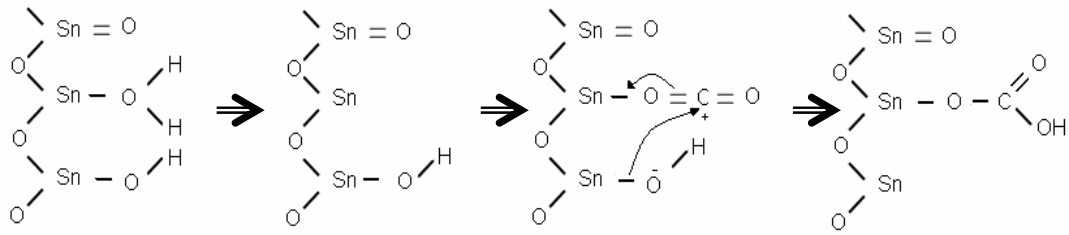
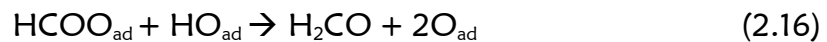


Figure 2.14. Bicarbonate formation

At the temperatures above 230° C, formate either decomposes to produce CO₂ and hydrogen (2.15) and increase the conductivity, or react with another hydroxy group to form aldehyde (2.16). The production of formaldehyde provides two adsorbed oxygen atoms and leads to conductivity decrease [41].



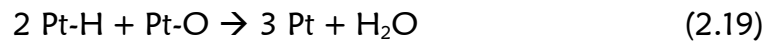
Surface dopants effect the response of the gas sensors by the spill over and Fermi level mechanisms. When the noble metal–tin oxide sensor is in contact with a reducing gas in the atmosphere, the reducing gas is first activated by the metal surface. Some forms of surface hydrogenic and hydrocarbon species are created on the noble metal surface, react with the adsorbed, charged oxygen molecules on the tin oxide underneath the support via a spill over process [5]. The spill over process can be simply defined as the migration of chemical specie from catalytic sites onto the inner support [42]. This process involves the transport of active species adsorbed on another phase which normally does not sorb or form the species. Spillover of CO in the catalytic oxidation of CO in the presence of Pd-SnO₂ is suggested by Corner *et al.* [43]. CO was chemisorbed on Pd and spills over to SnO₂, showing a faster oxidation than in the absence of Pd. So, it is an important part of the surface diffusion. Spillover reaction leads to the injection of electrons back to the bulk, thus increases the conductivity. As a result, the

reducing gas composition causes a change in the conductivity of the sensor material. The noble metal promoter in the semiconducting material activates hydrogen and the reducing gas dissociatively at low temperature, generating reductant species on the metal surface. As a result, in the spill over process the hydrogenic or hydrocarbon species are transported to the tin oxide surface, crossing the surface boundary between the promoter metal and the support. This makes the spill over process an important effect on the gas sensing mechanism.

This can be explained by an example of hydrogen and oxygen interaction with Pt promoter and formation of active hydrogen and oxygen ions:



The resulting active hydrogen can spill over onto the semiconductor support and react with the active oxygen.



In the case of gas sensing, this process causes a faster sensor response. The schematic explanation of the spill over and Fermi level mechanisms can be seen in Fig. 2.15. In the chemical sensing mechanism (spillover) change of the adsorbed oxygen concentration is effective; where in the electronic sensing mechanism (Fermi level) change of oxidation state of noble metal is effective.

Cha et al. [16] elucidated the hydrogen sensing mechanism of Pd promoted SnO₂ gas sensors and suggested that Pd promotion shifts down the optimum sensor operating temperature to 250 °C. This effect is explained by the spill over process, the d orbitals of the promoter metal transfer electronic charge into the antibonding levels of the adsorbate, resulting with dissociation of hydrogen molecules [44].

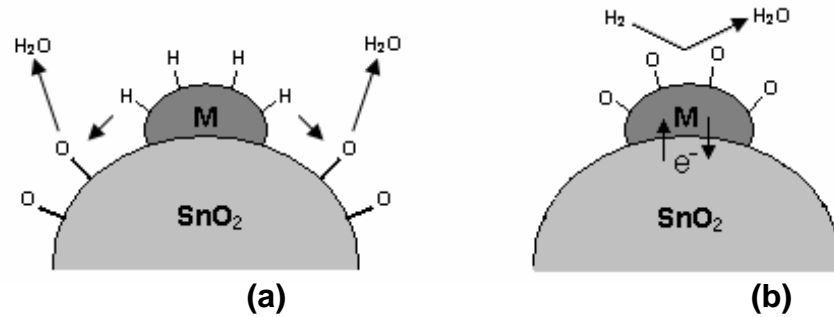


Figure 2. 15. (a) Spillover (e.g.Pt-SnO₂) and (b) Fermi level (e.g. PdO-SnO₂) mechanisms

In the Fermi level mechanism, gas detection takes place at the surface of the semiconducting oxide. The promoter metal changes the electrostatic potential at the metal-metal oxide interface resulting from the different electronic affinities. As a result, the conductance varies according to the Fermi level of the metal oxide modified by the promoter metal [10].

Cabot *et al.* [35] suggested that when considering the transduction of the chemical changes introduced by the gas reaction, distinction is made considering if the dominant electronic transduction takes place on the additive particle (electronic mechanism) or on the supporting oxide itself (chemical mechanism). Additive particle size is considered to be one of the parameters delimiting the dominant mechanism. Too large additive particles could not lead to such an electronic mechanism because a reduction – oxidation of the whole surface does not take place.

2.6. PARAMETERS AFFECTING THE SEMICONDUCTING OXIDE GAS SENSOR PERFORMANCE

The gas detection with semiconductor gas sensors can not be only completely explained by considering only the charge transfer occurring at the surface of the semiconductor. In determining the gas sensitivity of the sensor, reactivity, the difference in diffusivity between the target gas and oxygen are

also important factors. This makes the sensing properties to be dependent on the sizes of the pores, grain sizes, molecular size of the sensed gases, temperature, etc. [45].

Also the following parameters and their influence on the sensor response should be considered as Barsan [12] reported in his study:

- The SnO₂ based material with different dopings, crystallinity and thickness, including the details of the coating preparation
- The geometry of the material of the test substrate
- The aging and preconditioning procedure
- The porosity, adsorption and desorption properties of the material
- The sensing mode with external and internal modulations (partial pressures, temperatures)
- The modulation of measurement parameters such as potential, frequency and resistance.

2.6.1. EFFECT OF TEMPERATURE

Temperature has a pronounced effect on the sensitivity of tin dioxide based gas sensors, as it influences the physical properties of semiconductors like the charge carrier concentration. The oxygen injection experiments conducted at 195°C by Castro *et al.* [13] showed that the sintering temperature affects the responses of the sensors. Also, every reaction taking place at the surface of the semiconductor, as well as the most probable species adsorbed, and hence the reaction sites are temperature dependent [45]. Thus, temperature strongly affects processes occurring at the surface of the sensor. As an example sorption can be given; both adsorption and desorption processes are temperature activated. Also the surface coverage by molecular and ionic species, chemical decomposition and reactive sites are all temperature dependent. This means that, dynamic properties of the sensors such as response and recovery time and the static characteristics of the sensor depend on the temperature of operation. And there is always a temperature for which the sensitivity of a sensor is maximum. For example, in the case of pure SnO₂,

the most active oxygen specie is occurring the temperatures between the temperature range of 423-923 °C [45].

Thus, there are different possible temperature dependent elementary steps of molecular recognition with semiconductor gas sensors that have to be optimised for the specific detection of a certain molecule. The key for the controlled operation is the careful adjustment of the operation temperature, since conduction changes upon exposure to different gas components usually show different maxima as a function of temperature. Sanchez *et al.* [46] studied with HF gas and recorded the sensor signal in constant air flow and HF containing flow separately, to compare the sensor responses under air flow before and after being exposed to a single HF flow. They recorded that, an increase of the dilution in air more significantly causes the conductivity peak no longer be assigned to the analysis of the chemical compound, but to the carrier gas. The conductivity peak showed a maxima at the temperature where it is most sensitive to air. But there was still an inflexion point at the temperature where the material is most sensitive to HF. So they concluded that it is very important to determine the specific detection temperature for each chemical compound analysed.

In the report written by Barsan and Göpel [12], it is declared that if the SnO₂ sensor was operated in constant temperature mode, CO and NO₂ gases show opposite influence on the sensor resistance changes. In the cases both of these gases were of interest, they had a compensating effect on the sensor response. To detect the signals for each gas the sensor should be operated in a sinusoidal modulation of temperature or a charcoal filter should be used to eliminate the interference. In the same report they mentioned that the calorimetric and resistive measurements indicated a decrease in the temperature of the sensor was often associated with gases like CO, which were detected by their catalytic combustion.

Sciliano [7] conducted his experiments on SnO₂ sensitive layers with CO and reported that there was no appreciable response at temperatures lower than 100 °C. Also the response and recovery times depending on the sensor

temperature were both slow at low temperatures and faster at high temperatures. Sciliano also suggested that the Pd doped samples present an optimum detection temperature of about 200-250°C.

Licznanski *et al.* [47] studied the filterization effect of SnO₂/Rh layer for CH₄ detection in dry air. CH₄ injection experiments conducted at different temperatures such as 400, 500 and 600°C, and concluded that on the upper and lower layers of the multilayer tin dioxide sensors the best responses to methane achieved at 500°C.

2.6.2. EFFECT OF ADDITIVES

Oxygen ions cannot be chemisorbed on undoped stoichiometric n-type semiconducting oxides. For them to be adsorbed, their negative charge must be compensated by ionized bulk donors in a space charge layer [17]. The foreign metal atoms on SnO₂ serve as adsorption sites with an ionic bond strength depending on their electronegativity. Therefore, in order to enhance the sensing properties of the tin dioxide material, introduction of noble metal additives is usually performed. The dopant, not only act as a catalyst, but also modifies the electrical transport properties of the sensor by introducing new states in the band structure of the active materials and, the surface morphology of the material and the size of the crystalline grains [7]. The most important effects of noble metal addition are the increase of the maximum sensitivity, rate of response and lowering the operating temperature of the sensor [48]. A great number of additives have been studied being Pd [6,27,48,49,50,51], Pt [7,22,27,41,48,51] and Au [35,39,41] the most used.

In any case, the contact of the additive with the semiconducting oxide creates a barrier that is fully characterised by the electron affinity of the semiconductor, the work function of the metal and the density of surface states of the semiconductor that are located inside the energy band gap. This contribution creates a Schottky barrier through the formation of a depletion region in the semiconductor surface in contact with the cluster [45]. As a result the surface states created by the presence of the additives can shift the Fermi

level of the semiconductor to that of additive. Addition of alkali metal oxide creates an electron density on the semiconductor surface. Therefore, as Yang *et al.* [48] reported, the CO and C₃H₆ gas oxidation is significantly improved by effectively suppressing the self-inhibition of CO and C₃H₆.

Beside the noble metal addition, also many other studies have been focused on the capacity of dopants in the SnO₂ layer; the carbon nanotube promotion is also effective [9], as nanotubes exhibit very good adsorption properties and have a large specific area. It is also reported that carbon nanotubes alters the electrical properties enabling operating at room temperature on tin dioxide semiconductor oxides.

Mulla *et al.* [30] investigated the electrical response of ruthenium incorporated tin oxide thin films as a mean to improve the sensitivity and selectivity towards hydrocarbons. They recorded that 0.17 wt. % of ruthenium in tin oxide exhibited the highest sensitivity towards hydrocarbons at approximately 300°C.

Delgado [45] in his Ph.D. thesis explained that in general, under noble metal loading cluster forming at the surface of SnO₂ was expected, such as those obtained in the case of Pt and in the case of Pd. Depending on the deposited noble metal and loading of the interacting gas, these clusters would be in metallic or oxidised forms.

Sciliano [7] reported that doping sometimes increased the sensitivity of the sensors and reduced the temperature corresponding the best sensitivity. For example, for Pd-doped sensors, this effect was more pronounced for CO detection. He suggested this was because PdO trapped CO molecules causing to diffuse them inward and react with SnO₂, CO molecules might also diffuse to other PdO and react with each other.

2.6.3. EFFECT OF HUMIDITY

The presence of water strongly influences the sensing properties of SnO₂ based gas sensors. The influence of water vapor in the detection of CO may be evaluated by monitoring the changes in the electronic affinity

associated with CO exposure at different water vapor concentrations or, the changes in the catalytic conversion of CO to CO₂, associated with changes of water vapor concentrations, as reported in the study by Barsan and Göpel [12]. These results show that for Pd doped nanocrystalline layers an initial exposure to CO of 10 ppm in a humid air background causes changes in both the electronic affinity and the surface energetic barrier. And when the CO concentration further increased, just changes in the surface electronic barrier are recorded. And when the dry air is background, there are no changes in the electronic affinity associated with CO exposure. The results show that the sensing mechanism for CO also involves hydroxyl groups at the surface of the SnO₂ layer.

In the study of CO oxidation on Au/TiO₂, by Date [52], it was demonstrated that the amount of moisture adsorbed on the catalyst determines the activity, and there is an optimum concentration of moisture, where the CO oxidation shows a maxima. But when the concentration of moisture is further increased, the catalytic activity is depressed probably due to blocking of the active sites.

Barsan and Göpel also mentioned about the possibility of rooted OH groups could become donors, because such a mechanism could have explained the increase in conductance associated with water vapor adsorption as well as the interaction of CO with hydroxyl groups.

At temperatures between 100 - 500 °C the interaction with water vapor leads to molecular water and hydroxyl groups, but above 200°C molecular water is no longer present at the surface. These hydroxyl groups are formed due to an acid / base reaction with the OH⁻ sharing its electronic pair with the Lewis acid site (Sn) and leaving the weakly bonded proton, H⁺, ready for reactions with lattice or adsorbed oxygen [12]. And as the IR studies show, OH groups are bonded to the Sn atoms.

However a complete knowledge of the surface chemistry involved in CO detection is still not enough for the complete understanding about the

dependence of sensor resistance on the CO partial pressure at various water concentrations.

2.6.4. EFFECT OF FILM THICKNESS

The target gas can react with the adsorbed oxygen at the inner grain boundaries. Therefore the reaction-diffusion mechanism can be considered to explain the thickness influence of tin dioxide film in CO sensing mechanism. The thickness dependent response indicates that the reaction mechanism is dominated by diffusion as reported by Mandayo *et al.* [53]. Diffusion dominated mechanism means the diffusion is slower than the reaction and would explain the response increase as thickness decreases observed in the thickness range of 200-700 nm. On the contrary, in the case of the films with a thickness less than 200 nm., the resistance responses shows just the reverse behavior with the decreasing thickness. The decrease of response for the thinnest films could be produced by the lack of reaction sites when the thickness is comparable with the grain size. Mandayo determined the optimum film thickness as 200 nm. with the highest electrical response against CO.

In the study by Sakai *et al.* [54], it is concluded that the film morphology was depended on the film thickness. Looking at the films prepared, they reported the 100 nm. thick films had very few cracks with a very flat morphology. As the thickness of the films increased to a range between 300-1000 nm., the number and the length of the cracks were also increased (Fig. 2.17).

Sakai *et al.* [54] studied on tin dioxide layer thicknesses and reported an unusual result. They studied in the 100-300 nm thickness range and suggested the sensor response to H₂ decreased with an increasing film thickness. On the other hand, the sensor response to CO was found to be almost independent of the film thickness. This result indicates the gas response change; depending on film thickness shows variations with the types of gases. They thought this independency from the film thickness in the case of CO was because the film morphology of the films was all the same.

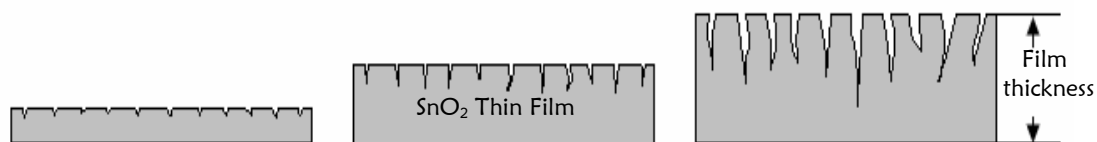


Figure 2.16. Model for the influence of film thickness on morphology

Also the SnO_2 concentration in the sol is a factor influencing the film thickness and the morphology of the coatings. In the same study [54], when the SnO_2 concentration was increased, the morphology tended to become rougher. It was suggested this change in the structure resulted because of the agglomerating state of colloidal particles of the sol suspension.

2.6.5. EFFECT OF FILM MORPHOLOGY

The degree of crystallization, grain size, and surface structure will determine the characteristics and the performance of the solid state gas sensors. The reduced size of crystallites means the increasement in the surface area. The gas sensing reactions are known to be surface sensitive and an increased surface area means more of the sensor surface is exposed to gas for reaction, thereby increasing the probability of reaction and the sensitivity. In the report prepared by Barsan and Göpel [12], it is declared that in the preparation of gas sensing layers aging and preconditioning steps are very important to obtain a stable sensor response signal and avoid drifts during the first use of the sensors. The main reasons for the need to precondition result are to obtain definite grain sizes and a definite conductivity by a definite concentration of intrinsic defects such as oxygen vacancies in the SnO_2 layer.

Gulati et al. [55] modelled the electrical behavior of the SnO_2 bulk sensors and concluded that the sensitivity depended on both on the ratio of the particle size and to the depletion width, not independent either one of them.

When the sensor surface is considered as a one dimensional chain of SnO_2 crystalites which are connected by a predominant number of necks and a small number of grain boundary contacts; for the case mean crystallite size much more larger than thickness of the depletion region ($D \gg 2L$), the electron conducting channels through necks are too wide to be influenced by the surface effect. The grain boundry contacts share most of the electrical resistance of the chain and so they govern the gas sensitivity. And when D decreases to a closer degree to $2L$, the necks become the most resistive part in the chain as a result they control the gas sensitivity. Both in the grain boundry and neck control models, a region existance is assumed in the grains in which the carrier concentration is constant and remains unaffected by any change in the charge carrier concentration in the boundry layer at the edge of the films. And it is also assumed that the resistance in the grain bulk is less than the resistance at the necks or in the grain boundries. For the case $D < 2L$, ultrafine particle control, each constituent grain is depleted of conduction electrons as a whole and grains share most of the resistance of the chain, so they control the gas sensitivity. This means a simultaneous change in carrier density throughout the entire grain when a change in the reducing gas concentration occurs [18]. In this region the sensitivity is strongly dependent on D , probably because the electron concentrations in air and in a gas inside the depletion layer depend on the distance to the surface. And the relative increase in the concentration increases with the decreasing distance to the surface. As a result the gas sensitivity increases as the thickness of the gas sensitive layer decreases. According to this explanation done by Yamazoe [10], usage of ultrafine particles of SnO_2 cause to achieve the grain control state which gives very high sensitivity.

In the case of compact layers, the interaction with gases only takes place on the geometric surface of the semiconductor and depending on the thickness/debye length ratio the layer can be partially or completely depleted. In the partially depleted layers, surface reactions do not influence the conduction in the entire layer, conduction process occurs in the bulk region.

As a result two types of resistances occur, one is surface reaction originated and the other is not. The other resistance occurs in parallel to the surface, indicating a limited sensitivity. For the completely depleted layer case, the layers can become partly depleted as a result of the reducing gas exposure. Because, reducing gas injects additional electrons to the conduction band. Also the oxidizing gas exposure can change the layers from completely depleted form to partly depleted form.

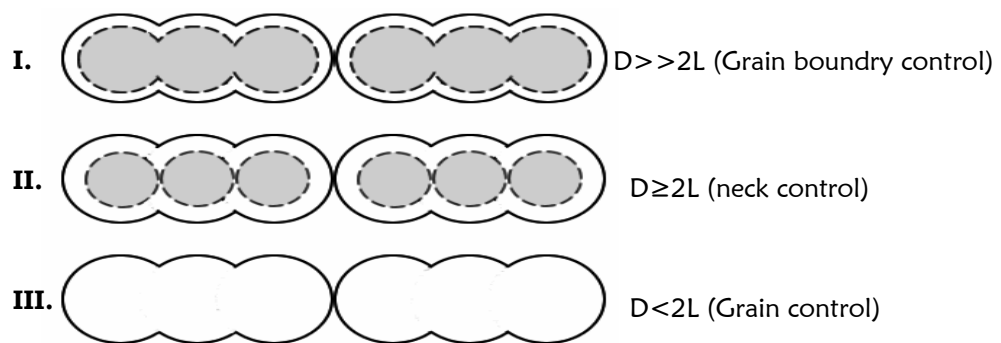


Figure 2.17. Schematic models for the grain size effects

In the porous layers volume of the layer is also accessible for the gases to penetrate into the sensing material. In this case, the active surface is much higher than the geometric surface area. And the situation in porous layers is more complicated because of the presence of necks between the grains.

The switching case from partly depleted to completely depleted layers in the presence of reducing gas is again valid for the porous layers. When the mean free path becomes comparable with the dimensions of grains, in the case of small grains and narrow necks, the surface influence of mobility should also be considered. The reason for this consideration is that the number of collisions by the free charge carriers in the bulk of the grain becomes comparable with the number of surface collisions.

It was determined by Blaustein *et al.* [56] that the resistance of the samples was modified by the grain size and the width of depletion layer. For example in samples with grain size larger than $0.1 \mu\text{m}$ and steep barriers, the oxygen diffusion into the pellet first produced a fast and then a slow increase of resistivity. That could be explained by considering that oxygen rapidly adsorbed at the grain surfaces and slowly diffused into the bulk. Therefore, Schottky barriers became rapidly higher and slowly wider. And since the barriers did not overlap, the resistivity increased monotonically. In samples with a grain size less or equal to $0.1 \mu\text{m}$ the oxygen diffusion into the pellet produced a fast increase and then a slow decrease of resistivity. When the oxygen made contact with the material, an increase in the resistance occurred as a consequence of the large barrier height. Then a few seconds later the oxygen vacancies concentration was reduced by oxygen indiffusion and that gave rise to a decrease in resistance. They explained this different behaviour with the overlapping of depletion layers, implying a different conduction mechanism.

Manorama *et al.* [57] investigated an obvious reduction in the particle size by using sol-gel synthesis method than hydrolysis method. The ultimate particle size of the aggregates was about $1\text{-}2 \mu\text{m}$ when the material was prepared by using hydrolysis method, and about $0.2 \mu\text{m}$ in the sol-gel prepared material. Also the responses of the sol-gel prepared sensors were much faster compared to the ones prepared by hydrolysis method. They concluded that the sol-gel technique was available for a crystallite size in range of nanometers. Barsan and Göpel [12] reported that $0.2 \text{ wt. } \%$ doped SnO_2 films showed the best responses to 50 ppm CO at a particle size of around 15 nm . Choi and Lee [14] investigated the K, Ca and Mg impregnated SnO_2 sensors and concluded that the sensitivity had increased corresponding to reverse order of crystallite sizes. They also reported that the crystallite size became coarser upon heat treatment, such as calcination or sintering. And they commended on the Ti doped SnO_2 sensor study giving the lowest

sensitivity by the sensor produced with finer grain size conducted by Lee [58] as; insufficient adhesion between constituent particles.

Korotcenkov et al. [6] investigated the influence of bulk Pd doping on gas sensing characteristics of SnO₂ films, and explained the reason why they found it difficult to separate the Pd effect of chemical influence on gas detecting. That is, the doping results in changes of film morphology, and decreases both the crystallite sizes, and the concentration of free charge carriers.

2.6.6. EFFECT OF ELECTRODES

Electrodes control the transfer of conduction of charge carriers to the external circuit to produce a proper signal. The contact with the electrodes forms a metal-semiconductor junction that influences the overall conduction process. With the different metals used as electrodes the Schottky barrier in the metal-semiconductor interface, the overall activation energy and the conductance of the sensor changes. Then the chemical reactions between the atmosphere and metal-semiconductor interface would effect strongly to the overall conductivity of the sensor.

In order to get more information about the electrode effects, the gap between the two electrodes should be narrow. Therefore the number of energy barriers at the grain contacts between electrodes is reduced and there are only a few SnO₂ grains will fit in the gap. And hence in the electrode-semiconductor interfaces would have a greater significance in the sensor response. Saukko et al. [15] studied with Au and Pt electrodes, which are also utilized as catalyst activators in the gas detection, with a gap of 5 μm. Their experiments conducted at several concentrations of CO showed that the Pt electrodes are more sensitive at lower temperatures like 230 °C and Au electrodes at high temperatures like 475°C. And the samples with Au electrodes show a linear increase in the response, on the other hand samples with Pt electrodes shows a non-linear response increase with the increasing

CO concentration. So they concluded that utilizing different electrode materials, it was possible to modify the sensing properties of the gas sensors.

For compact structured layers they appear as contact resistance in series with the tin dioxide layer resistance. For partly depleted layers this contact resistance can be dominant and the reactions occurring at the three face boundary (electrode / tin dioxide / atmosphere) control the sensing properties [12]. For the porous layers the electrode contact resistance is minimized because of the thousands of resistances with comparable values connected in series.

In the case of thick tin dioxide films the electrode resistance was not apparent when compared to noises in the CO and NO₂ Transmission Line Measurement experiments. Though in the case of thin films the existence of electrode resistance was quite clear [12]. As Choi and Lee [14] reported, the location of electrodes influenced the gas sensitivity because of difficult penetration of gas into the small pores in sintered SnO₂ film.

In the status report of Barsan and Göpel [12], it has been declared that the Pt electrodes enhanced the CO sensitivity of SnO₂ based sensors. The reasons for this effect is suggested as, catalysis at the three phase boundary the doping of the near electrode region of SnO₂ by diffusion, contamination related to the additives used for the screen printing of the electrodes or the appearance of an intermediate layer between electrodes and SnO₂. They reported that some other studies also include the drastic influence of different electrode geometries and layer characteristics, which lead to different current paths characteristic for different thicknesses of the sensing layer, contact effects and the electrode - SnO₂ interface.

Still the electrode influence on the sensing mechanism of semiconductor gas sensors is not clear. However, an optimum electrode material modifying the electrode geometry and sensor construction can enhance the sensing properties of the sensors.

2.7. EFFECT OF ALKALI METAL PROMOTION

Alkali metal compounds are usually employed as promoters of metal catalysts [59] or crystallite growth stabilizers of SnO₂ particles [14]. They are electropositive promoters acting as electron donors and therefore enhancing the chemisorption of electron acceptor adsorbates [59]. In the case of alkali promotion over transition metal surfaces, the adsorption of diatomic molecules and their dissociation probabilities increase [60].

Lambert *et al.* [61] investigated the effects of alkali promoter Na on dispersed Cu metal catalysts. As the result of the experiments in NO and CO containing atmospheres, it is reported that Na spilled over onto the surface of the metal catalyst and strongly altered its properties by changing the catalyst work function, adsorption enthalpies of adsorbed species and the activation energies of reactions involving these species. Electrochemical promotion of Na resulted in serious improvements in selectivity for NO, from 20 to 80%, accompanied by a drastic rate enhancement of an order of magnitude.

Choi *et al.* [14] investigated the effect of K, Ca and Mg promotion on the SnO₂ thick films and reported that the sensitivity of the films was increased in the order of Mg, pure, K and Ca tin dioxide films. This order is corresponding to the reverse of the particle size order of metal-tin dioxide powders.

Previous studies showed that even at 50°C the Na promoted SnO₂ thick films exhibited electrical response to methane. This is resulted from the reduction of activation energy caused by the alkali metal promotion. Sodium promotion also reduced the saturation at the surface and therefore enhanced the desorption rate of the reaction products from the surface [28].

As Karakas reported [73], alkali metal promotion increases the electron density on the transition metal, as a result; increases the strength of the surface. On the other side, has a weakening effect on the C-O bond and therefore causes an easier CO dissociation.

The objective of this study is to investigate the effect of sensor temperature, the effect of additives in the sensor material and the effect of limited oxygen concentration in the medium in detecting carbon monoxide with SnO₂ based gas sensors. More specifically, to investigate the applicability of Na-promotion to Pd/SnO₂ multilayer thin films to improve CO selectivity was studied at different temperatures and in different ambient atmospheres. This study is also in parallel to the early study by Severcan [28], which takes methane as the reducing gas for the investigation of tin oxide based thick films' dynamic resistivity behavior under step change in concentration between 50 – 200 °C.

CHAPTER 3

EXPERIMENTAL PROCEDURE

Metal promoted tin oxide films on glass substrates show good responses to reducing gases, if the coating applied on the surface is obtained carefully and the films are deposited in appropriate conditions to achieve a reasonable morphology and thickness. In order to get satisfactory results, every step should be conducted carefully starting from the choice of materials to the final installation into the reaction chamber. In this study, two types of sensors; palladium (Pd) over tin dioxide (SnO_2) and sodium (Na) promoted Pd over SnO_2 , were produced to examine with carbon monoxide. The catalysts were prepared using the sol-gel technique and the films were produced by spin coating method. The gas sensing tests were performed mainly at 150, 175 and 200°C.

3.1. MATERIAL SELECTION

The precursors used in the sol-gel catalyst synthesis were:

SnO_2 precursor: $\text{SnCl}_4 \cdot 5\text{H}_2\text{O}$ [Tin (IV) chloride pentahydrate, 98+%]
(Acros Organics)

- Pd precursor: CH_3CO_2 [Palladium (II) Acetate] (Aldrich Chemical Co.)
- Na precursor: NaCl [Sodium Chloride 99.5%] (Merck) and for the hydrolysis step DI water and $i\text{-C}_3\text{H}_8\text{O}$ [isopropanol, 99.5%] (Riedel de-Haen) were used.

The supplies used in the preparation of the substrates ready for the measurements:

- Highly conductive silver colloid [SPI Supplies, Kwick Stick]
- Silver paste [Spi Supplies 1050621]
- Silver electrodes [50 gauge, 0.7 mm.]

The analyze gases used during the testing were:

- He [Helium, 99.99%] (Air Products and Chemicals Inc.)
- CO [Carbon monoxide, 1%CO, balance He] (Air Products and Chemicals Inc.)
- O₂ [Oxygen 5%O₂ , balance He] (Air Products and Chemicals Inc.)

3.2. CATALYST SYNTHESIS BY THE SOL-GEL METHOD

There is a wide range of techniques for the film preparation of tin dioxide such as spray prolysis [6, 63], chemical vapor deposition [19], thermal evaporation [64], sputtering [6, 16], screen printing [65] and the sol-gel process [57]. Thermal evaporation and sputtering generally produce compact films which reduces sensitivity [18]. The synthesis method of sol-gel is the most common technique due to the advantages of low processing temperatues and possibility of tailoring the starting solutions, resulting better compositions and better control of the final structure [66]. Also the dopants can be incorporated in the sol gel before deposition which has resulted in high quality films with a more homogeneous distribution of dopant material within the film structure [18].

Two different approaches are generally employed in the sol-gel synthesis of SnO₂. One of these approaches consists in the hydrolysis of a tin alkoxide with low H₂O/Sn ratio to avoid precipitation of the sol. This procedure has the advantage of minimising the impurities in the final material, but the high cost of he precursors and the low time stability of the sols against the incerase in viscosity makes this approach inconvenient. For this reason,the sol-gel preparation of SnO₂ is more commonly achieved through the hydrolysis of inexpensive precursors such as SnCl₂ or SnCl₄ [7].

Both SnO₂ based catalysts are synthesized according to the molar ratios for 5 gr. of product. In tin dioxide sol-gel preparation, 11.64 g SnCl₄.5H₂O is dissolved in 13.95 g of isopropyl alcohol and 3.21 g of water and 9.42 g of isopropyl alcohol mixture is added drop by drop to the first solution for the hydrolysis reaction [66]. During this process SnCl_x.(OC₃H₇)_y molecules are formed in the sol, depending the extend of the hydrolsis reaction [62]. For the 1% wt. Palladium (Pd) over tin dioxide (SnO₂) catalyst synthesis 0.0925 g of palladium acatate and for the 0.1% wt. Sodium (Na) promoted Pd over SnO₂ catalyst synthesis 0.0915 g of palladium acatate and 0.013 g of sodium chloride is added to the sol (See Appendix A for the catalyst preparation calculations). Then the sol is stirred on a magnetic stirrer (Velp Scientifica) over night under closed conditions before applied on the substrates.

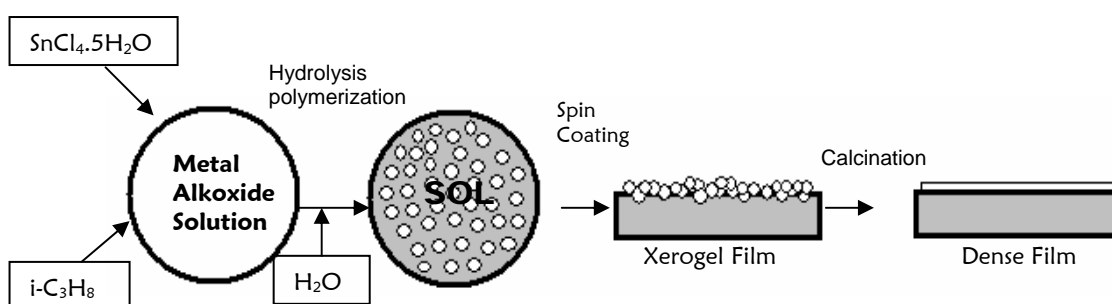


Figure 3.1. Flow diagram of tin oxide film preparation

3.3. SUBSTRATE PREPARATION

For the coating process, in order the sol not to spil, the surface of the substrates must be porous with a higher surface tension. Therefore, the soda-lime glass substrates are etched in 10 M sodium hydroxide (NaOH) solution at room temperature over night in order to get the sol stuck onto the surface and have a stable coating base. After etching, the substrates are cleaned with

detergent and water and rinsed with distilled water. Before coating, substrates were cleaned again in an ethyl alcohol bath. Dry substrates were ready for attaching to the spin coater.

3.4. COATING PROCESS

The methods of application of the film can be dipping [28], spinning [9,51,67], spraying [6,63] or even painting [68]. Deposition conditions play an important role with respect to the final film characteristics [69]. In order to overcome the difficulties of CO detection, thin film technology is one of the potential ways [53]. Spraying and spin coating methods have the advantage that only small amounts of liquids are needed to coat large surface areas [69]. As well as the coating parameters, solution viscosity and the chemical additives in the solution are of great importance for the film thickness and morphology. There for a brief elaboration on coating process is needed [67].

For the film formation, the solution must;

- wet the substrate
- remain stable with aging
- have some tendency toward crystallization into a stable high temperature phase
- heat treated to get insoluble before subsequent deposition for the multiple layers

Spin coating is an inherent batch process to produce thin films on a rigid flat surface or slightly curved substrate. The substrates used for this process is limited to a smaller size that can be held down steadily for spinning at high rotational speeds, ie. 1000-4000 rpm [70].

Spin coating can be divided into four stages; deposition, spin up, spin off, and evaporation. The first three stages are sequential, while the fourth normally proceeds throughout the coating process [70].

In the first stage an excess amount of liquid is delivered to the substrate at rest or spinning slowly. In the 2nd stage the liquid flows radically outward,

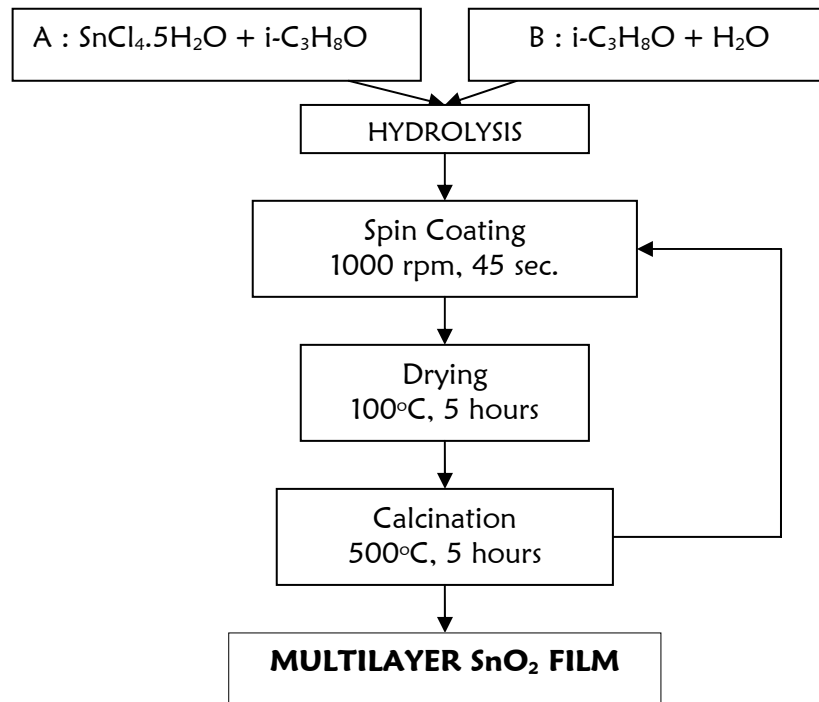


Figure 3.2. Flow Diagramm for the chemical solution deposition of the multilayer thin films

driven by the centrifugal force generated by the rotating substrate. This stage generally occupies the time it takes the substrate is being spun to reach a maximum speed of thousands revolutions per minute (1000-4000 rpm). In the third stage, excess fluid in the liquid film covering the substrate flows radially to the perimeter, accumulating there temporarily in unwanted swelling from which droplets form and fly off. As the film thins flow of the remaining liquid slows. The fourth stage is further thinning of the film by evaporation. Evaporation generally continues after spin off has totally halted by solidification brought out by the concentrating of non volatile solutes and particulates. Final film thickness is found to be minimally affected by deposition and spin up. The key spin coating is the spin off stage. Apart from the edge effect, similar to the dip coating process, a film of liquid tends to become uniform in thickness as it thins by spin off and remain so as it thins

further, provided its viscosity is intensive to shear and does not vary over the substrate. Film uniformity is the result of two counteracting forces: the rotation induced centrifugal force, which drives radially outward flow, and the resisting viscous force, which acts radially inward.

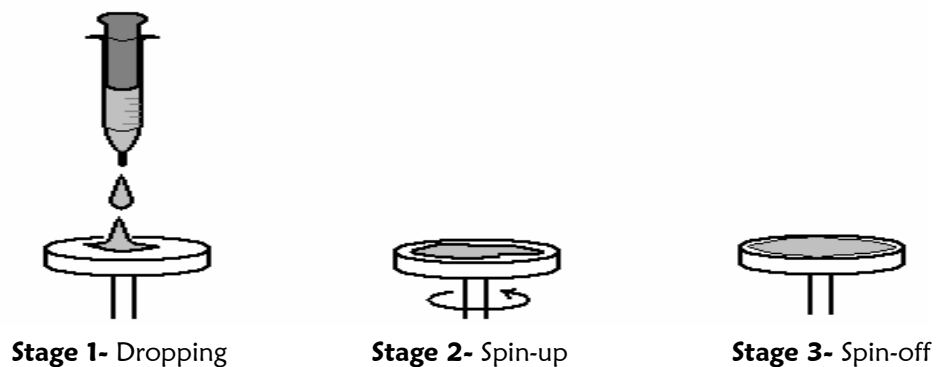


Figure 3.3. Schematic diagram of spin coating process

The thickness of a spin coating is the result of the delicate transition by which evaporation takes over from spin off. Nonvolatile constituents can leave the substrate solely by flow. Whatever quantities of them are left when the film becomes so thin and viscous that flow halts, must remain as the coating after all the volatile species have evaporated [71].

An advantage of spin coating is that the film of liquid tends to become uniform in thickness during spin-off and tends to remain uniform provided that the viscosity does not vary over the substrate. This tendency arises due to the balance between two main forces: centrifugal force, which drives flow radially outward and viscous force (friction), which acts radially inward. During spin-up, centrifugal force overwhelms the force of gravity, and rapid thinning quickly squelches all inertial forces other than centrifugal force [71].

Disadvantages of this technique are that it is less economical than dipping because the excess solution is lost during deposition and it is not a continuous process. It is suitable for coating small discs and lenses [67].

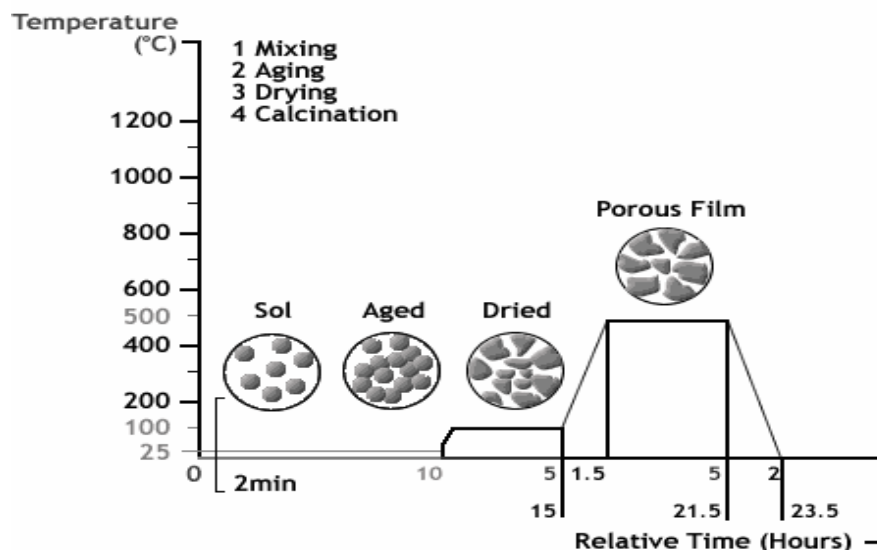


Figure 3.4. Process time vs. process temperature graph

In the current study a home made computerised spin coater was used in the spin coating process. The software was designed to regulate the acceleration, the spin frequency and the spin duration of the coater. For this particular experiment the frequency was set to 800 rpm and the total spin duration was set to 45 seconds. The substrates were attached via a double sided tape on to the spinner.

3.5. DRYING

After the coating of each layer on the substrates the sol-gel system is by no means stagnant. Firstly, the water and the volatiles in the solution must be removed by the drying process and the network shrinks as the further condensation occurs [28, 67]. Ordinary drying is performed in a furnace at a temperature ranging between 100 – 200 °C. In the current study, drying of the substrates was performed in a furnace at 100 °C for 5 hours. During the drying process, the physico-mechanical and the physico-chemical transformations occur in the gel structure [28].

3.6. CALCINATION

Calcination turns the precursor films into ceramic films with the removal of organics in the coatings. The coatings are heat treated at higher temperatures (350-750 °C) than the previously specified drying temperature. Delabie et. al. [17] reported that the non-calcined films show a smaller degree of transformation of CO to CO₂ than the calcined films. In this study the calcination was performed by a maximum central furnace temperature of 500 °C in air medium. In each calcination process the same profile was applied; temperature increase from room temperature to 500°C was realised in 90 min. and for the samples were cooled down from 500°C to 100°C at the same rate. During the 5-hour-lasting calcination procedure, various physico-chemical transformations occur such as creation of a macroporous structure causing from the volatilization of solvents, thermal synthesis reactions with elimination of volatile compounds followed by modification of the structure through sintering [28]. The calcination process affects cracking, the grain size, crystal structure, surface roughness and transparency of the films [67]. Therefore, the larger pores are formed during the calcination process.

3.7 ANALYSIS OF THE FILMS

Film morphology and composition analysis of the films were investigated by Jeol JSM-6400 Scanning Electron Microscopy (SEM) equipped with an Energy Dispersive Spectrometer (EDX). During SEM studies film thicknesses and film surfaces were investigated. SEM samples were coated by 250°A thick Au film using SCD 050 sputter coater. EDX analyses were carried out at selected areas and maps of some samples were obtained. Also, X-ray diffraction patterns were scanned for calcined Pd/SnO₂ and Na-Pd/SnO₂ using Nickel filtered CuK α radiation.

3.8 SENSOR PREPARATION

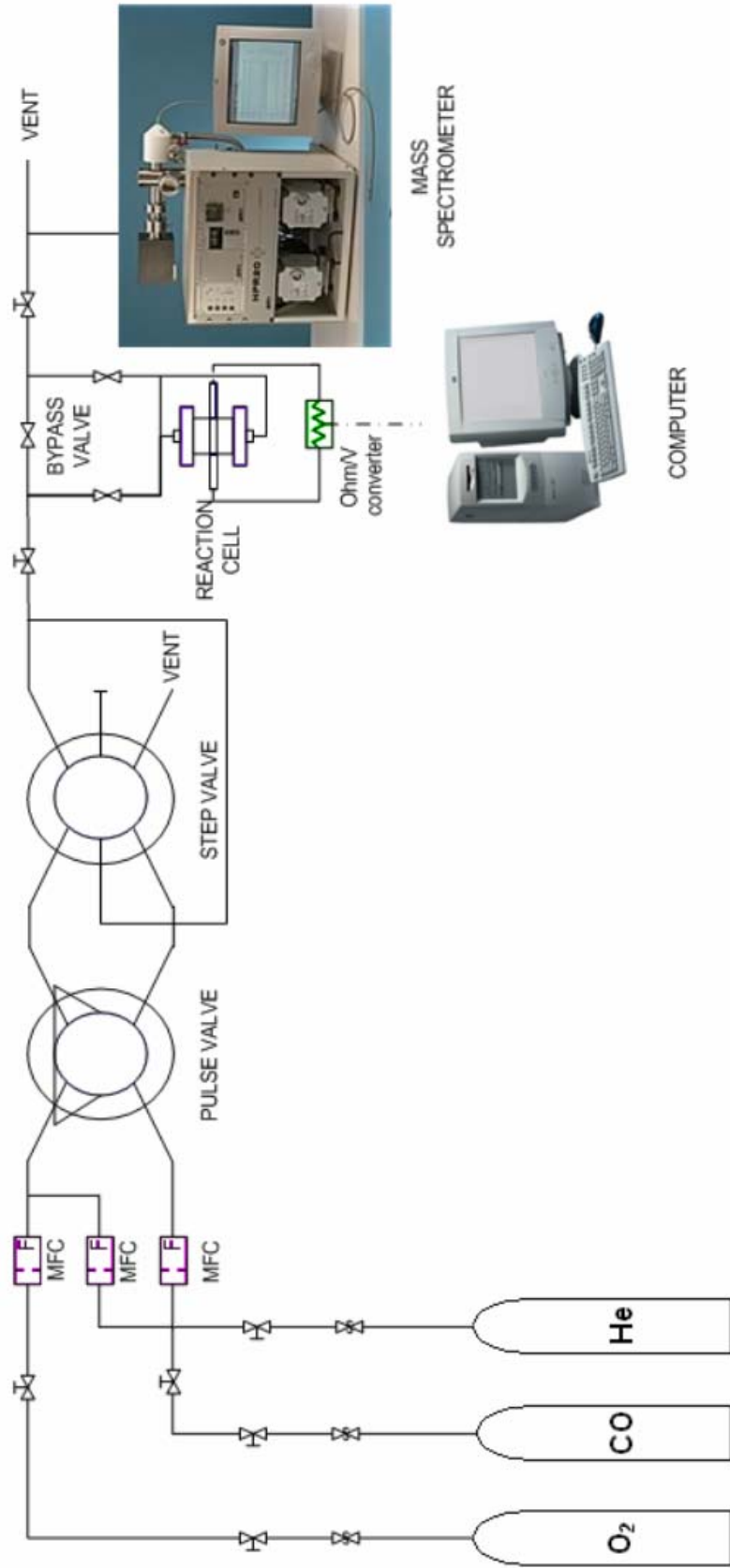
For the gas analysis, the electrodes must be attached onto the surface on the opposite sides, to collect the resistance change in the gap between the two specified points. A highly conductive pure silver colloid (Silver Kwick Stick – Spi Supplies 5008 - AB) was applied on the surface to the opposite edges where the electrodes would be in contact. The silver colloid applied gains conductivity during waiting over night at room temperature. After this 0.7 mm. (OD) silver electrodes with a length of 15 cm. and an electrode spacing of 4 mm. were attached on glass substrates by an electrically conducting silver paste (Spi Supplies 1050621), which has to be calcined at 200 °C for 30 minutes in a furnace. Then the test sensor was installed into the glass reaction chamber and connected to the computerized digital multimeter via signal wires.

3.9. EXPERIMENTAL SETUP

Gas detection apparatus, comprised primarily of gas suppliers, mass flow controllers, valves, heaters, reaction chamber, temperature controller, computerized digital multimeter and mass spectrometer as can be seen in Figure 3.5. The experimental setup can be generalized in 4 main units as; Feed Unit, Injection valves, Reaction Chamber, and Data Acquisition Unit, respectively.

3.9.1. FEED UNIT

Feed unit is comprised of 99.5% He, 1% CO + 99% He mixture, 5% O₂ + 95% He mixture, dry air, 99.5% CH₄ gas cylinders (supplied by Air Products and Oksan Ltd. Şti.) and 3 flow controllers. 99.5% He, 5% O₂ + 95% He mixture and dry air are used as carrier gases. To establish the desired flow rates, each gas was directed into 3 mass flow controllers (Aalborg GFC 17). Each gas is fed through their own mass flow controller, except the O₂ +



3.5. Experimental Setup

He gas mixture entering as the carrier gas with dilution. The calibrations of the mass flow controllers had been done by a soap bubble meter before the gas fed to the reaction chamber (See Appendix B for calibration curves). All the gas lines were constructed via 1/8" stainless seamless tubing and stainless steel connections and fittings.

3.9.2. INJECTION VALVES

There are two six-port valves (VICI Valco Instruments Co. Inc.) and a by-pass line for directing the gas flow either to the reaction chamber or to vent. One of the six port valves is operating for impulse input and the other one is for the step input to the reaction chamber. There is a 5 ml. sampling loop connected to the injection valve.

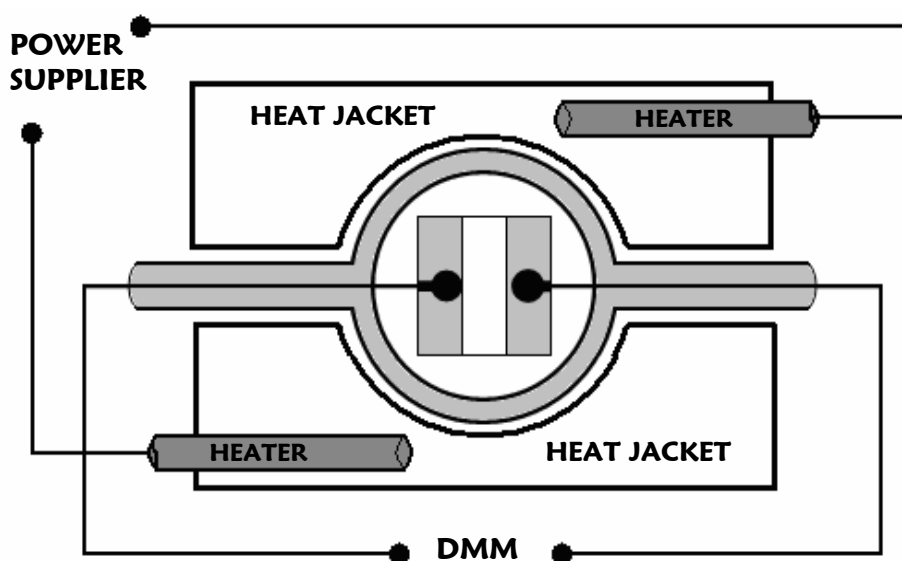


Figure 3.6. General presentation of reaction chamber

3.9.3. REACTION CHAMBER

Reaction chamber is a Pyrex glass reaction cell, which has a 4 mm. wall thickness with a diameter of 2.1 cm. and a height of about 2.4 cm which is

designed to work at atmospheric conditions. In the cell the substrate was attached to two 0.7 mm. (OD) silver electrodes from the opposite edges.

Inside the cell, just on the top but not in contact with the substrate, there is a K type thermocouple located to continuously monitor the temperature inside the cell.

3.9.4. DATA ACQUISITION UNIT

In the data acquisition unit, there is a mass spectrometer, capable of scanning up to 200 amu (HPR20 Hiden Analytical Ltd., England), to which the gas mixture leaving the reaction cell is fed and a computerised digital multimeter (DMM), connected to the test sensor.

3.10. EXPERIMENTAL PROCEDURE

In the current study, CO injection experiments were performed on two different tin oxide based test sensors, namely 1 wt.% Pd promoted and 0.1 wt.% Na- 1 % PdO SnO₂ multilayer thin films, to find out the effect of ;

- Promoting metal in the SnO₂ support,
- Temperature and
- The oxygen concentration of the atmosphere

The calcined films were tested at several temperatures respectively 150, 175 and 200 °C, in oxygen free and 1% oxygen containing dry conditions. During the experiments the volumetric flow of the carrier gas was kept constant at 40 ml/min. and the pulses were introduced to the reaction cell by means of a 5 ml sampling loop containing 1 % CO in Helium.

After heating to the desired temperature, each test sensor was exposed to a constant carrier gas flow for 4 hours before conducting the experiments. This process was allowed for desorption of pollutant chemical compounds on the sensitive layer and the film resistance to reach a constant value. The electrical response of the test sensor was obtained by monitoring the resistance changes. And the concentration changes in the reaction cell exit gas were

detected by a mass spectrometer. CO pulses were injected until the quantity of the exit CO pulse reached a steady value. Injections were repeated every 10 minutes, for 10 times in average; 8 of which were sent to the reaction chamber and 2 passing through the by-pass line directly to the mass spectrometer for checking the injection concentration. The same procedure was applied to each sensor for the resistivity response tests.

3.10.1. TEMPERATURE EFFECT ON THE GAS SENSING RESPONSES

In the current study first the effect of operating temperature on sensing properties of 1 wt.% Pd promoted and 0.1 wt.% Na- 1 % PdO SnO₂ test sensors was examined. The experiments conducted at 150, 175 and 200°C where the sample temperature was controlled with $\pm 1^\circ\text{C}$ accuracy.

3.10.2. EFFECT OF OXYGEN ON THE GAS SENSING RESPONSES

Because in the combustion and sensing reactions oxygen concentration is a limiting factor during testing He, 1% O₂ in He and dry air were used as carrier gases. Each test sensor was exposed to carrier gas flush for 4 hours before the first CO injection. The tests were performed at 150, 175 and 100 °C in oxygen free and 1% oxygen containing atmospheres. And the dry air experiments were conducted only at 200 °C.

CHAPTER 4

RESULTS AND DISCUSSION

In the present study, SnO₂ based 1 wt. % Pd promoted and 0.1wt. % Na with 1wt. % Pd promoted multilayer thin films on glass substrates were exposed to carbon monoxide. The semiconductive films on glass substrates were formed by Chemical Solution Deposition (CSD). The CSD technique has been chosen because of its convenience and inexpensiveness, thus the feasibility for various applications.

Simultaneous measurements were recorded for the change in resistance of the films by a computerized digital multimeter and the change in the gas concentration by a mass spectrometer. Scanning Electron Microscopy (SEM) and Energy Dispersive Spectrometer (EDX) analyses were used for structure and composition investigations of the SnO₂ based semiconductive films.

The tests were performed at selected temperatures in different oxygen containing atmospheres. The experiments were performed to find out;

- The effect of temperature increase on the responses
- The effect of doping on the responses, and
- The effect of oxygen content in the atmosphere.

4.1. FILM CHARACTERIZATION

In this study, two different SnO₂ based semiconductive catalysts were deposited on soda-lime glass substrates. The morphology and the composition of the 1 wt. % Pd promoted and 0.1 wt. % Na - 1% Pd promoted SnO₂ films

were investigated by Jeol, JSM-6400 Scanning Electron Microscope (SEM) equipped with Noran series II, Energy Dispersive Spectrometer (EDX), and X-ray diffractometer, respectively.

4.1.1. SEM ANALYSIS

As SEM image can show only a small portion of the film at a time, it needs to be confirmed that the region shown in the image is representative of the whole film. If the film is known to vary in crack density or thickness over the surface, more different regions of the film need to be examined to have a valid idea of the film characteristics. In the current study, SEM examinations were performed viewing many regions of the film, then characteristic regions were photographed on each coated sample. As the spin coating yields very little variation in film morphology across the surface most images show representative film features.

The microstructure of the sensing surface directly influences the sensitivity of a sensor. The surface area to volume ratio and the pore size of the film affect the sensor performance [9]. A gas sensor must be porous and have a large surface area. In the Figures 4.2, 4.3 and 4.4, the surface morphologies of the pure SnO₂, Pd and Na/Pd doped SnO₂ films are represented. Although the pure SnO₂ film surface was smooth the Pd and Na-Pd modified films showed a relatively porous and cracky structure, as Siciliano and co-workers had also reported in their study [66]. In the top views of the films, it can be seen that the alkali promoted SnO₂ films have a more cracky structure than the films with only Pd doping, therefore has a larger surface area. This result is also in agreement with the previous studies [28].

Carbon monoxide and methane can penetrate in the sensing film in bulk, therefore these gases can react with oxygen ions at inner SnO₂ grain boundry surfaces. Other gases with larger molecules like methanol react mainly on the film surface [53]. Due to the fact that the molecules can react with the oxygen molecules at the inner grain boundries, the diffusion coefficients play a major role in the sensing mechanism. The thickness of

growing films is a major effect in the sensors response. Thickness influence can be explained by a reaction-diffusion mechanism which means diffusion is slower than reaction. Therefore thin films are more effective than thick films in carbonmonoxide sensing [53], and a better reversibility can be obtained in the thin films. Silver and co-workers also concluded that the use of thin films instead of thick ones could improve the sensitivity and the stability of the sensor [32]. Thin film gas sensors with high surface area have advantages like, fast recovery, lower energy input, device compatibility miniaturization and overall cost effectiveness [30].

Although the thin film studies are more successful in sensing carbon monoxide, a thickness less than 200 nm. is not sensitive as expected, as Mandayo and co-workers had already declared [53]. Also, Korotcenkov and co-workers recorded that high sensitivity films had a thickness of more than 200-300 nm [63]. In Korotcenkov's study the explanation of this thickness behavior is the lack of reaction sites when the thickness is near the grain size. In the current study, after coating 8 layers, the film thickness was determined as app. 450 nm from the image of the cross-section (Fig.4.1).

The cracks in the films were formed after drying with the removal of water and isopropanol. Sakai and co-workers [54] found out that the number and the length of the cracks have increased with increasing thickness to 300 and 1000 nm. They also reported that the cracks did not penetrate through the film down to the bottom. Cracks were also formed in the calcination process when the films shrink as a result of grain growth. In many studies it was reported that the average size of particles got larger as the calcination temperature got higher [23].

Film morphology is mostly dependent on the deposition method used and the specific parameters used during the film deposition. In the current study, the resulting average particle size of the tin dioxide supported films was determined app. 35 nm. (Fig. 4.5.), and this result is in agreement with the conclusion made by Manorama et. al. [57], mentioning about the success of sol-gel technique in preparing gas sensor material in the range of nanometers.

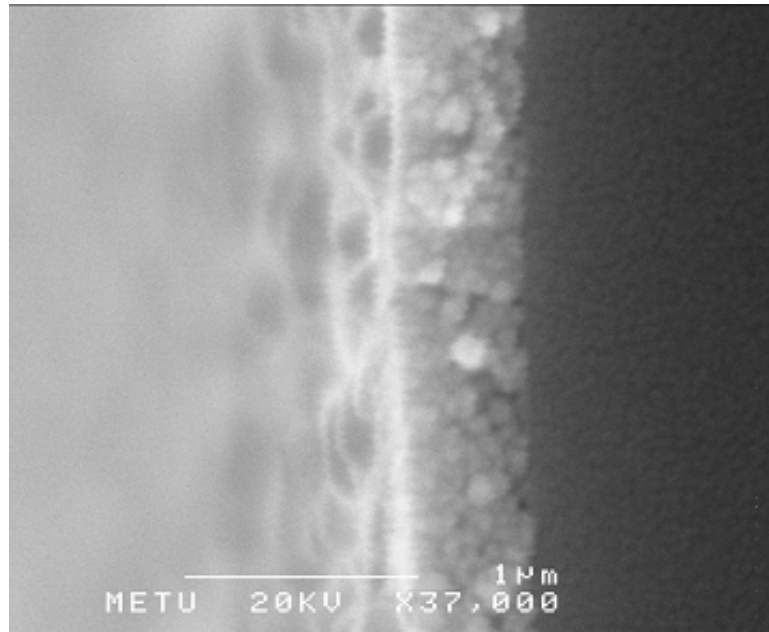


Figure 4.1. SEM image (cross-sectional view) of Na-Pd/SnO₂ film

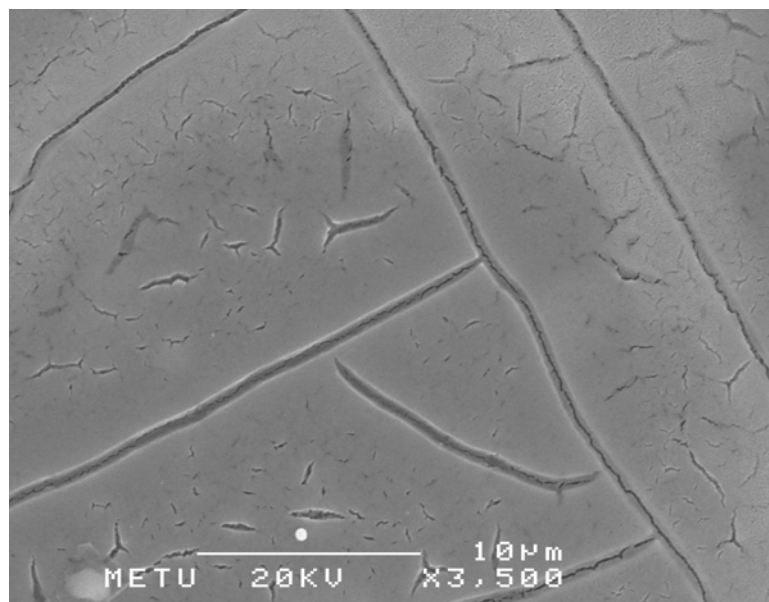


Fig. 4.2. SEM image (top view) of SnO₂ film

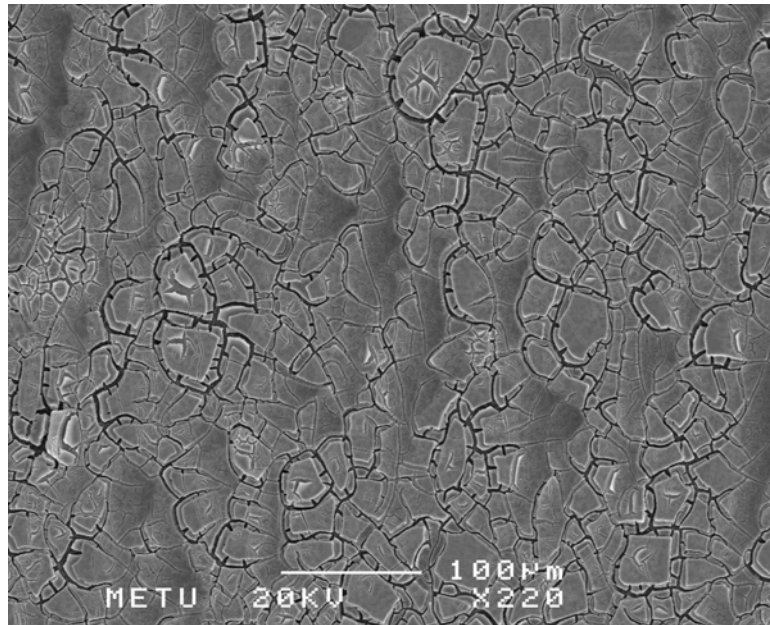


Fig. 4.3. SEM image (top view) of Pd/SnO₂ film

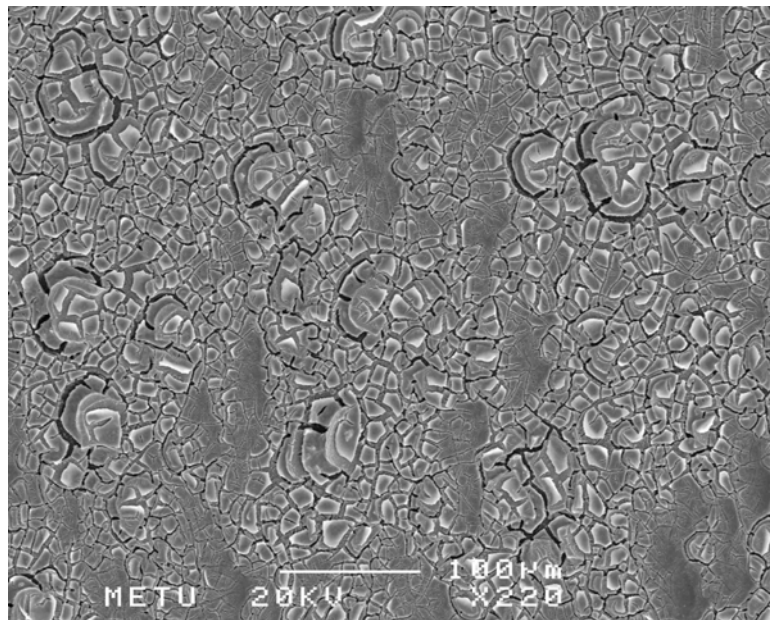


Fig. 4.4. SEM image (top view) of Na-Pd/SnO₂ film

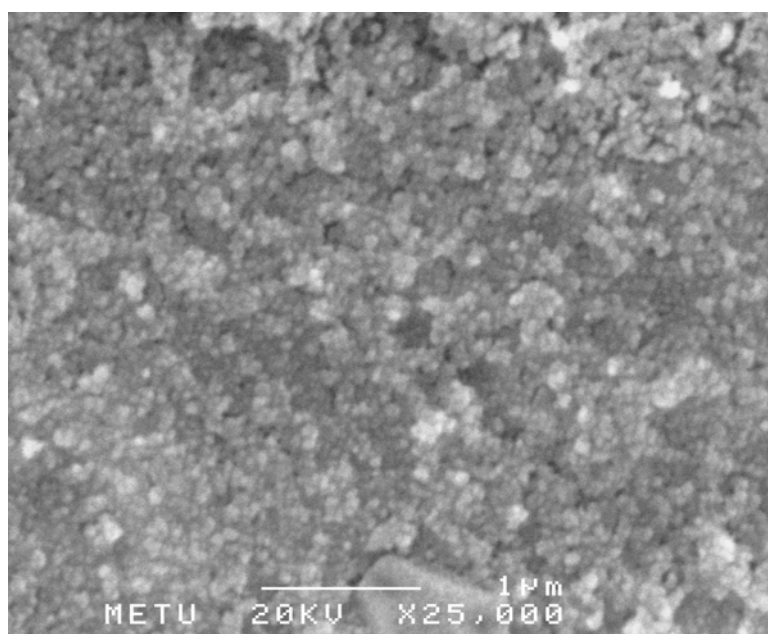


Figure 4.5. High magnification SEM image of SnO₂ film spin coated 8 layers

As seen in the figure 4.3. and 4.4, the doping did not lead to visible particles in SEM investigations. Besides as Briand and coworkers [19] reported, the palladium doping alters the specific area and the surface roughness.

The SnO₂ supported Pd and Na promoted Pd films could easily be removed before the calcination process just by scratching, since the film layer was much softer than the glass substrate. After being calcined at 500°C for 5 hours in air the colour of the layers turns from mustard to brown and the film surface got rougher. As reported by Starke *et al.* [2] the Scanning Tunneling Microscope (STM) surface analysis showed a significant increase in particle size above 500°C. And the experiments conducted on pure SnO₂ films by Hammond and Liu [18] showed that among the test sensors calcined at the temperatures 500, 600, 700 and 800°C, the highest conductivity sensitivity to H₂ was achieved by the sensor calcined at 500°C, at the operating temperature of 250°C. Though the typical operating temperatures for the pure tin oxide films are reported in the range of 350-400°C in the literature.

In the same study, it is also reported the average grain size of the films increased with the increasing calcination temperature.

4.1.2. EDX ANALYSIS

The produced films had homogeneous thicknesses throughout the film due to spin coating technique, and the EDX analysis also yielded a homogeneous composition throughout the films both for the Pd and Na/Pd doped SnO₂ coatings (Fig. 4.6-7).

As in an EDX study, the composition at a point is being analysed, it should be conducted at several points to confirm that the composition analysis is valid for the whole surface of the film. In the current study, EDX studies were performed at many points of the film resulting with the same composition through the entire film.

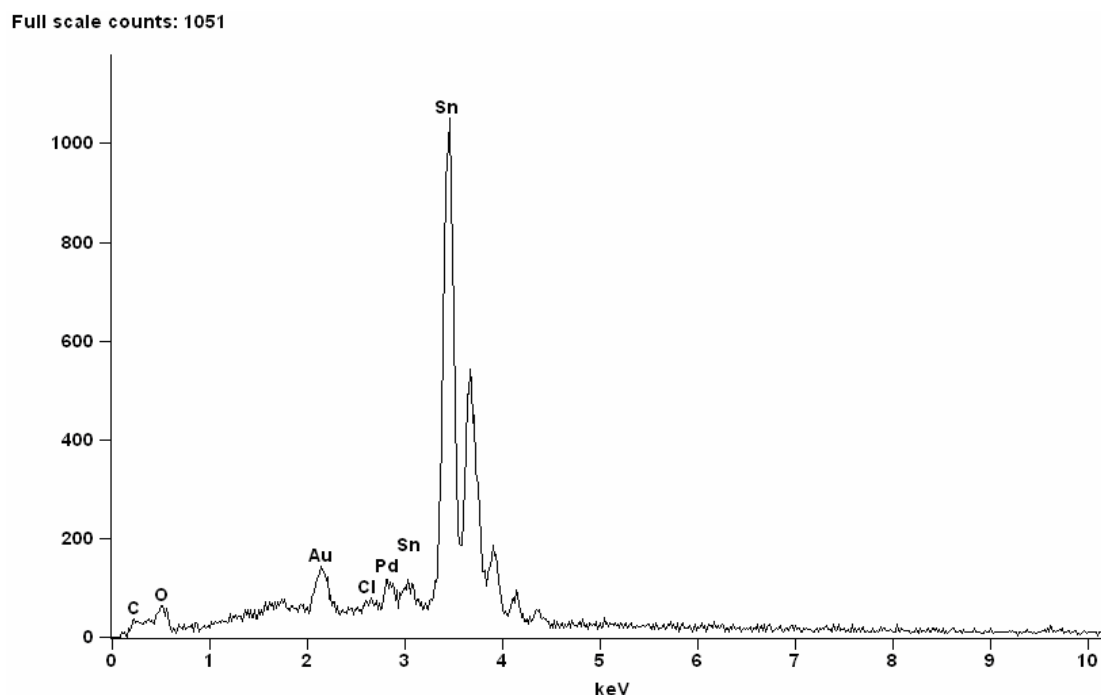


Figure 4.6. EDX analysis of 450 nm thick Pd/SnO₂ films calcined at 500°C

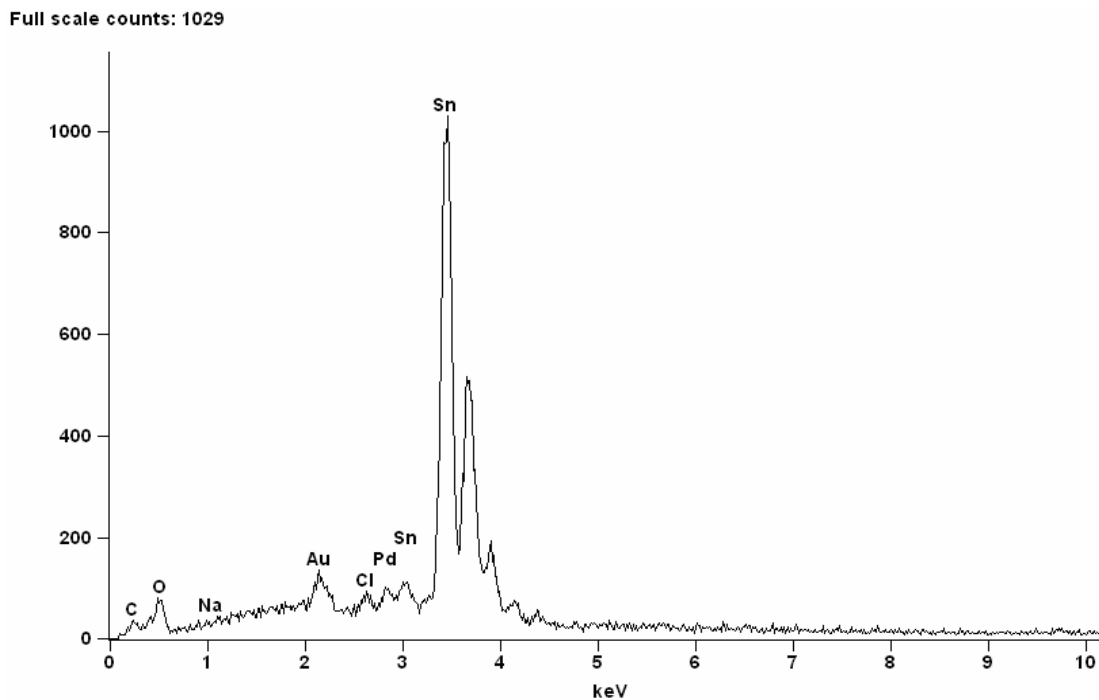


Figure 4.7. EDX analysis of 450 nm thick Na-Pd/SnO₂ films calcined at 500°C

In Figure 4.6., it can be seen that 1 wt. % Pd promotion is clearly observed in the analysis. Though, Na promotion can only slightly be identified when the EDX results are compared with each other. The reason for this slight difference comes from the very little composition of Na in the catalyst solution which is only 0.1 wt. %.

4.1.3. X-RAY DIFFRACTION ANALYSIS

X-ray diffraction patterns were scanned for calcined Pd/SnO₂ and Na-Pd/SnO₂ using Nickel filtered CuK α radiation. Intensities obtained for the samples were between 20-80° 2 θ angles.

Figure 4.8 and 4.9 shows the X-ray diffraction pattern of the calcined Pd/SnO₂ and Na-Pd/SnO₂ films, respectively. From the diffractograms it can be said that the identification of the phase is cassiterite SnO₂. The X-ray patterns of the Pd/SnO₂ and the Na-Pd/SnO₂ films are quite similar since in this frequency range, only the major phase of tin oxide catalyst can be seen.

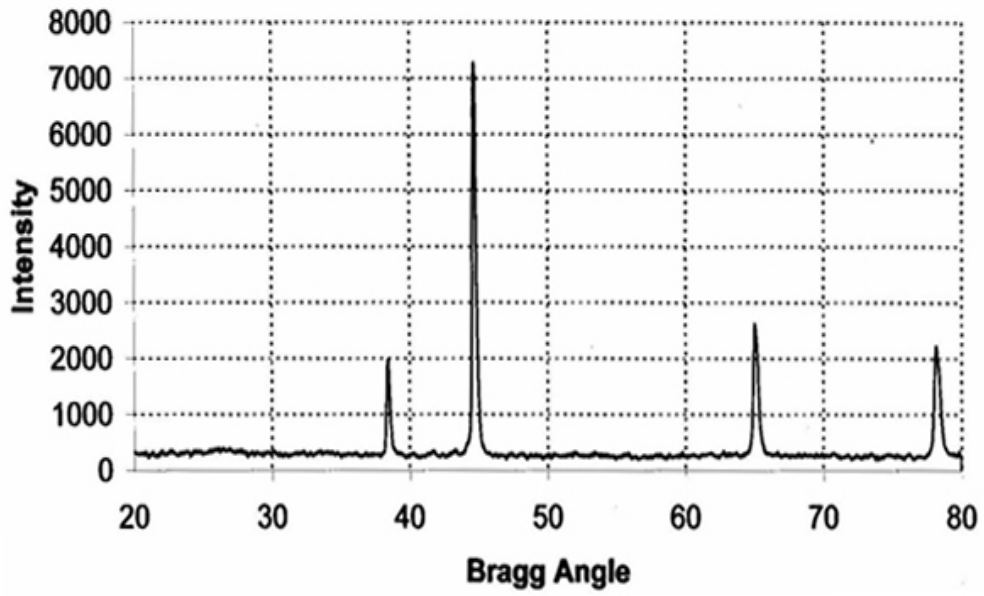


Figure 4.8. XRD Patterns of calcined Pd/SnO₂ substrate

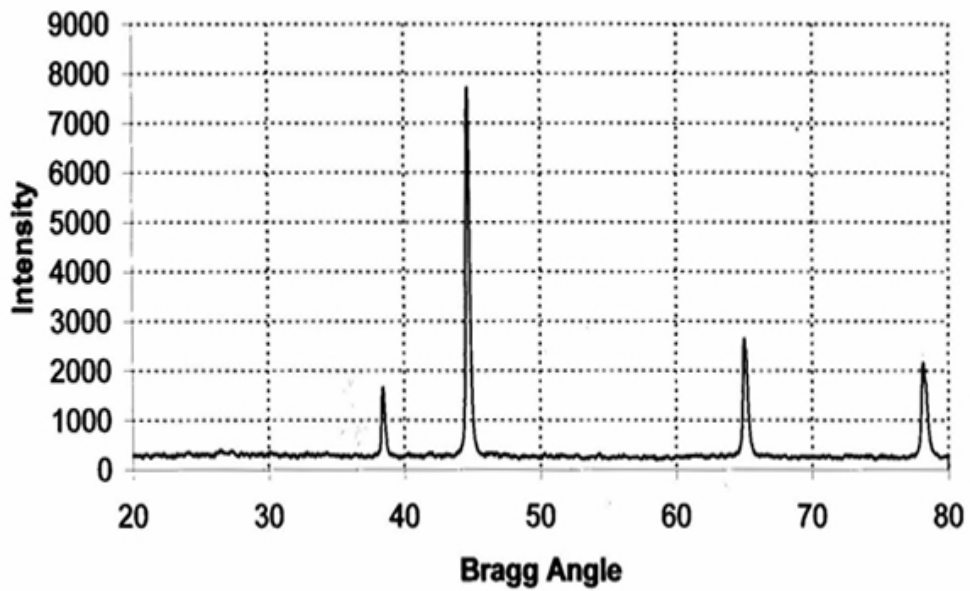


Figure 4.9. XRD Patterns of calcined Na-Pd/SnO₂ substrate

4.2. RESPONSE ANALYSIS OF THE TEST SENSORS TO METHANE

Methane response analysis pulse and step experiments were conducted after carbonmonoxide experiments, at the maximum temperature selected (200 °C), to decide by considering the best responses of both types of the sensors. In a preliminary study by our study group [28], it was concluded that thick film Pd/SnO₂ and Na-Pd/SnO₂ gas sensors responded satisfactorily towards step CH₄ concentration changes. Though, in the case of injection type of CH₄ changes the same result could not be achieved.

In Figures 4.10 and 4.11 the responses of the Na-Pd/SnO₂ and Pd/SnO₂ test sensors in 99.9% He atmosphere to pure methane injections at 200 °C are given. At 200 °C, it has been observed that both of the test sensors show slight variations in resistance to pure methane, and these variations were not stable.

Mandayo et. al. [53] reported that, carbon monoxide and methane penetrate in the sensing film in bulk, and the molecules can react with the oxygen molecules at the inner grain boundaries. So, the diffusion coefficients play a significant role in the sensing mechanism and the thickness of the films is a major factor in the sensor response. In the same study by Mandayo, influence of thickness is explained by a reaction-diffusion mechanism which means diffusion is slower than reaction. This shows that methane can not diffuse within the pores of the catalytic surface in such a short time of the injection. When the molecular diameters of carbon monoxide (0,316 nm.) and methane (0,380 nm.) are considered, it is logical that methane has a difficulty in penetrating in the sensing film. This result was supported by another test on the sensor with 5% methane in Helium with step changes like done by Severcan [28] in 2002.

When the carbon dioxide and water production of the test sensors are considered, the concentration change in water can clearly be seen in the case of Na-Pd/SnO₂ substrate. This result is probably due to the Na promotion increasing the oxygen storage at the surface and causing the formation of

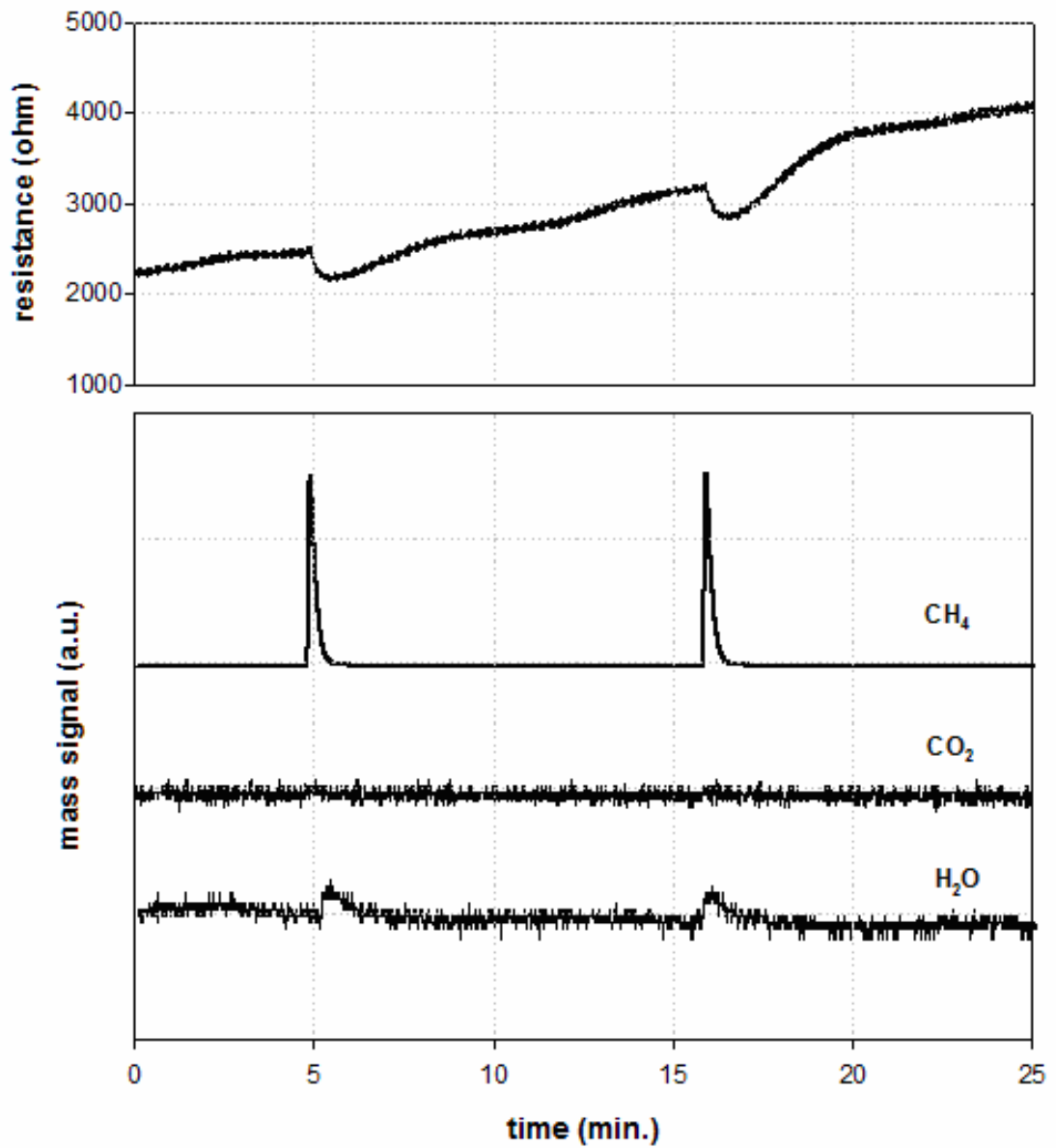


Figure 4.10. Response of Na-Pd/SnO₂ test sensor to pure CH₄ injections at 200°C in He atmosphere

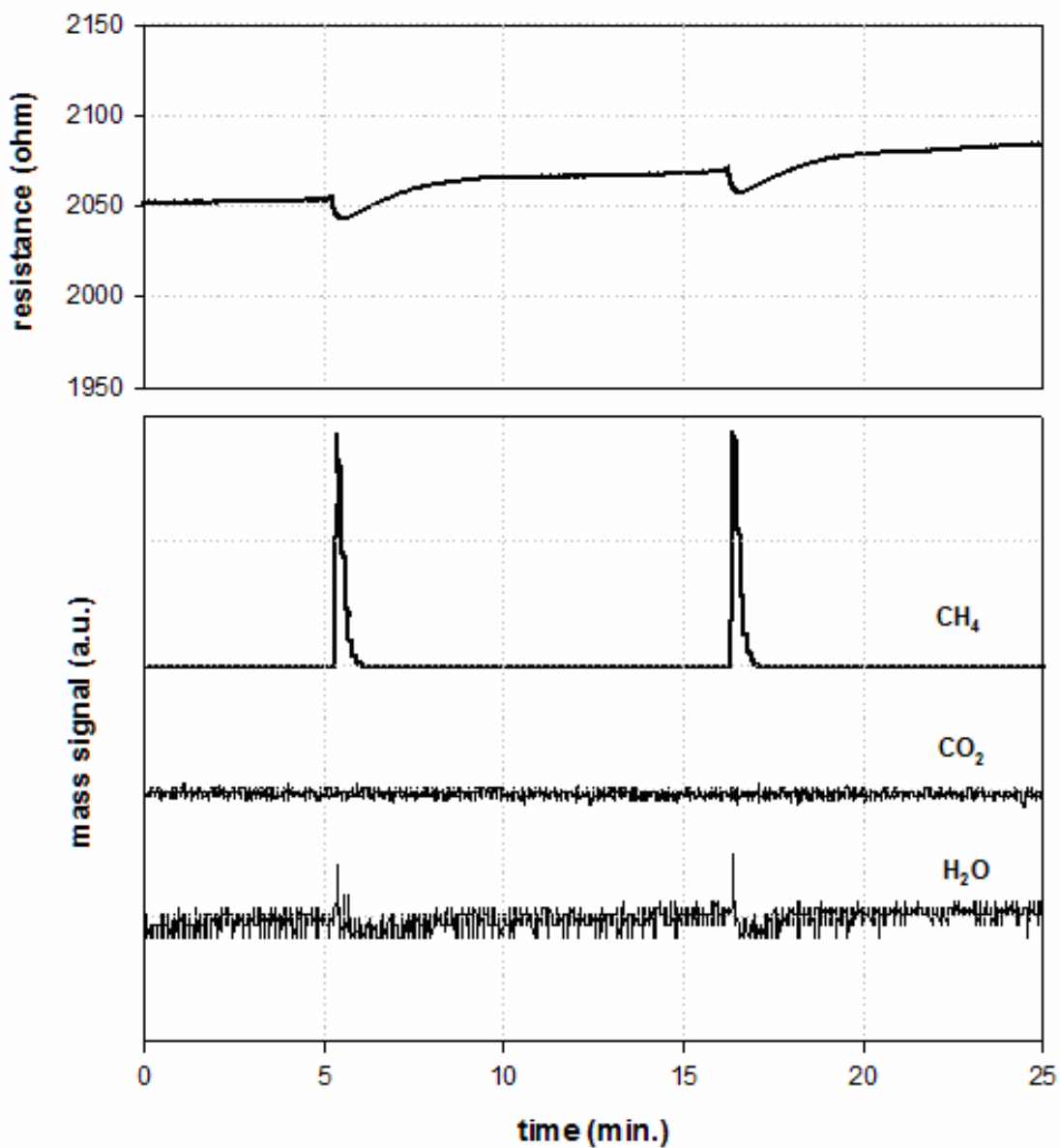
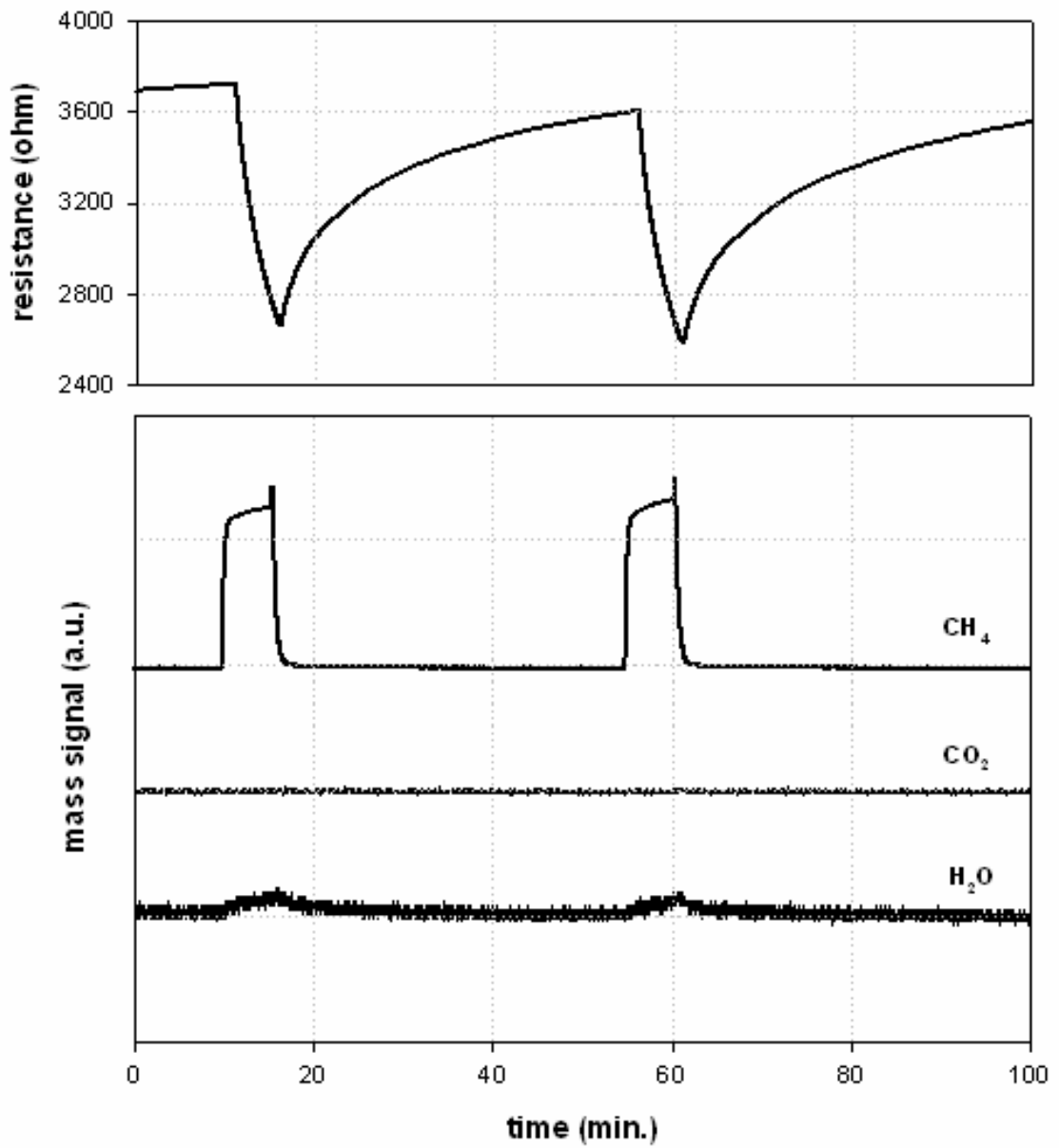


Figure 4.11. Response of Pd/SnO₂ test sensor to pure CH₄ injections at 200°C in He atmosphere



4.12. Response of Na-Pd/SnO₂ test sensor to 5% CH₄ step changes at 200°C in He atmosphere

higher oxides of Palladium [75]. This result is also supported by the resistance values which are higher in Na-Pd/SnO₂ sensor when compared to Pd/SnO₂.

It is well known that there is a relationship between the concentration of the reducing gas and the resistance response of the sensor [37]. In the step study conducted at 200 °C with 5% CH₄ in helium, although the methane concentration was reduced from 100% to 5%, the responses were more significant than the responses to the 5 ml. pure methane injections. This is because in the case of pulse input, only the initial response of the test substrate can be seen, then sensor resistance begins to increase again when the methane is cleared off and helium washes away the surface adsorbed reducing gas. When, the step injections are considered, the resistance signal continuously decreases to a point in the time interval of methane injection, until almost all the adsorption and reaction sites are full.

4.3. RESPONSE ANALYSIS OF THE TEST SENSORS TO CARBON MONOXIDE

Carbon monoxide response analysis experiments were conducted at the selected temperatures and in different oxygen containing atmospheres. The electrical and compositional responses of the sensors were recorded in order to have idea on both the electronic interactions and the reactional changes. In the literature various workers advocated different mechanisms, such as;

- The presence of the gas can cause the catalyst to change chemically and alter the response of the device,
- The catalyst dissociates the gas molecules into elemental atoms which can spill over onto the surface of the semiconductor oxide grains. And therefore speeds up the surface reactions,
- The electronic interactions between the catalyst and the SnO₂ can cause changes in the surface energy state,

- The catalyst can produce new chemical species by partial combustion, providing a modified response, and
- The catalyst can affect the reaction rate leading to an enhanced response at a lower temperature.

The studies were performed to understand which of the proposed mechanisms are valid and/or dominating for the Pd/SnO₂ and Na-Pd/SnO₂ test sensors.

4.3.1. TEMPERATURE EFFECT ON THE RESISTANCE BEHAVIOR

Tin oxide semiconductor gas sensors are used to detect minority gases in the atmosphere by measuring the resistance difference in the presence and absence of the impurity gases. Since the resistance is not uniform throughout the material, the surface resistances of the films are taken into account.

The base line of a sensor is defined as the resistance in clean, dry atmosphere and all the steps during the fabrication, like fabrication of electrodes and film coating, affect the base line. Changes over long operating times of baseline and sensitivity are important in the utilization of any sensor. Though the reducing gas caused resistance changes at low temperatures, the studied sensors did not show any distinguishable resistance change from the base line to CO gas at 100 and/or 125 °C in He atmosphere. In the figure 4.13 and 4.14, the resistance responses of Pd promoted SnO₂ films, to two serial injections of 750 ppm. CO in He atmosphere, at 100 and 125 °C are given. Upon exposure to CO gas, a decrease in the resistance was observed, as was expected, which is a result of the reducing effect of CO on oxidised Pd/SnO₂ film surface. By looking at the responses at 100 °C it has been observed that; the variation in the sensor resistance is small, unstable and negligible when compared to the resistance oscillation of Pd promoted SnO₂ films. This can be a result of the insufficient thermal energy to decrease the band gap energy. Because of the low temperature, a physical adsorption dominating mechanism

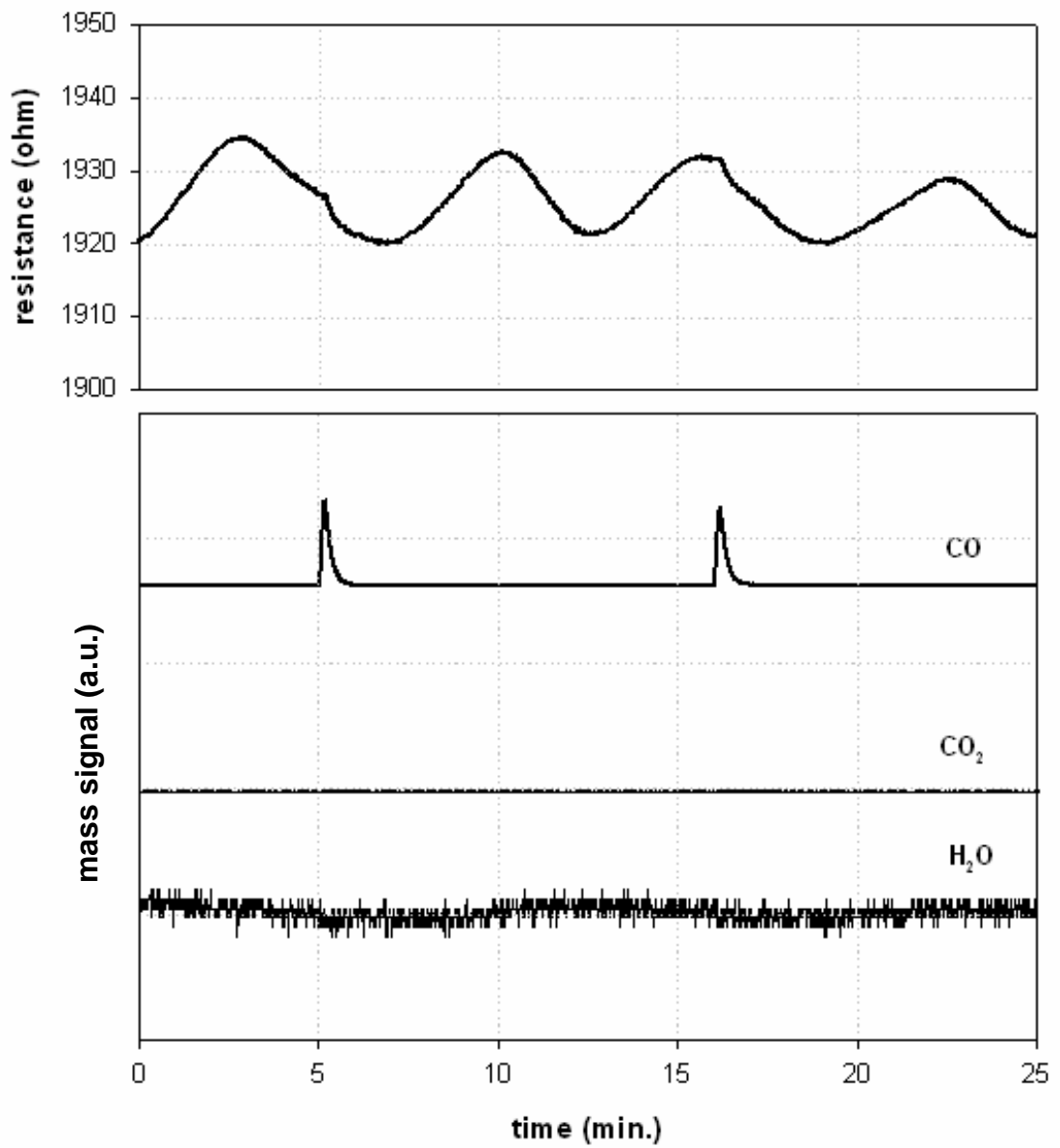


Figure 4.13. Pd/SnO₂ multilayer thin film resistance behavior in He atmosphere under 750 ppm CO injection at 100 °C

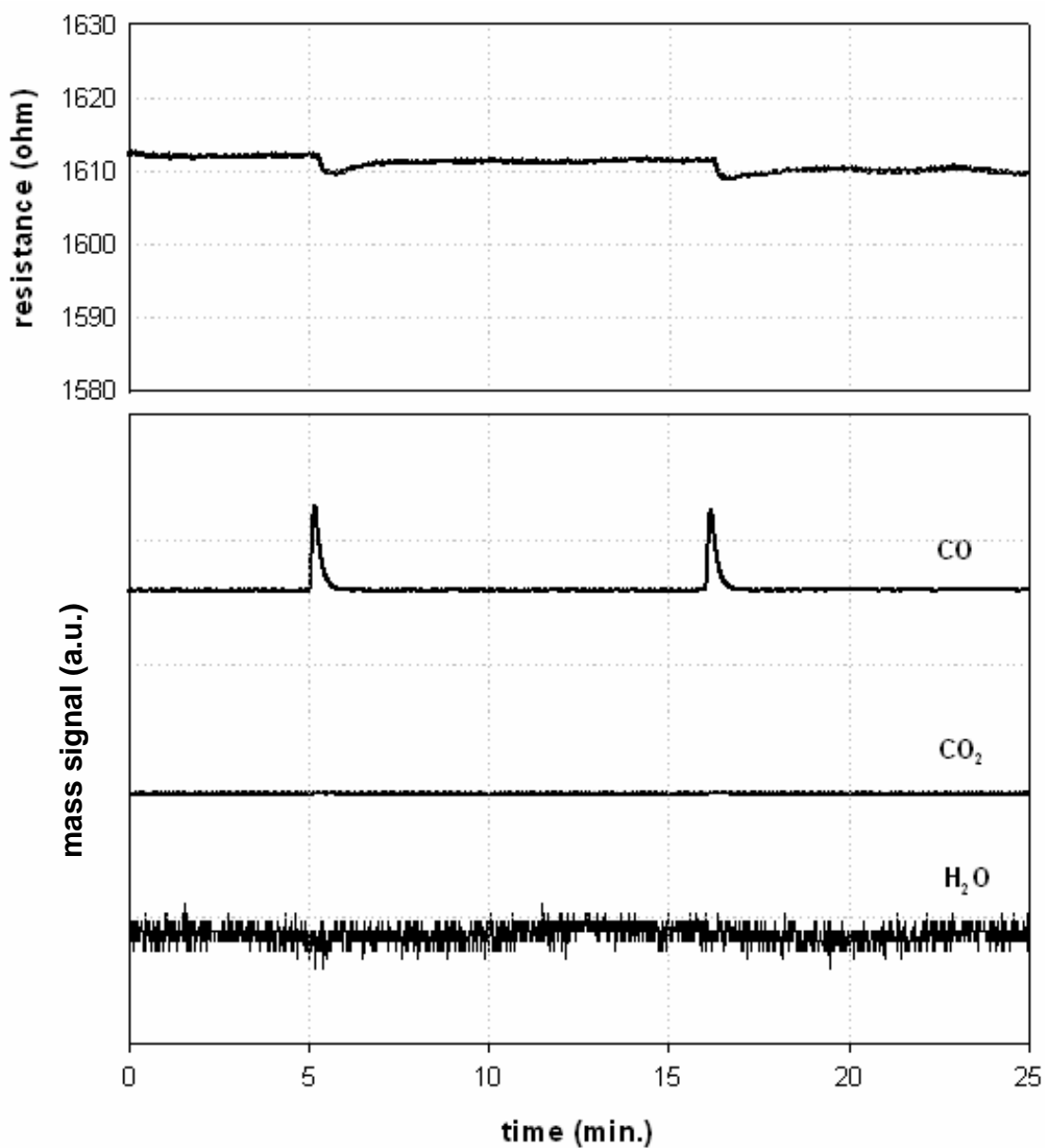


Figure 4.14. Pd/SnO₂ multilayer thin film resistance behavior in He atmosphere under 750 ppm CO injection at 125 °C

was expected that did not result in a significant compositional change in the reaction cell exit gas as can be seen on the bottom of the resistance response graph. Considering the fact that, the compositional changes in the reaction reflect as resistance changes in the sensor, at 100 °C the mass spectrometer data supports the weak resistance response of the test sensor when the CO₂ and H₂O production curves are considered.

At 125 °C, the Pd promoted SnO₂ films did not show an oscillation in the resistance but the responses were only 3 - 4 ohm which is still negligible, obviously the compositional change in the reaction cell exit gas was still not distinguishable at all.

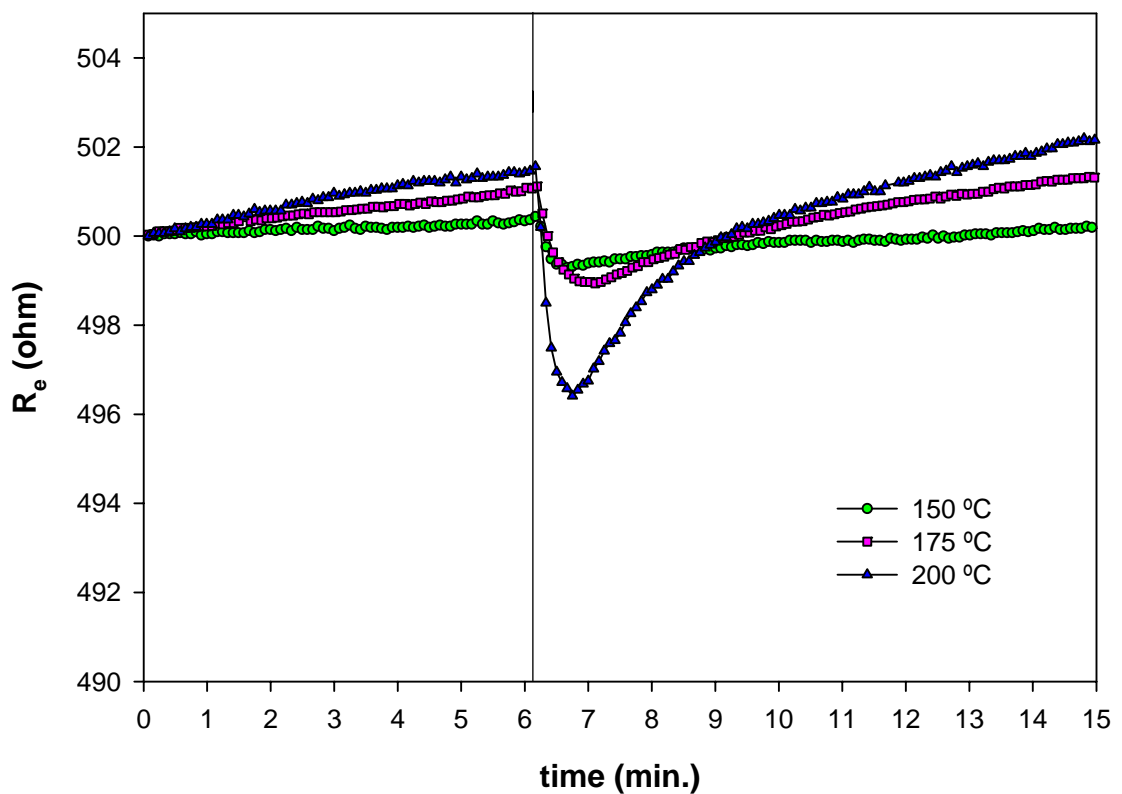


Figure 4.15. Na-Pd/SnO₂ multilayer thin film resistance behavior in He atmosphere under 750 ppm. CO gas injection at 150, 175 and 200 °C

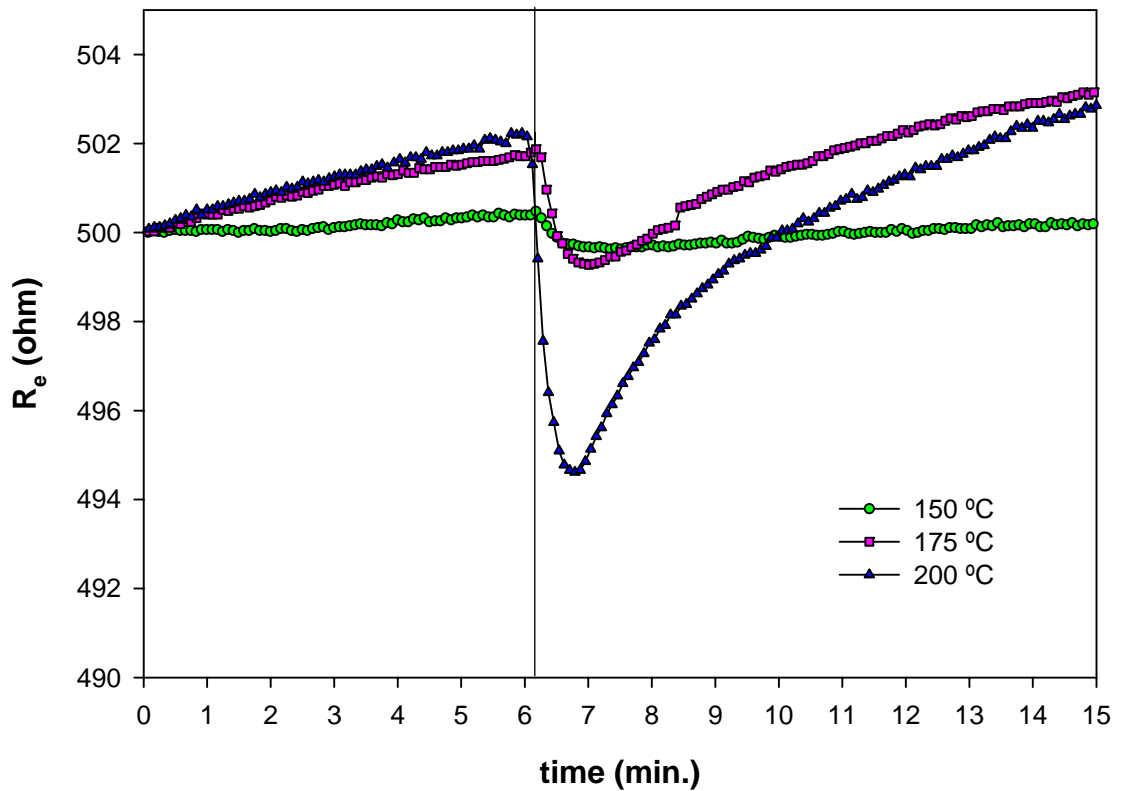


Figure 4.16. Pd/SnO₂ multilayer thin film resistance behavior in He atmosphere under 750 ppm. CO gas injection at 150, 175 and 200 °C

In order to detect a CO injection with this concentration, both of the studied gas sensors need to be heated to a higher operating temperature, like the other conventional tin oxide gas sensors. In the literature usually the distinguishable responses were recorded at high temperatures in the range of 250-350 °C. But as reported by Martinelli *et al.* [65], Pd promotion enhances the sensitivity at lower temperatures, and the maximum sensitivity of the semiconductor to the reducing gas occurs at lower temperatures. As a result the recognition of the gas takes place at lower temperatures.

In the figures 4.15-16, the comparison of resistance responses to the CO gas in the pure helium atmosphere at different temperatures can be seen. The resistance values are calculated equivalent resistance values in the range of 490 – 505 ohm. for an easy comparison (See Appendix D for R_e calculations).

When reducing gas is injected to the testing atmosphere, it either reacts or adsorbs on the surface of the catalytic layer. Figure 4.15 summarizes the Na-Pd/SnO₂ test sensor resistance changes at 150, 175 and 200 °C. At 150 °C, the rate of the reaction taking place between the surface adsorbed oxygen species and the reducing gas is not so significant. Therefore the resistance response is not clear. Looking at the poor resistance response, one could say there was no reaction occurring with the catalytic surface, but the CO injections resulted with the water concentration changes as can be seen in Figure 4.32. Upon increasing the temperature to 175 °C, resistance response becomes more pronounced, but the response time also increases as the magnitude of the response increases. By increasing the temperature more to 200 °C, the resistance response sharpens and the response time becomes almost equal to the response time observed at 150°C. So the best result was achieved at 200 °C with the largest response and the shortest response time.

In the case of Pd/SnO₂ test sensor, at 150 °C the rate of the reaction is smaller than Na promoted Pd/SnO₂ test sensor. This is clear when the resistance responses of the both types of the sensors are considered. There can be two reasons for this result; the alkali promotion may weaken the C-O bond in CO chemisorbed and therefore causes a better response even at low temperatures and/or the addition of alkali metal act to enhance oxygen adsorption and the increase in the number of oxygen species causes an easier reaction with the reducing gas in the same oxygen free testing conditions [73]. Increasing the temperature from 150 to 175 °C, increases the resistance response up to the level of Na promoted Pd/SnO₂ sensor. Upon increasing the temperature more to 200 °C, response time almost stays constant but the magnitude of the resistance response grows almost 1.5 times larger of the response taken with Na promoted test sensor at 200°C (Fig. 4.16).

In the Figures 4.17-18, the comparison of the resistance responses in the 1% O₂ containing Helium atmosphere are shown at the same operating temperatures. Although the Na-Pd/SnO₂ sensor show slight variations in quite long response time at 150 °C, at 175 °C response time gets shorter and the

magnitude of the resistance response gets 5 times larger than at 150 °C (Fig. 4.17). Then with increasing the testing temperature to 200 °C, the response becomes 7 times larger when compared to the one at 150 °C, and the response time again gets shorter different than in the case of oxygen free conditions.

In Figure 4.18, the resistance responses of the Pd/SnO₂ test sensor can be seen. Like in the case of Na- Pd/SnO₂ in oxygen containing atmosphere the magnitude of the responses grows larger and the response time gets shorter as the temperature increases. But the change of the magnitude of resistance responses with increasing temperature is not as sharp as it is in the case of Na promoted Pd/SnO₂ test sensor. The reason can be the increased oxygen chemisorption capacity of the alkali promoted surface again [73].

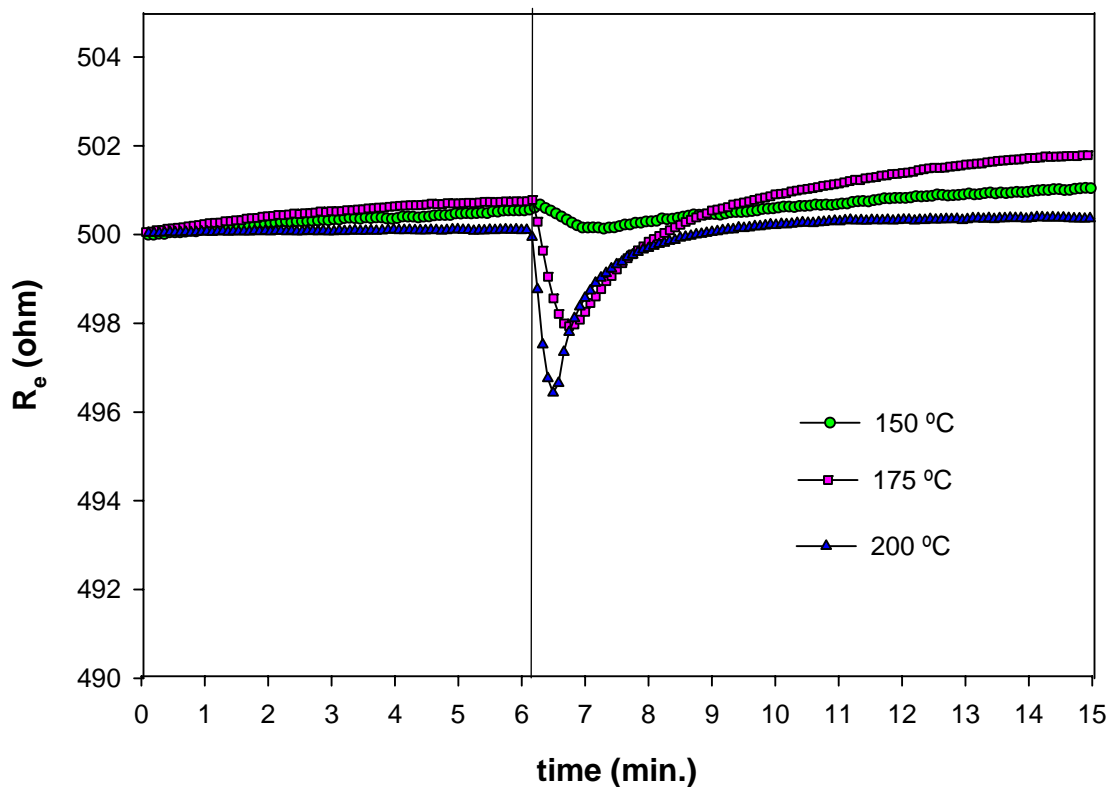


Figure 4.17. Na-Pd/SnO₂ multilayer thin film resistance behavior in 1% O₂ + 99% He atmosphere under 750 ppm CO injection at 150, 175 and 200 °C

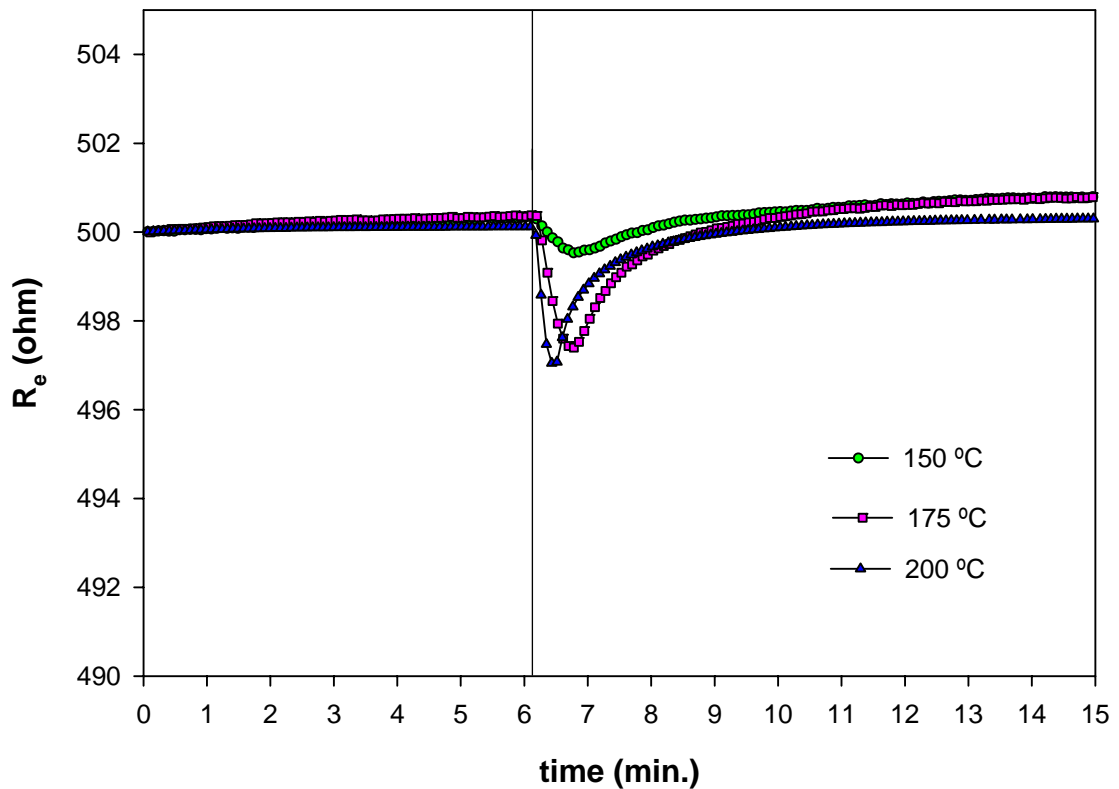


Figure 4.18. Pd/SnO₂ multilayer thin film resistance behavior in 1% O₂ + 99% He atmosphere under 750 ppm CO injection at 150, 175 and 200 °C

When resistance responses are plotted as a function of time, upon exposure to carbon monoxide gas, the resistance decreases which indicates the reducing activity of carbon monoxide over oxidized SnO₂ supported catalyst surface. This result is in agreement with the earlier studies [28, 37]. Also, there is a power law relationship between sensor conductivity and reducing gas concentration as observed by Göpel [37] that explains the conductivity was proportional with the reducing gas concentration.

The CO injections resulted with the CO₂ and water production in the sensing layers. In the study of Schmid *et al.* [50], the IR spectroscopy measurements showed that in the sensing mechanism of methane, propane and toluene, there were only water and carbon dioxide could be found

related to the sensing process, and there were no side products from the oxidation.

4.4. PROMOTION EFFECT ON THE RESISTANCE BEHAVIOR

The most important objective of the doping is to improve the sensor sensitivity to the particular gases. In the literature, most reported catalysts have high work functions, which is defined as the minimum amount of energy required to remove an electron from the surface of the metal.

Pd and Ag are known to form stable oxides in air, which extract electrons from the tin oxide structure and form an electron depleted region in the SnO_2 grains. PdO and Ag_2O can easily reduced to metals accompanied by

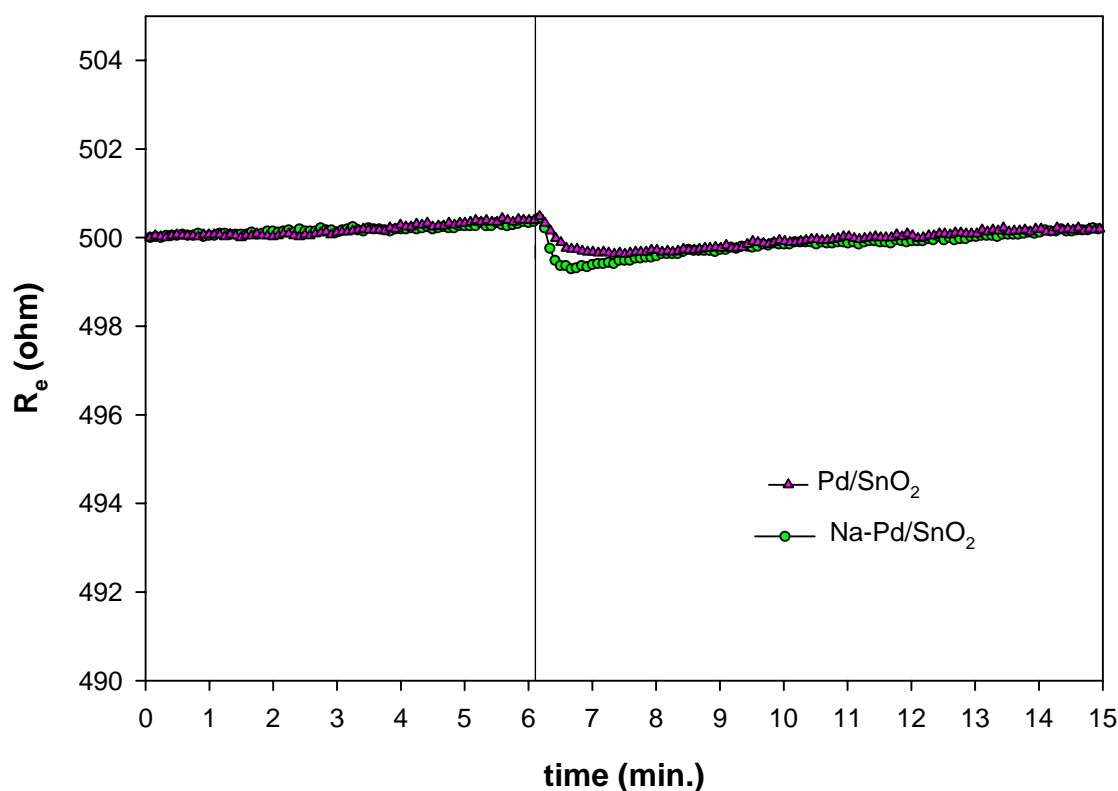


Figure 4.19. Comparison of Pd and Na-Pd/SnO₂ multilayer thin film resistance behavior in He atmosphere under 750 ppm CO injection at 150°C

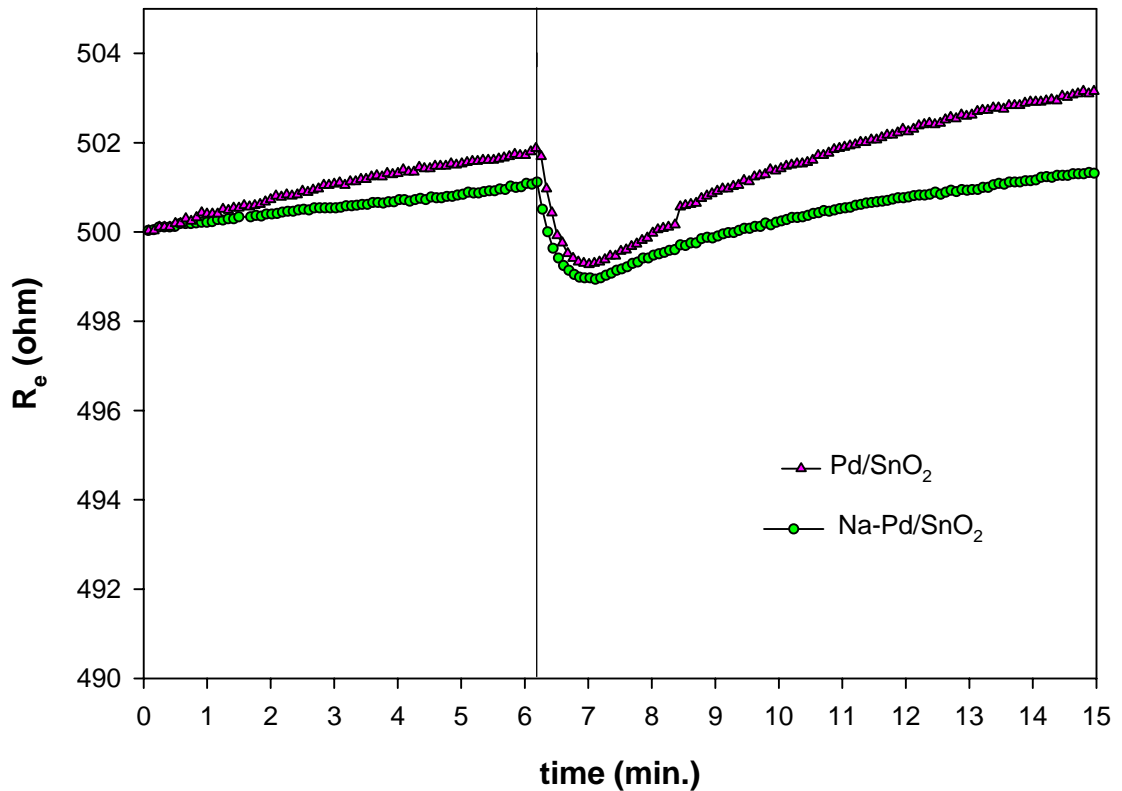


Figure 4.20. Comparison of Pd and Na-Pd/SnO₂ multilayer thin film resistance behavior in He atmosphere under 750 ppm CO injection at 175°C

the release of electrons back into the bulk SnO₂. Thus these particles are receptors to the reducing gases, which otherwise is provided by the adsorbed oxygen.

The catalyst effects are influenced by the amount, chemical form and the physical form of the catalyst. In this work 1 wt. % Pd and 0.1 wt. % Na are used as catalysts in the SnO₂ support.

The work function of Pd is reported as 5.12 eV. in the study conducted by Tang [33]. It is investigated by Capone, that the Pd doped SnO₂ films have a higher resistivity than undoped films and this might be due to the transfer of electrons from the tin dioxide to the metal which can occur since the palladium work function is higher. In particular good properties are observed for Pd and Os which act as activators for CO and CH₄ respectively, improving

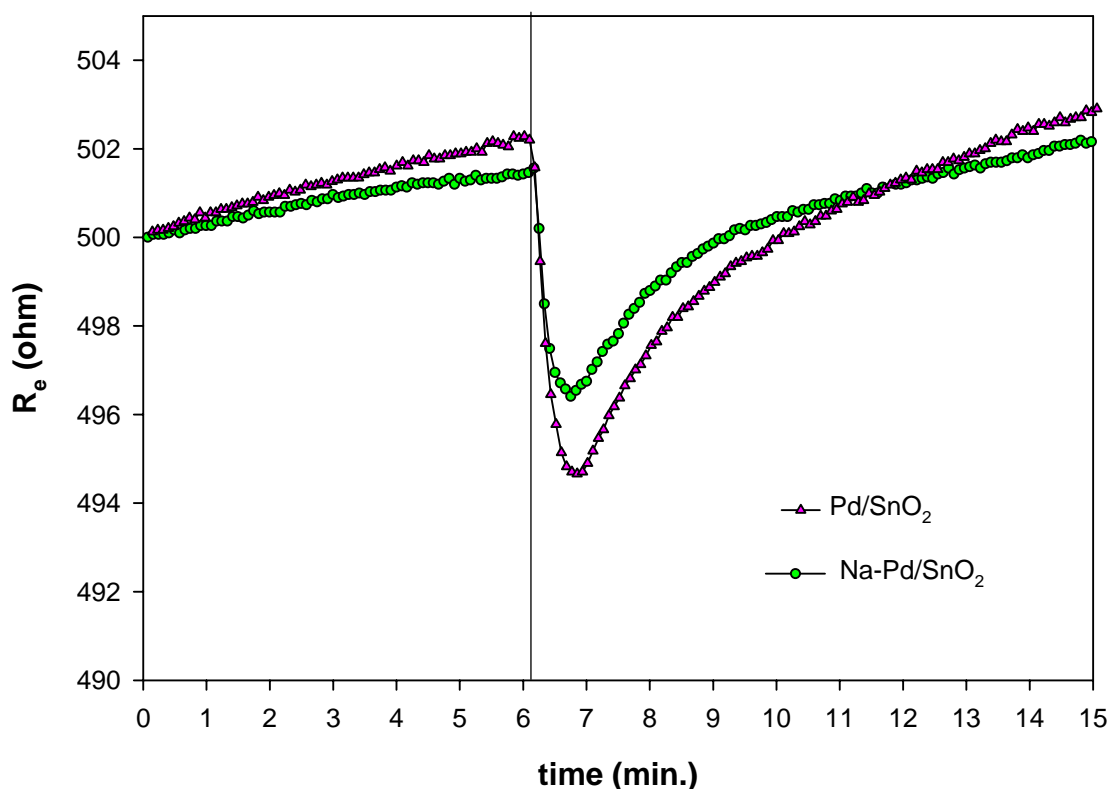


Figure 4.21. Comparison of Pd and Na-Pd/SnO₂ multilayer thin film resistance behavior in He atmosphere under 750 ppm CO injection at 200°C

also the response [51]. Catalyst selection is based on the understanding that there are electronic interactions changing the surface energy states between the catalyst and the SnO₂ support. Adding alkali metal oxide is likely to create an electron density on the surface which will reduce the affinity of nucleophilic reagents like CO and C₃H₆ to the catalyst due to the electronic effect [48].

In Figure 4.19, 4.20 and 4.21, the comparison of Pd/SnO₂ and Na-Pd/SnO₂ test sensor responses in oxygen free atmosphere at 150, 175 and 200 °C can be seen respectively. Looking at the responses at 150 °C, the Na promoted test sensor give a better result with respect to the unpromoted test sensor (Fig.4.19). At 175 °C, though there is only a slight variation in the resistance response in magnitude in favor of Pd/SnO₂, Na- Pd/SnO₂ test sensor

has a more stable base line (Fig.4.20). In Figure 4.21, it is clear that the response of Pd/SnO₂ is better both in magnitude and response time.

When palladium is added, a maximum of conductance appears at low temperature (75-100 °C) in 300 ppm CO/air and 100 ppm C₃H₅OH/air. Then the CO sensitivity clearly drops at an operating temperature higher than 150 °C. Addition of palladium is the main cause for this high sensitivity at low temperature. It was already known the palladium decreases the activation energy of the CO oxidation reaction, but its interaction with CO and tin oxide is not well understood. Under 1000 ppm CH₄ /air, the maximum conductance is located at a higher temperature (200-300 °C) because of the better stability of this molecule with temperature [51].

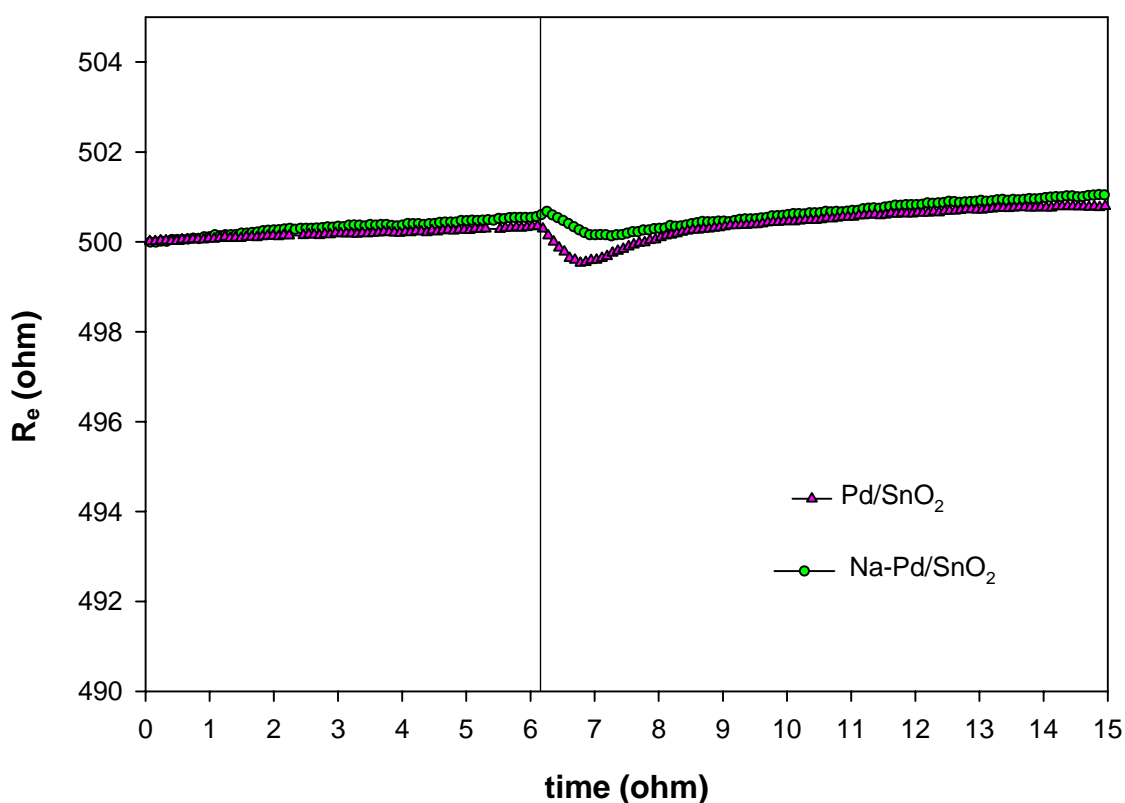


Figure 4.22. Comparison of Pd and Na-Pd/SnO₂ multilayer thin film resistance behavior in 1% O₂ + 99% He atmosphere under 750 ppm CO injection at 150°C

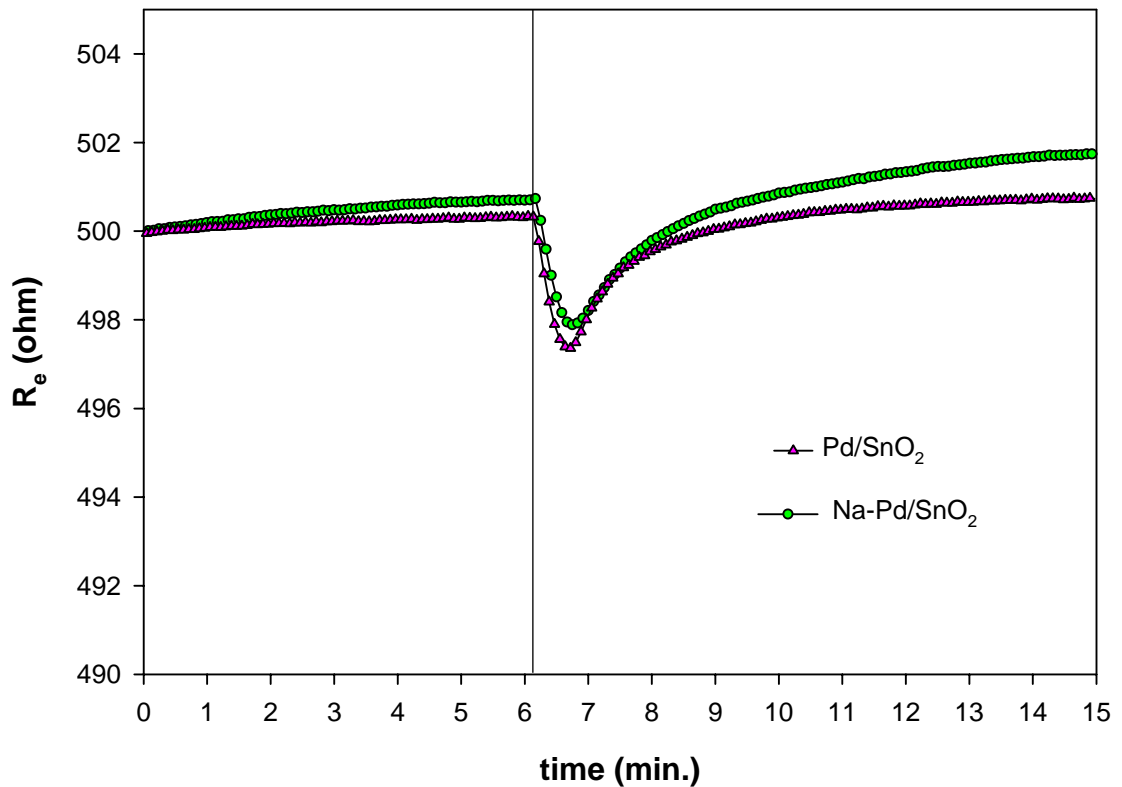


Figure 4.23. Comparison of Pd and Na-Pd/SnO₂ multilayer thin film resistance behavior in 1% O₂ + 99% He atmosphere under 750 ppm CO injection at 175°C

In Figure 4.22, 4.23 and 4.24, the comparison of Pd/SnO₂ and Na-Pd/SnO₂ test sensor responses in 1% oxygen containing helium atmosphere at 150, 175 and 200 °C can be seen respectively. At 150 and 175 °C, the Pd/SnO₂ test sensor give better resistance response results and shorter response times with respect to the other type (Fig.4.22 & 4.23).

Besides, at the same temperatures, Pd/SnO₂ test sensor has a more stable base line. At 200°C, though there is only a slight variation in the response time, in favor of Pd/SnO₂, the Na- Pd/SnO₂ test sensor has a larger resistance response in magnitude (Fig.4.24) and the base lines of the both sensors are seem to follow the same pattern. The rising resistance base line in the case of Na promoted Pd/SnO₂ sensor is not a surprise, because from the

earlier studies, it is known and proved with the XPS results, that the Na promotion increases the oxygen storage at the catalytic surface [75]. In another study by Mirkelamoglu [73], pointing the TPD studies, it is concluded that at the temperatures below 200 °C, sodium promoted catalysts are more readily oxidized than unpromoted Pd/SnO₂.

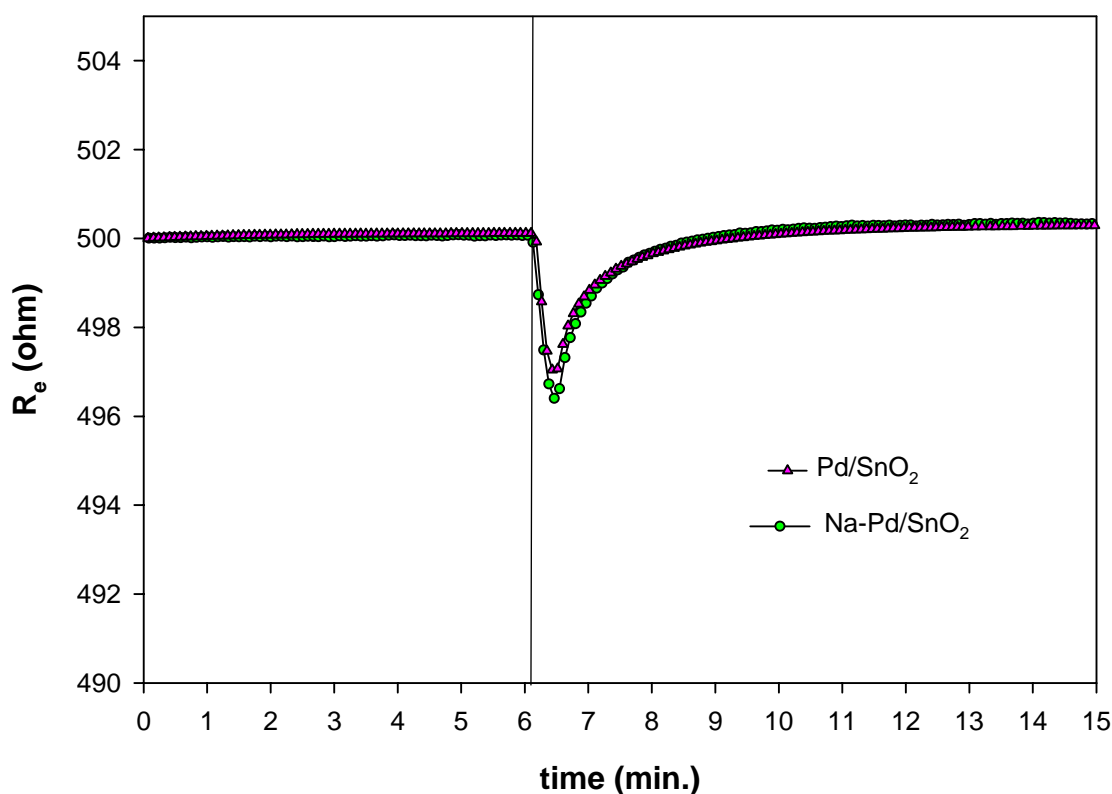


Figure 4.24. Comparison of Pd and Na-Pd/SnO₂ multilayer thin film resistance behavior in 1% O₂ + 99% He atmosphere under 750 ppm CO injection at 200°C

4.5. OXYGEN EFFECT ON THE RESISTANCE BEHAVIOR

The resistance curves show that Na promoted and unpromoted Pd/SnO₂ test sensors achieve the best responses at the operating temperature of 200 °C. Also, the responses of the same type of sensors show so much

variance in oxygen containing atmospheres especially at relatively high temperatures.

In the study by Mirkelamoglu [73], it is pointed that the addition of alkali metals enhanced oxygen adsorption on the catalytic surface and addition of oxygen during the adsorption stage hinders the CO adsorption by the blokage of the active sites by oxygen. When a relatively low temperature is considered, Figure 4.25 tells that the insufficient number of active sites may preferably adsorbed oxygen and therefore the resistance response in the case of oxygen containing atmosphere is smaller in magnitude.

Figure 4.26 and 4.27 compares the Na promoted Pd/SnO₂ films resistance responses at 175 and 200 °C respectively. The resistance curves indicate a more stable base line and the response time gets shorter in the case

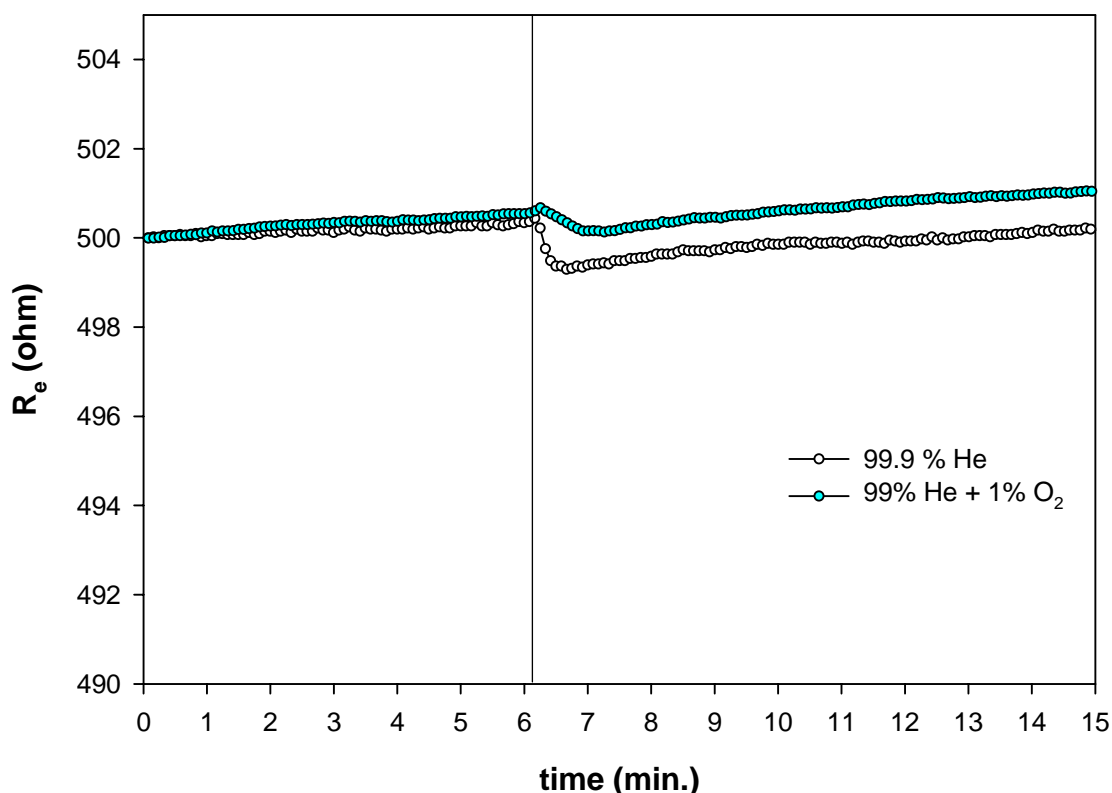


Figure 4.25. Comparison of Na-Pd/SnO₂ multilayer thin film resistance behavior in oxygen free and 1% O₂ containing He atmosphere at 150°C

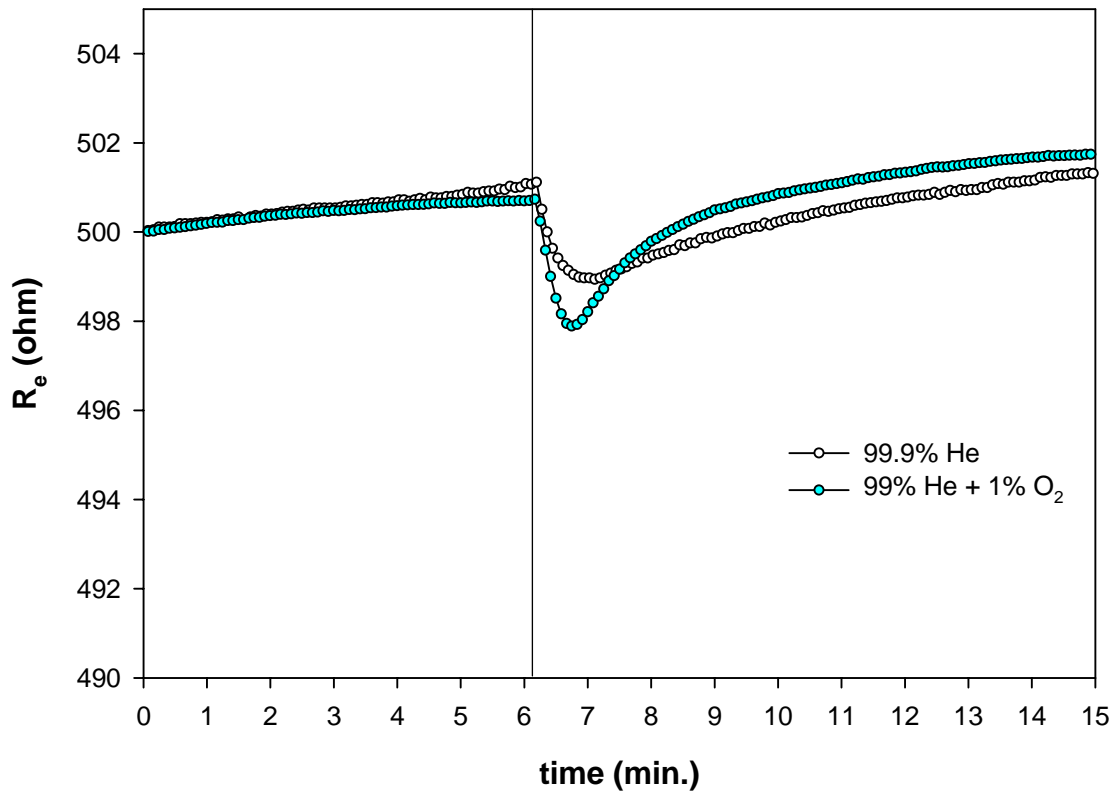


Figure 4.26. Comparison of Na-Pd/SnO₂ multilayer thin film resistance behavior in oxygen free and 1% O₂ containing He atmosphere at 175°C

of oxygen containing atmospheres at the both temperatures. The reason is the enhanced affinity of the films with the increasing temperature, and as a result increasing their resistance by oxidizing the catalytic surface in the case of oxygen containing atmospheres; therefore the reducing effect of the gas gets stronger. On the contrary, in oxygen free atmospheres, at high temperatures, smaller resistance values were obtained because temperature has a stronger effect on resistance decrease compared to that of reducing gas. When these resistance values are calculated in the equivalent resistance form, differences in the resistance values are seen as if they are in the same range. Actually, they are just calculated results to normalize the signal. In Figures between 4.32 and 4.43, the actual resistance values can be seen with the carbon dioxide and water concentration changes in the reaction cell exit gas.

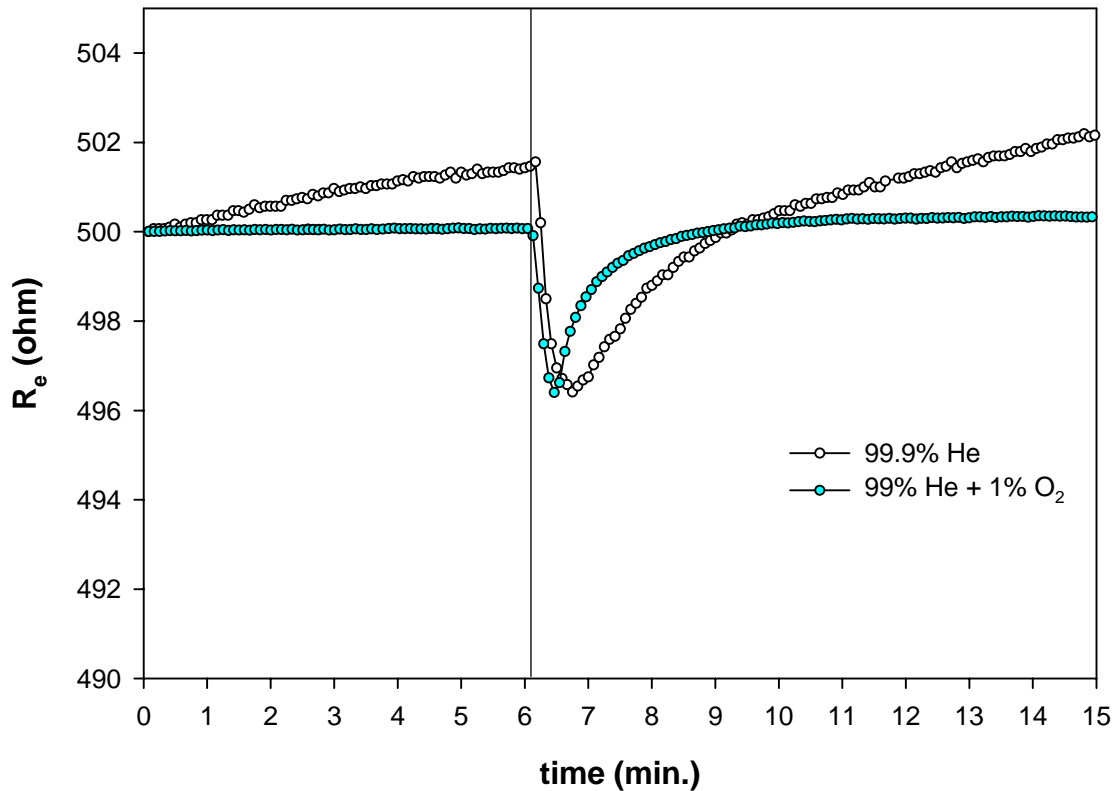


Figure 4.27. Comparison of Na-Pd/SnO₂ multilayer thin film resistance behavior in oxygen free and 1% O₂ containing He atmosphere at 200°C

In the study of Barsan and Schmid [72], it was reported that the oxygen needed for the reaction can be originated from 2 different sources as;

- The surface or the lattice near the surface of the sensitive layer,
- The surface of the electrodes or heater

In the first case an increase in the conductance can be expected, while in the second case no changes in the electrical behavior of the device would be expected. But, the density of the surface adsorbed oxygen species is influenced by the composition and the temperature of the ambient atmosphere, when there is oxygen in the testing atmosphere the oxygen affinity of the catalytic surface also increases with the increasing temperature and the resistance changes get more obvious. In Figures 4.28-29 and 30, the comparison of

Pd/SnO₂ film resistance behavior in oxygen free and 1% O₂ containing He atmosphere at 150, 175 and 200 °C can be seen. It is clear that in the case of oxygen free atmosphere, the variation in the Pd/SnO₂ resistance is small and not sufficient to have a stable signal at 150 °C. This is because the reducing gas can only react with the lattice oxygen. It can be said that at relatively low temperatures, in oxygen free atmospheres only the adsorption of CO is dominating effect on the resistance. Tang et. al. [33] explained this result as the reaction rate is much slower than the surface reaction it can be neglected.

The possible surface reactions can be described as follows where R represents the reducing gas;

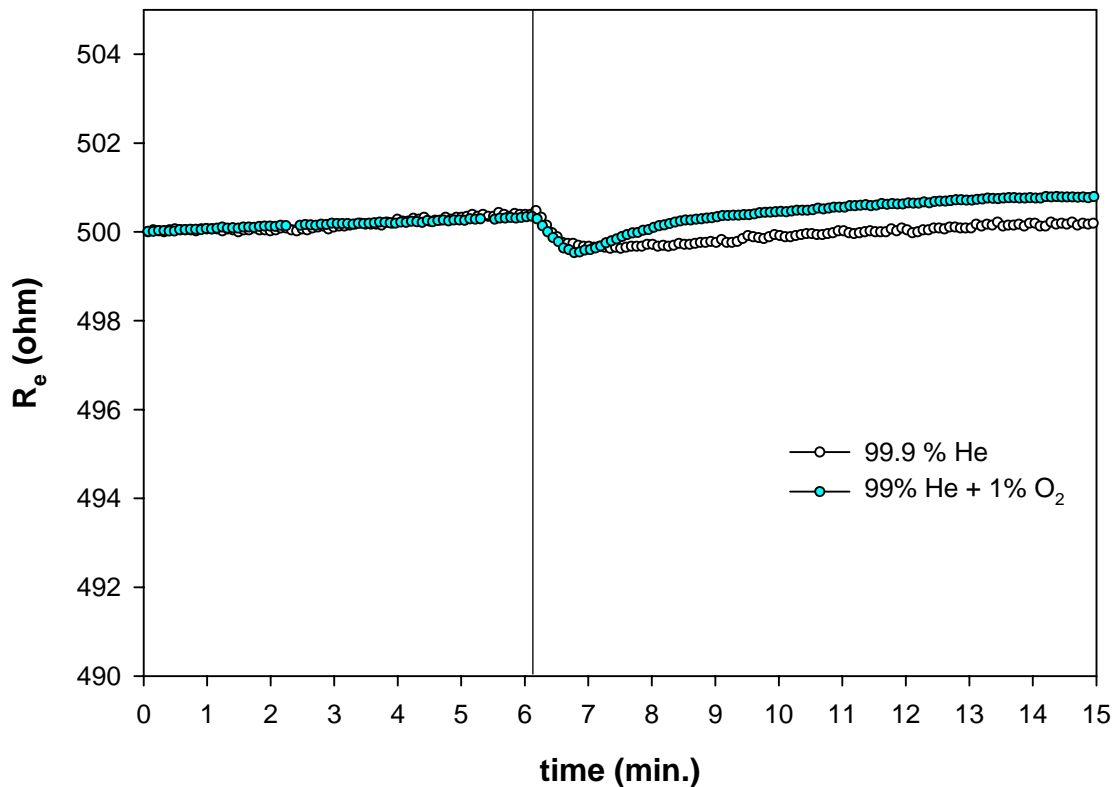
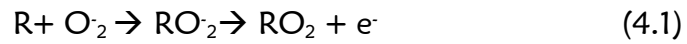


Figure 4.28. Comparison of Pd/SnO₂ multilayer thin film resistance behavior in oxygen free and 1% O₂ containing He atmosphere at 150°C

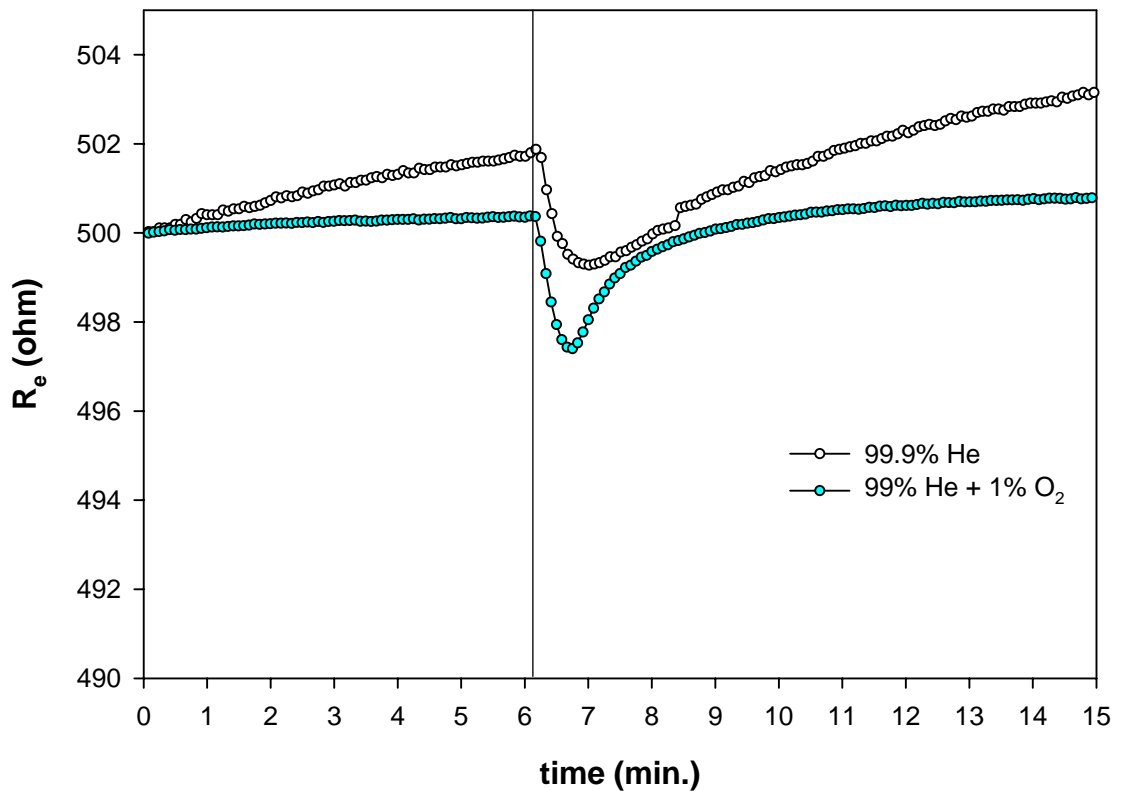


Figure 4.29. Comparison of Pd/SnO₂ multilayer thin film resistance behavior in oxygen free and 1% O₂ containing He atmosphere at 175°C

But as the temperature increases further, the resistance responses become stable. The same explanation is still valid as in the Na promoted Pd/SnO₂ films. The temperature increases the oxygen affinity of the films and as a result increasing their resistance by oxidizing the catalytic surface in the case of oxygen containing atmospheres, and in the oxygen free atmospheres, only the surface adsorbed oxygen reacts with reducing gas and oxygen is depleted. Therefore the resistance of the films decreases as the temperature increases.

In Figure 4.28 unpromoted Pd/SnO₂ sensor resistance responses are compared. In oxygen containing atmosphere the resistance response is more significant because in oxygen free atmosphere reducing gas only adsorbs on the surface and /or can only react with the lattice oxygen.

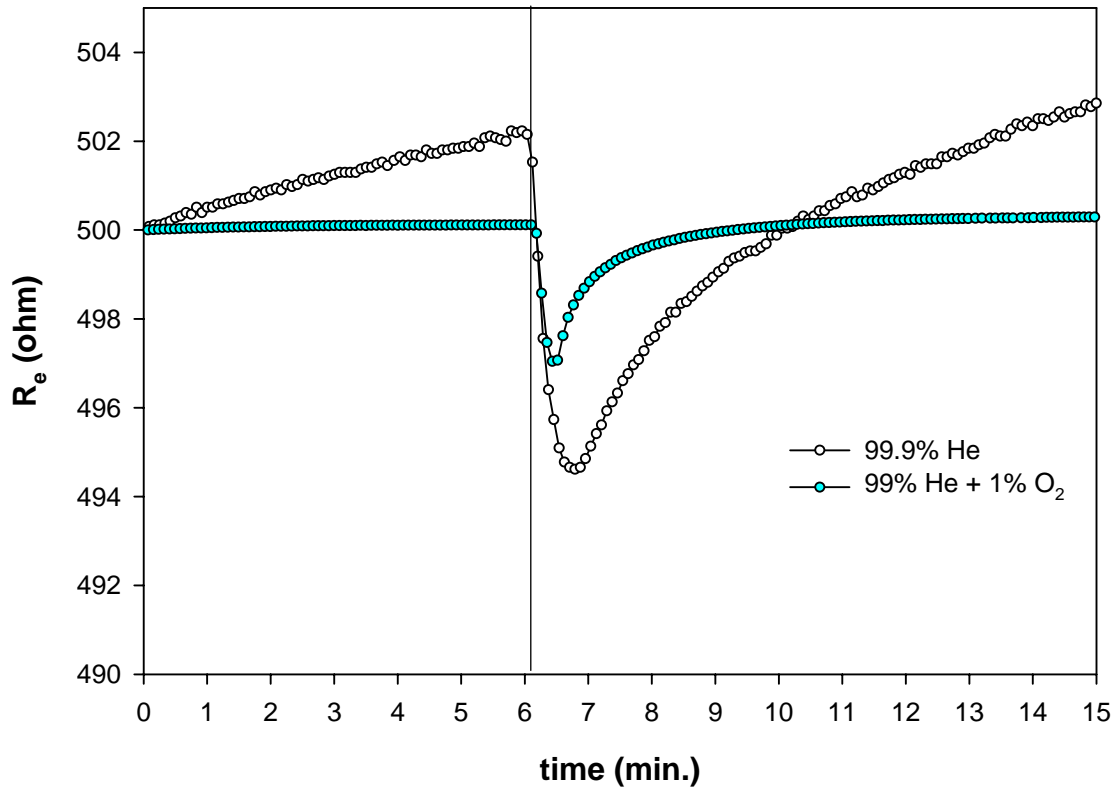


Figure 4.30. Comparison of Pd/SnO₂ multilayer thin film resistance behavior in oxygen free and 1% O₂ containing He atmosphere at 200°C

In Figure 4.29 and 4.30 unpromoted Pd/SnO₂ films resistance responses at 175 and 200 °C are compared. The resistance curves again indicate a more stable base line and the response time gets shorter in the case of oxygen containing atmospheres at the both temperatures as they do in the case of Na promoted Pd/SnO₂ films.

There was always a combustion reaction seem to occur in the sensing layer in the studied temperature range, which causes CO₂ evolution with a conversion depending on the temperature and the oxygen concentration in the atmosphere. The produced CO₂ peak was in lag with the CO injection peak, which was a result of CO₂ adsorption over the catalyst surface. Both peaks were not symmetric with respect to their maxima, which indicates the

adsorption and the desorption rates of the both gases in the catalyst was different from each other (Fig. 4.31).

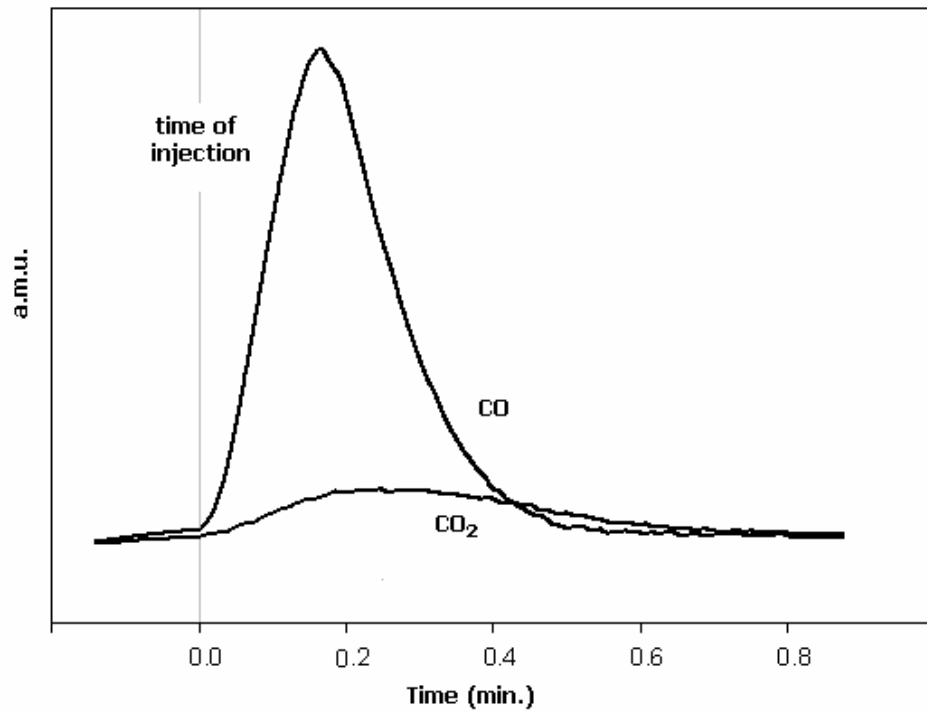


Figure 4.31. Typical CO injection, CO₂ production mass signal over the studied SnO₂ based test sensors

In the injection studies, when the CO gas introduced into the reaction chamber the resistance sharply decreased to a lower level and as the surface was cleaned by the carrier gas, it gradually reached to a higher point than the previous one, until the next injection is applied. Except this increasing resistance behavior, the response of sensor to the reducing gas was similar to the other kinds of gas sensors. This behavior can be arisen as a result of the gas trying to penetrate into the film. In this case, an initial rapid response takes place, but the sensor does not reach to a stable value of the resistance because of the difficulty of gas diffusion imposed by the structure of the film, as explained by Delgado [45].

In the Figure 4.32, the resistance response and the concentration changes at the exit of the reaction cell can be seen as a mass spectrometer signal. From the carbon dioxide concentration change it is obvious that there is not only adsorption also a reaction occurring at the surface as described in the Eqn. 4.1 and 4.2. There is also a change in the water concentration in the reaction cell exit gas. Another reason for the water desorption from the catalytic layer can be the reaction between the chemisorbed CO and the surface hydroxyl groups as explained by Karakaş et. al. [73]. In the same study they proposed the reaction sequence as,



where S indicates an active site for adsorption.

Na promotion increases the oxygen affinity of the surface. And therefore during the calcination process of the films the number of oxygen ions adsorbed on the surface increases in the presence of Na. At low temperatures, in oxygen free atmospheres the unpromoted Pd/SnO₂ films' surface preferentially adsorbs O₂⁻; therefore the sensitivity of the material is small. Because the O₂⁻ species are unstable and do not play much role in determining the sensitivity. So, Na promotion is advantageous at low temperatures and in oxygen free conditions. This difference is evident when the resistance response of the unpromoted Pd/SnO₂ films is considered (4.33). The production of carbon dioxide is obvious but there is no water formation in the reaction cell exit gas.

In 1% oxygen containing atmospheres at 150 °C, unpromoted Pd/SnO₂ film has a better resistance response curve and a more evident carbon dioxide production in the reaction cell exit gas (Fig. 4.34-35).

In the oxygen containing atmospheres there are greater amount of surface hydroxyls, so the reaction sequence can be explained as followed, where S indicates an active site again;

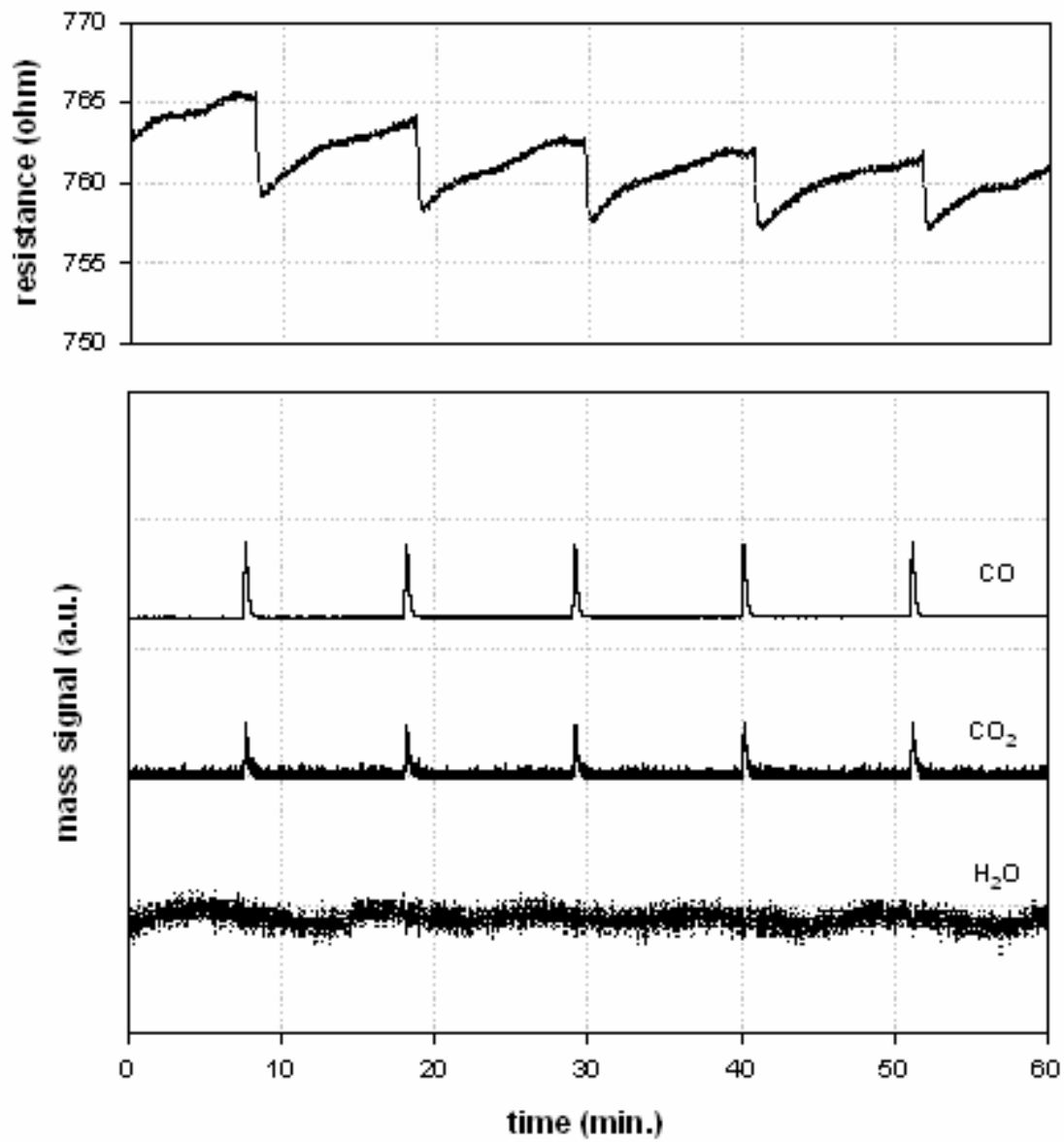


Figure 4.32. Response of Na-Pd/SnO₂ test sensor to CO injections at 150°C in He atmosphere (CO₂ and H₂O mass signals enlarged 50 times)

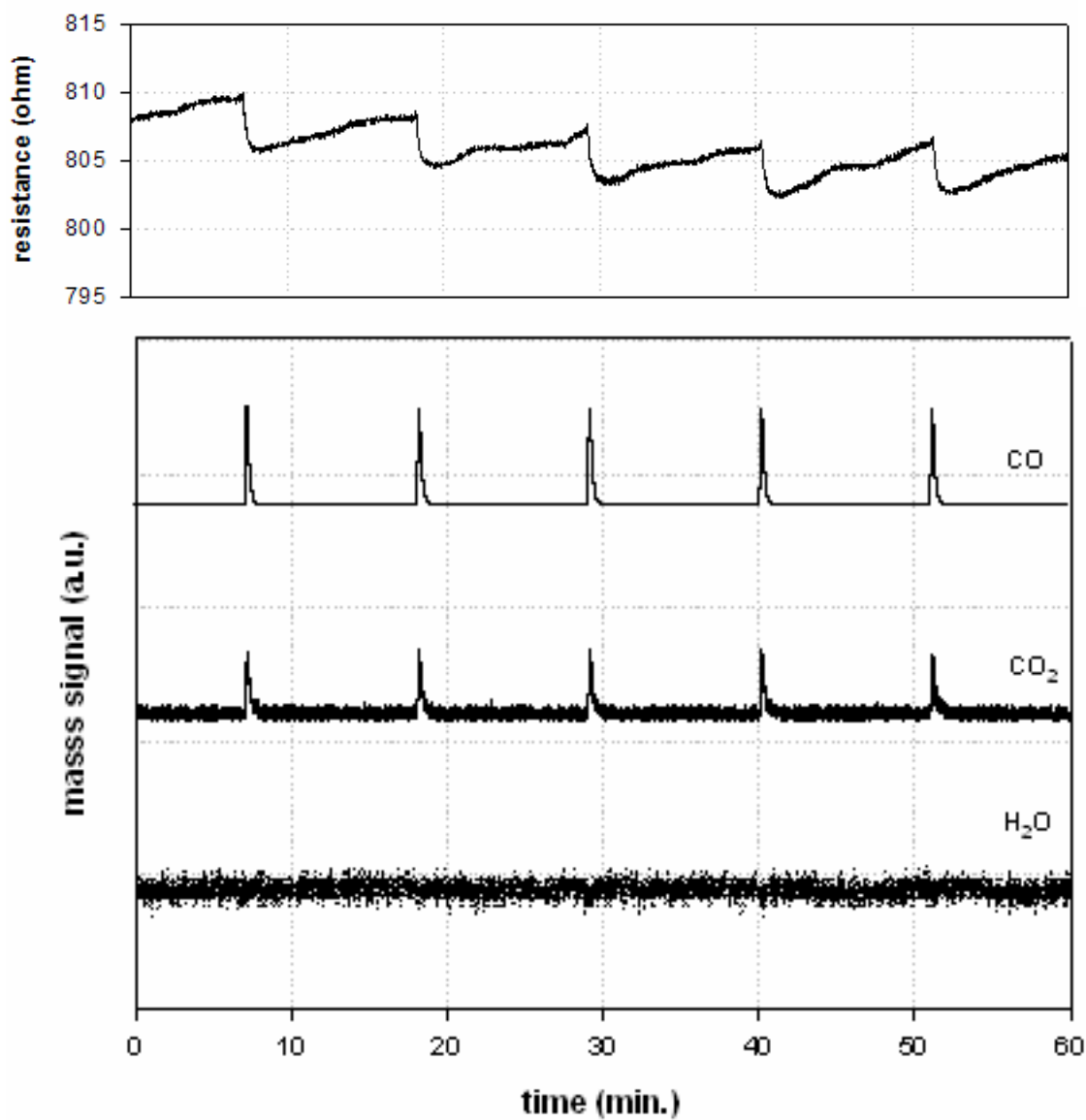


Figure 4.33. Response of Pd/SnO₂ test sensor to CO injections at 150°C in He atmosphere (CO₂ and H₂O mass signals enlarged 50 times)

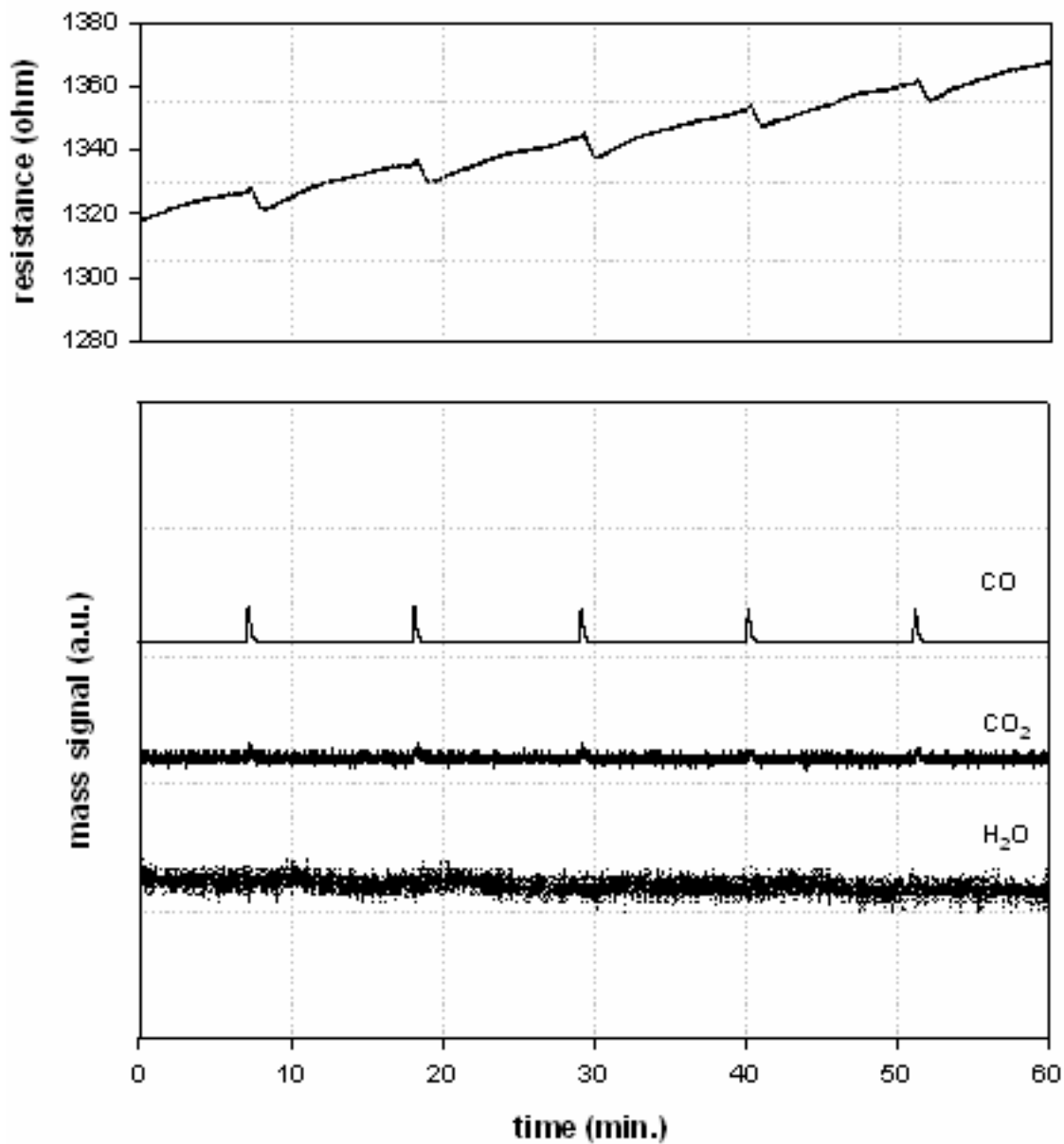


Figure 4.34. Response of Na-Pd/SnO₂ test sensor to CO injections at 150°C in 1% O₂ + 99% He atmosphere (CO₂ and H₂O mass signals enlarged 50 times)

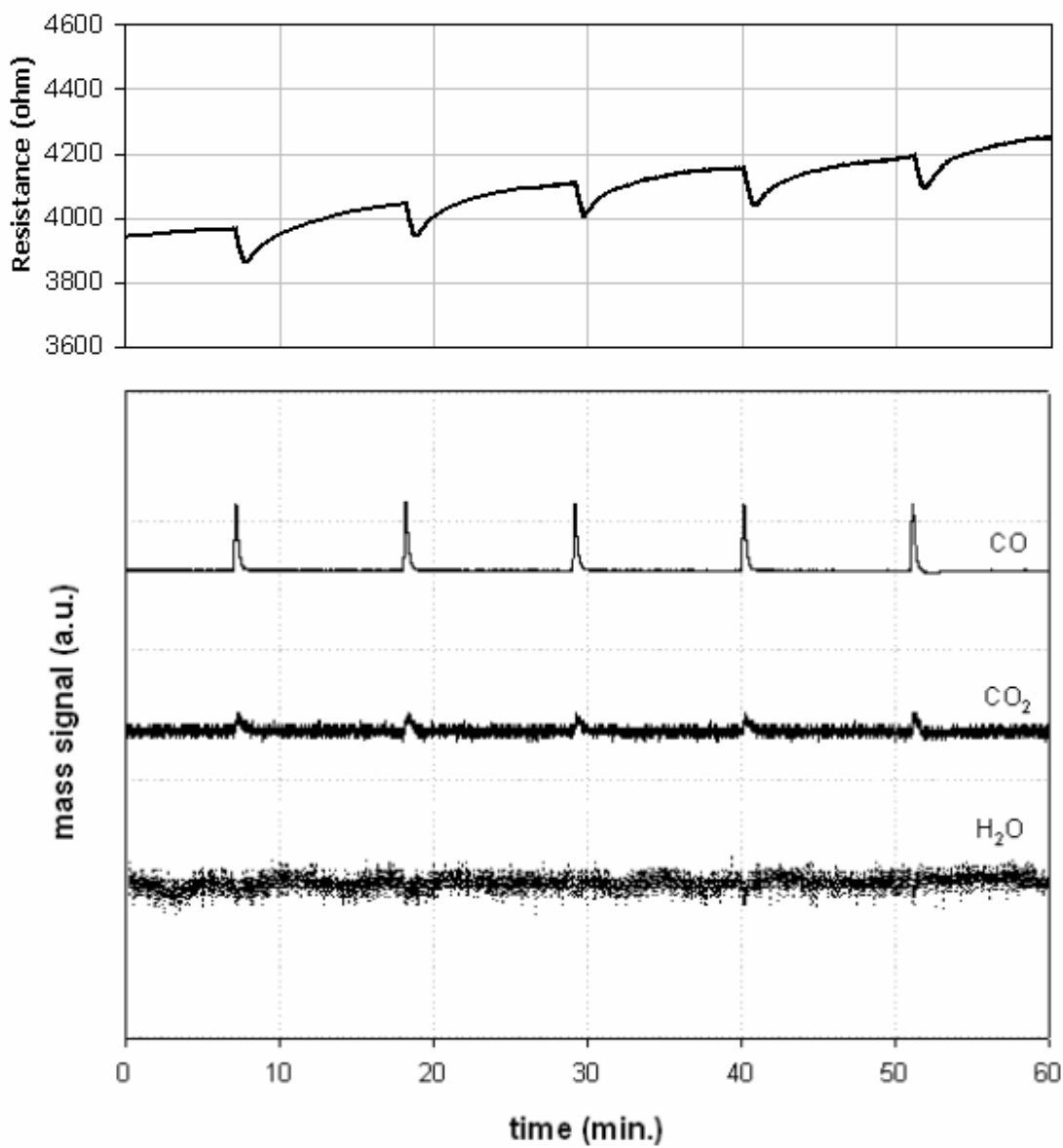
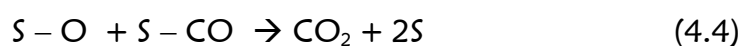


Figure 4.35. Response of Pd/SnO₂ test sensor to CO injections at 150°C in 1% O₂ + 99% He atmosphere (CO₂ and H₂O mass signals enlarged 50 times)



The Na promoted Pd/SnO₂ films show a good response reversibility at a low temperature of 150°C in oxygen free atmospheres when compared with the unpromoted Pd/SnO₂ films (Fig. 4.33). But, the number of cycles was too small to reach a stable response. However the electrical response under CO seems to tend toward a reproducible value.

When the experiments conducted at 175 °C are considered in oxygen free atmosphere (Fig. 4.36-37), there is a slight change in the resistance responses though the carbon dioxide formation is quite evident in the case of Na promoted catalyst. This shows the sensor signal is not directly correlated to the CO₂ production. At lower temperatures than 200°C, CO adsorption may occur without oxidation of the adsorbed gas and the subsequent release of electrons into the conduction band. Starke [2] et al. reported that the nanoparticles and multilayer coating have increased the surface area the adsorption of the CO molecules might have a marked affect on the conductivity of the film without an oxidation reaction taking place. They had also mentioned this behavior was supported by the fact that CO adsorbs strongly at temperatures below 200°C. And the CO signal is not related directly with the CO₂ production.

A larger sensor signal is not necessarily seen in the result of consumption reaction. Schmid et al. [38] explained this result telling that in the presence of very small amount of oxygen and water, CO could adsorb on the surface of the sensitive layer and act as an electron donor. The released electron was inserted into the conduction band of the material and this resulted with an increase in the conductivity of the material. But in higher oxygen containing atmospheres the generation of CO₂ is the main reaction, though resulting with a less electrical effect than the adsorption.

Looking the experiments conducted with Pd/SnO₂ and Na-Pd/SnO₂ at 175°C in the oxygen containing atmosphere (Fig. 4.38-39), it can be seen that

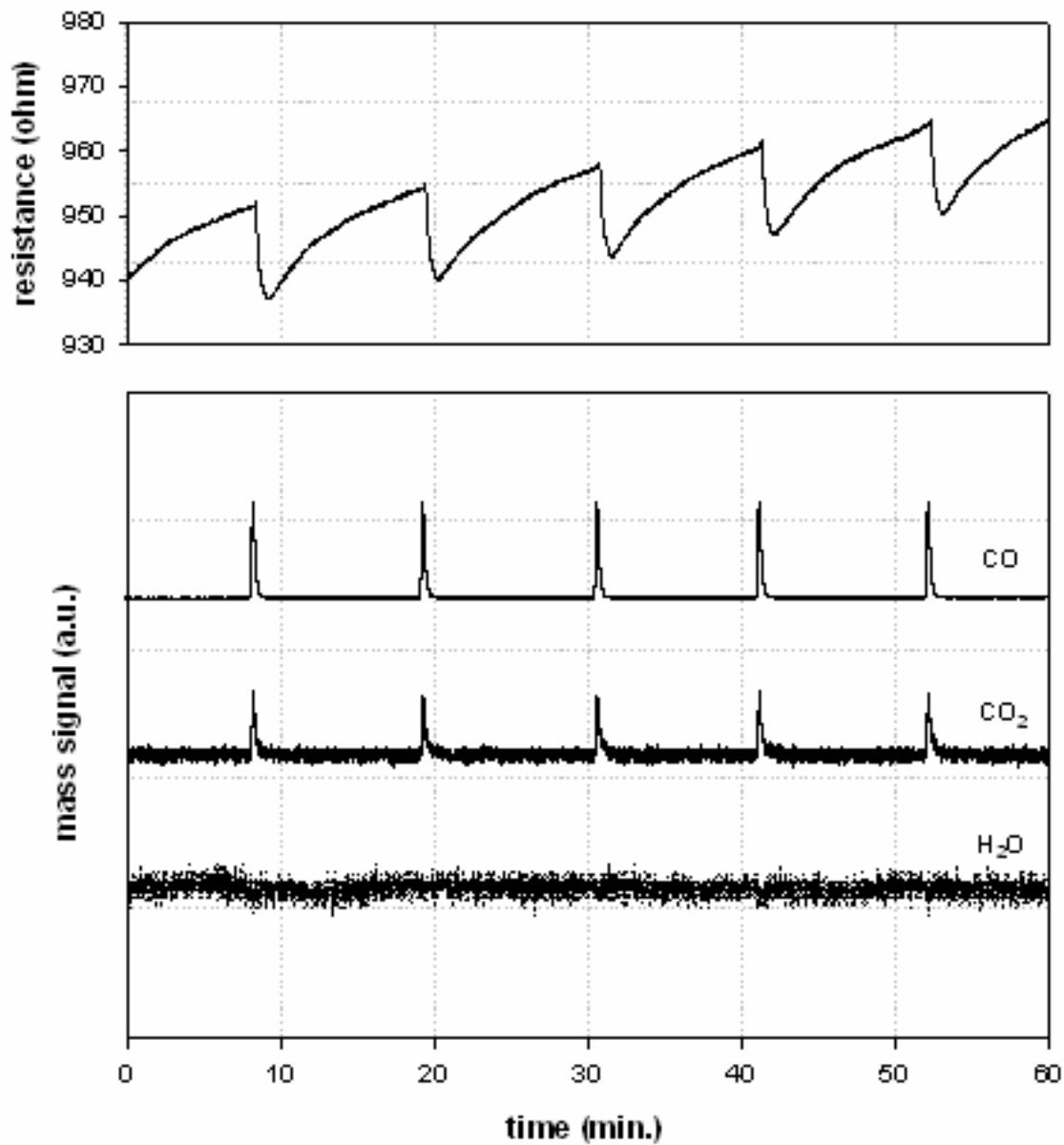


Figure 4.36. Response of Na-Pd/SnO₂ test sensor to CO injections at 175°C in He atmosphere (CO₂ and H₂O mass signals enlarged 50 times)

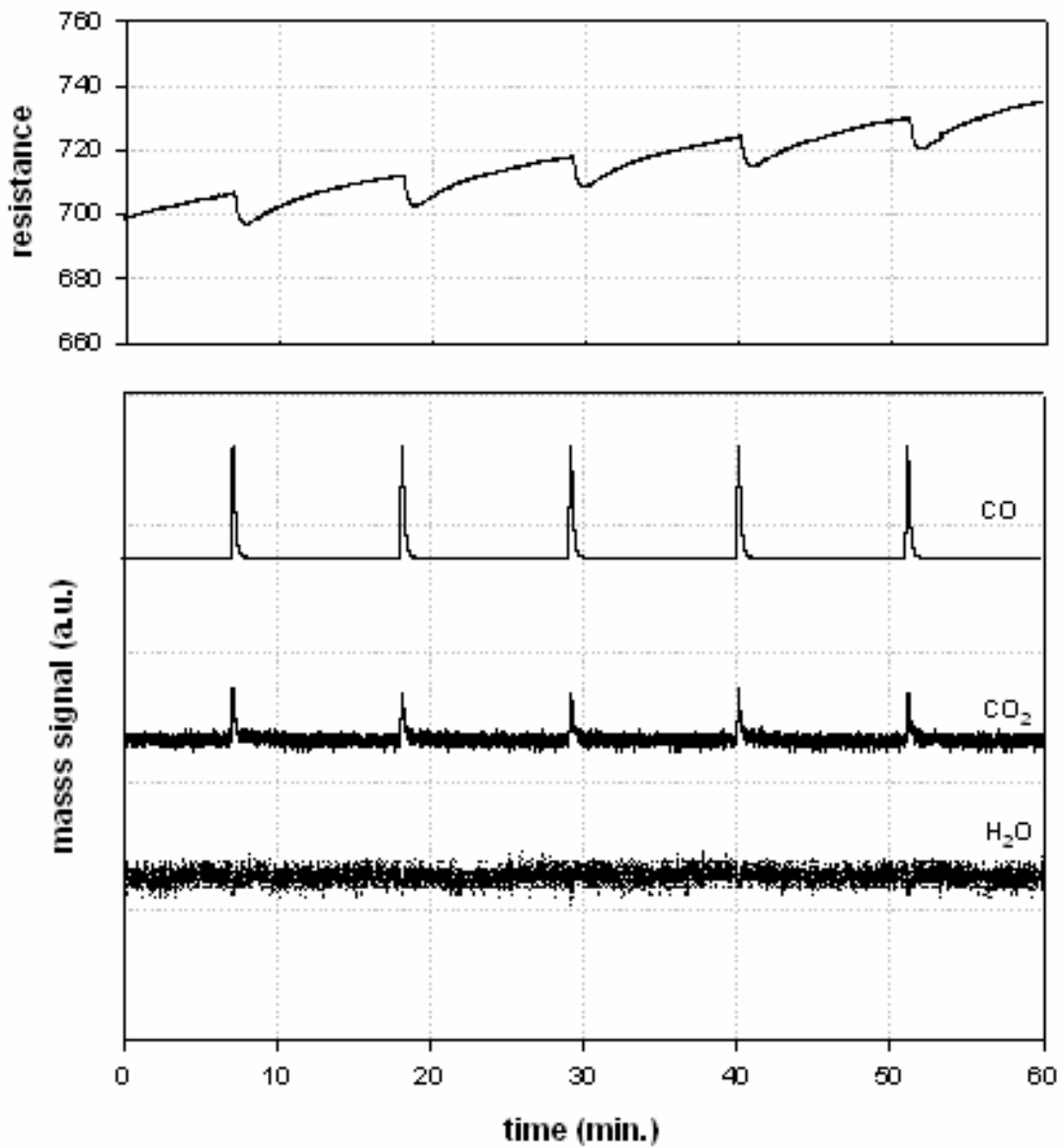


Figure 4.37. Response of Pd/SnO₂ test sensor to CO injections at 175°C in He atmosphere (CO₂ and H₂O mass signals enlarged 50 times)

there was a significant water formation in the exit gas. The water molecules apparently block the adsorption or reaction sites for the CO molecules, which leads to a smaller CO consumption in the Na promoted Pd/SnO₂ films.

The study by Mirkelamoğlu [62], also supports the water evaluation from the surface upon exposure to CO, both in the semiconductor support and the metallic catalyst. Semiconductor oxide gas sensor performance is also dependent on the water vapor concentration and the responses to combustible gases are affected by the ambient atmosphere humidity. It was investigated that the surface of tin dioxide adsorbs approximately 40 times greater quantities of water than oxygen [33].

Kappler et al. [73] reported in their study on Pd promoted SnO₂ thick films, the CO consumption was increased with the increasing temperature in the 200-400°C range. They also declared that the CO consumption was decreasing with the increasing humidity in 0-50 % r.h. range, at all investigated temperatures, however, the sensor signal of the sensor were increased with humidity.

Water can be absorbed in the form of physisorbed neutral molecules, hydrogen bonded molecules and chemisorbed reactive water molecules or as surface Sn-OH groups [33]. The H₂O molecules also interact with the semiconductor surface and lead to complex effects on the conductance evolution as a function of temperature. Adsorption of water on the surface results with the CO₂ production and protonated water, which affects the electrical response through the insertion of an electron into the conduction band (Fig. 2.13). The hydrogen atoms can also react with lattice oxygen atoms and produce oxygen vacancies as donors and surface hydroxyl groups. Thus chemisorbed water increases surface conductivity of the tin oxide.

It was reported in the study by Briand et al. [19], that in the films produced by the spray pyrolysis method, Pd doped SnO₂ films had higher resistivity than the undoped films that might be due to a transfer of electrons from the SnO₂ to the metal which could occur since the palladium work function is higher. In the experiments conducted in He atmosphere, generally

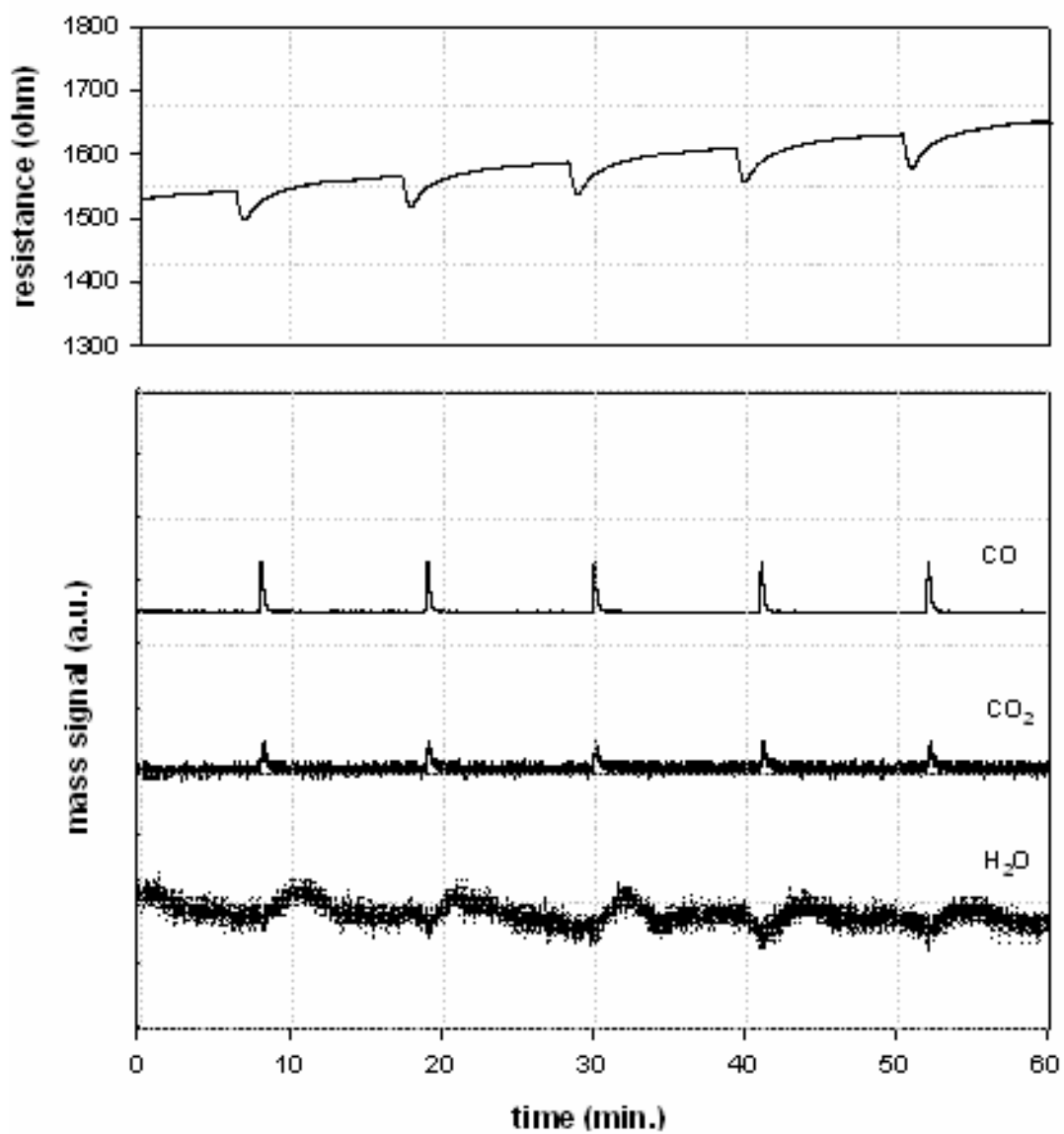


Figure 4.38. Response of Na-Pd/SnO₂ test sensor to CO injections at 175°C in 1% O₂ + 99% He atmosphere (CO₂ and H₂O mass signals enlarged 50 times)

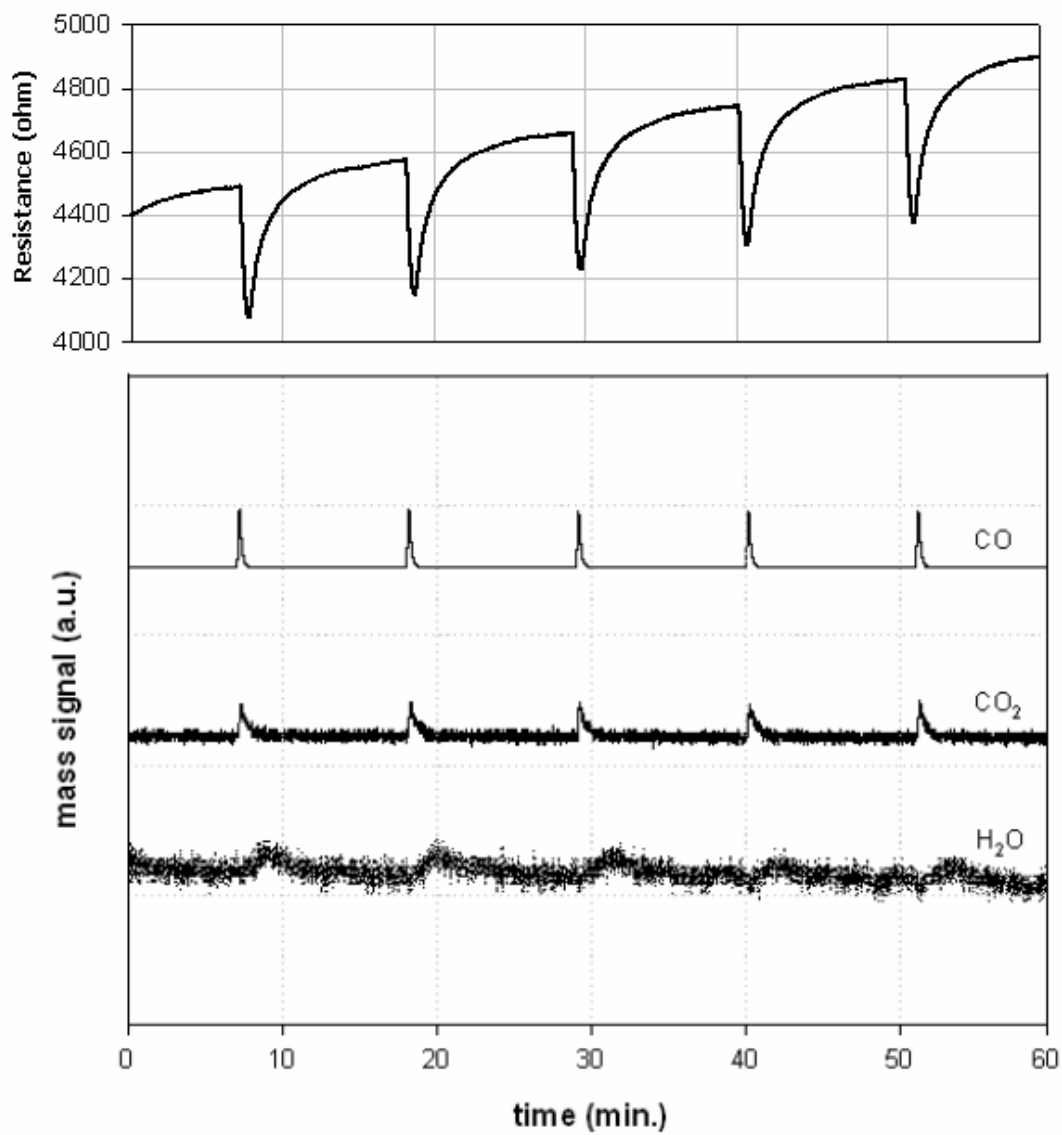


Figure 4.39. Response of Pd/SnO₂ test sensor to CO injections at 175°C in 1% O₂ + 99% He atmosphere (CO₂ and H₂O mass signals enlarged 50 times)

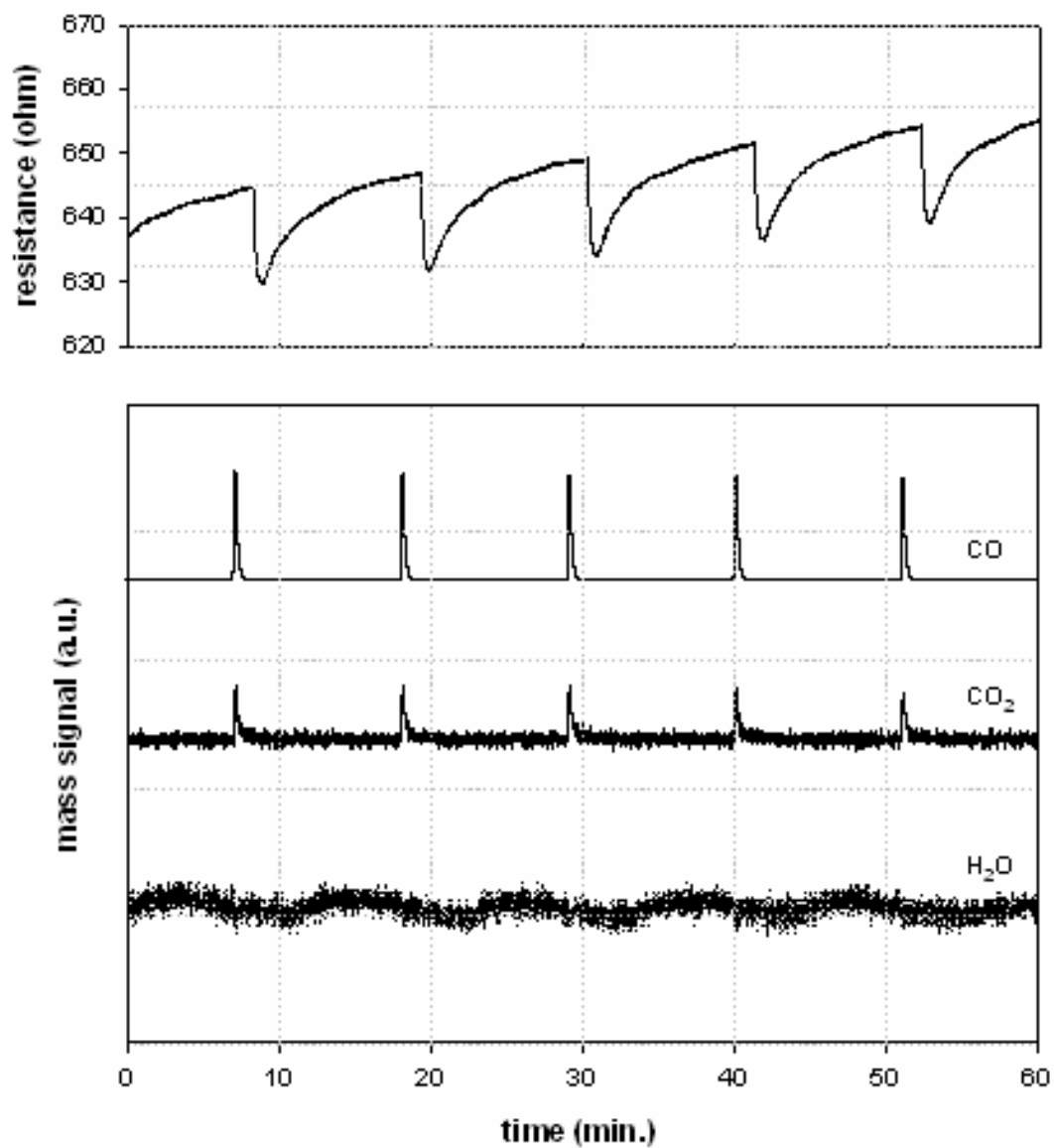


Figure 4.40. Response of Na-Pd/SnO₂ test sensor to CO injections at 200°C in He atmosphere (CO₂ and H₂O mass signals enlarged 50 times)

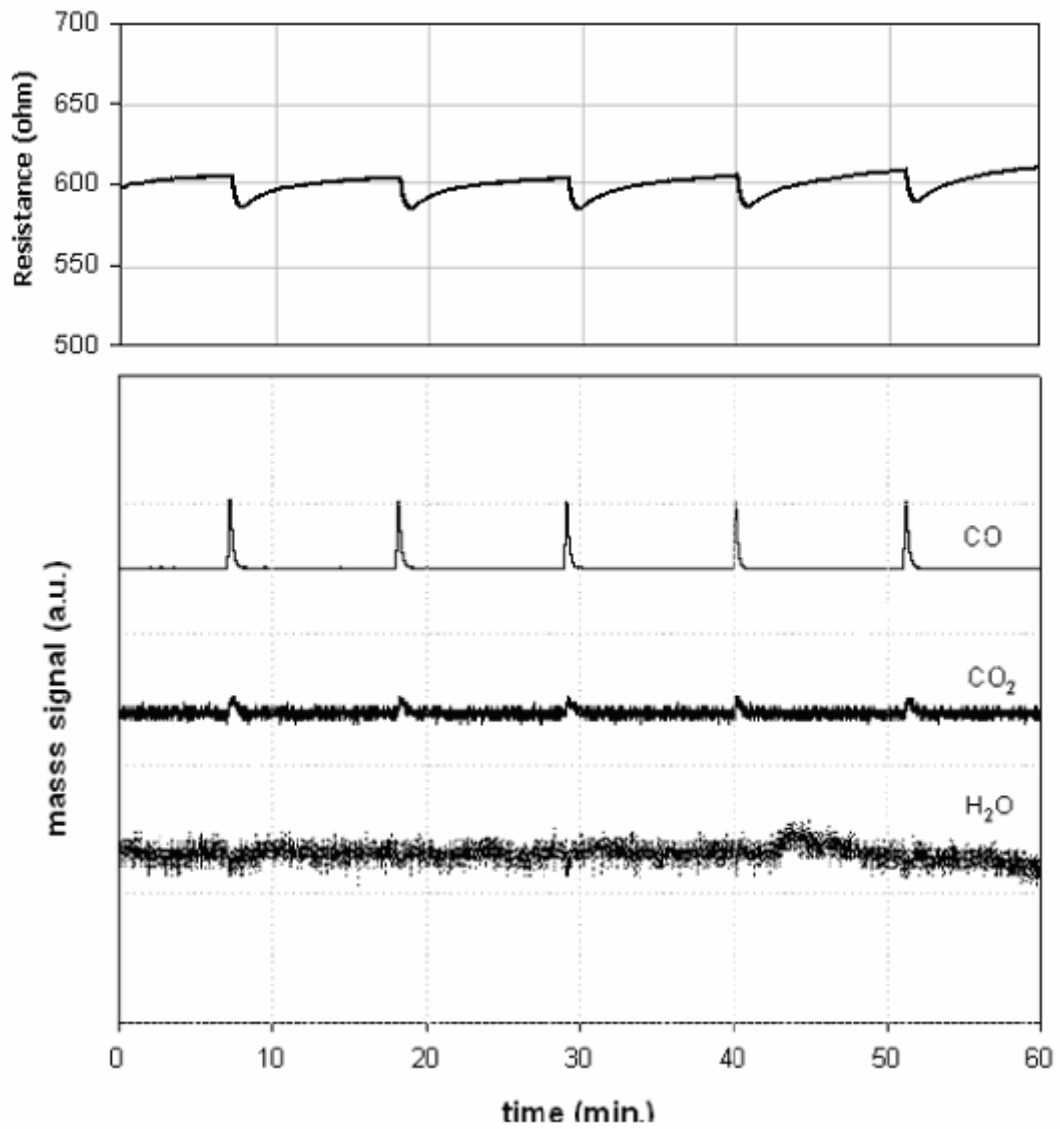


Figure 4.41. Response of Pd/SnO₂ test sensor to CO injections at 200°C in He atmosphere (CO₂ and H₂O mass signals enlarged 50 times)

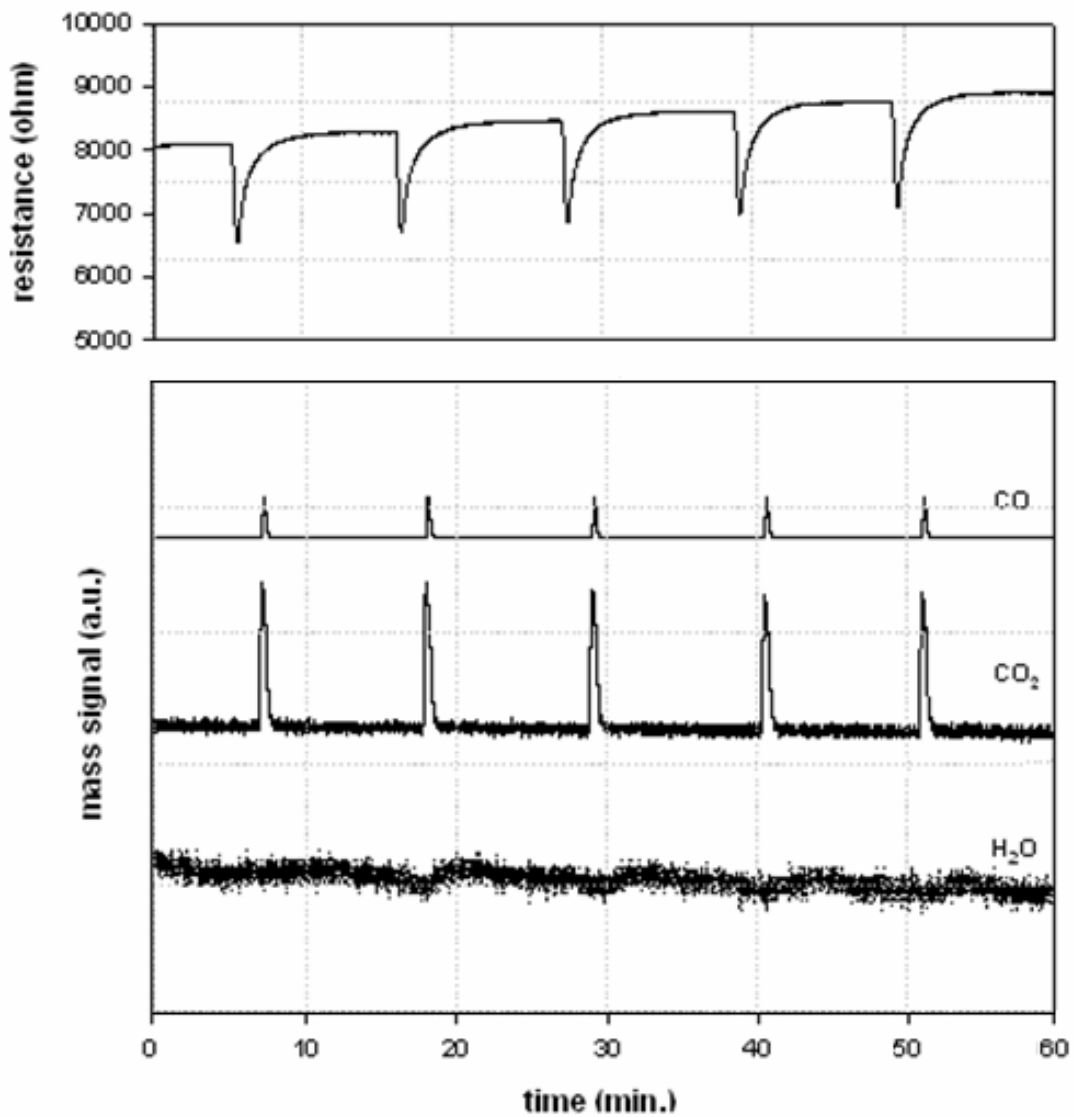


Figure 4.42. Response of Na-Pd/SnO₂ test sensor to CO injections at 200°C in 1% O₂ + 99% He atmosphere (CO₂ and H₂O mass signals enlarged 50 times)

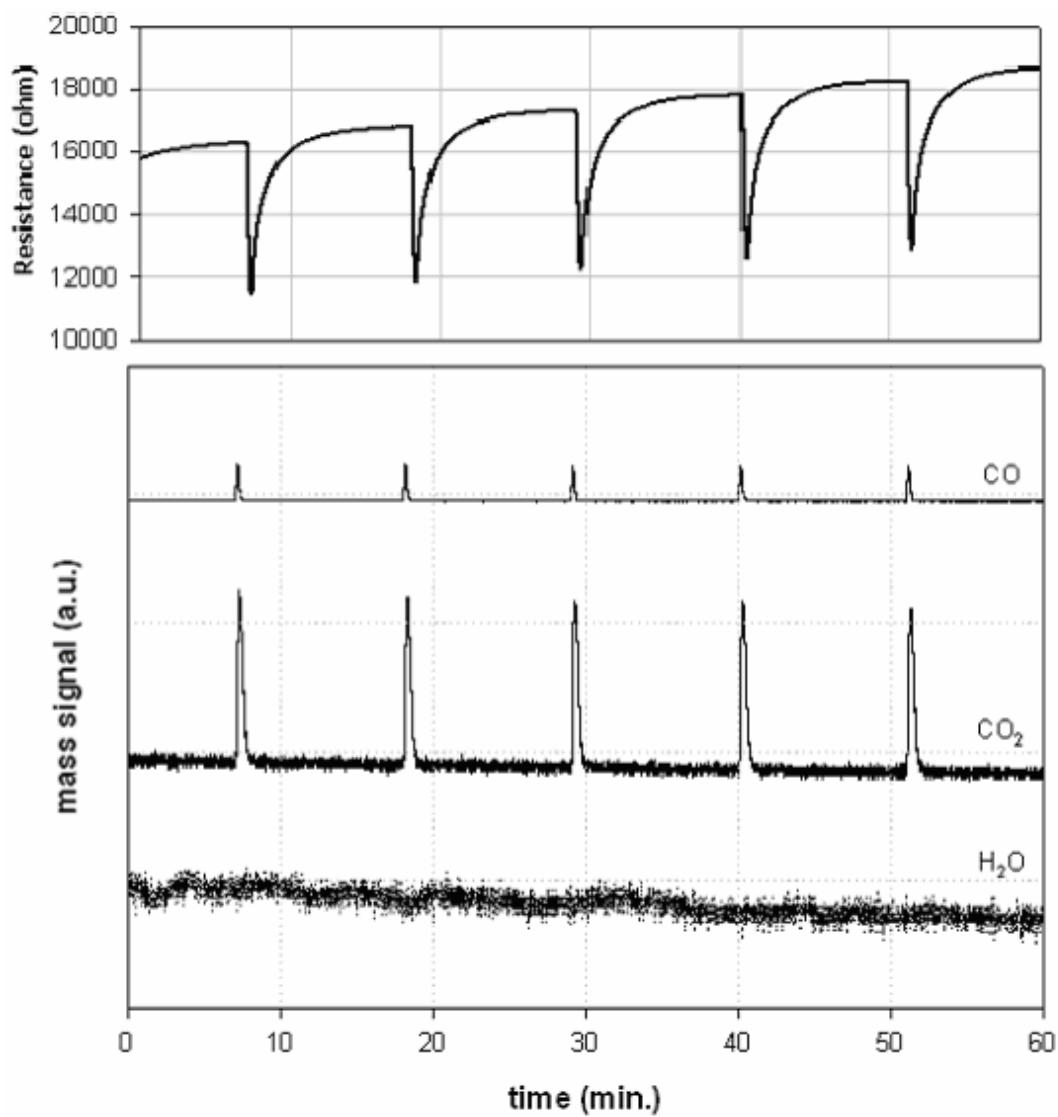


Figure 4.43. Response of Pd/SnO₂ test sensor to CO injections at 200°C in 1% O₂ + 99% He atmosphere (CO₂ and H₂O mass signals enlarged 50 times)

the surface resistance of the films were decreasing as the operating temperature increases as was expected, except the one conducted at 175°C with Na-Pd /SnO₂ test sensor. The resistance was surprisingly larger at 175°C than 150°C. On the contrary, in the experiments conducted in 1% oxygen containing atmosphere the resistance was increasing continuously which shows a continuous surface oxidation. In the oxygen containing atmosphere, the resistance drastically increased from 175°C to 200°C. This increase in the resistance is more obvious in the case of Pd/SnO₂ test sensors, which is in agreement with the resistance responses. At 200°C, the resistance responses of Pd/SnO₂ is 3 times larger than the Na-Pd promoted test sensor responses in the oxygen containing atmosphere (Fig. 4.42-43).

When unpromoted Pd/SnO₂ sensor response results are considered, at 150, 175 and 200 °C, in oxygen free atmospheres (Fig. 4.33, 4.37 and 4.41), it is clear that in the possibility of adsorption and reaction, the direct adsorption results with a larger electrical effect.

Investigations showed that on heating to 100°C only a minor water loss was observed, and the major loss occurred between the 240-450°C temperature range. Among the possibilities of adsorption, reaction with hydroxyl groups or ionosorbed oxygen, the direct adsorption results in the largest electrical effect followed by the reaction with hydroxyl groups and the reaction with ionosorbed oxygen [38].

CHAPTER 5

CONCLUSIONS AND FURTHER SUGGESTIONS

1 wt. % Pd promoted SnO₂ and 0.1 wt. % Na, 1 wt. % Pd promoted SnO₂ multilayer thin films have been prepared by sol-gel synthesis and coated on the soda-lime glass substrates by spin coating method. Injection studies with carbon monoxide were performed at the selected temperatures of 150, 175 and 200 °C in oxygen free and 1% oxygen containing helium atmospheres. The following conclusions are drawn from the data elaborated:

- Sol-gel synthesis is a proper method to obtain a homogeneous structure through a coated layer. Besides, the film morphology is mostly dependent on the deposition method. Spin coating technique provides a homogeneous structure throughout the film.
- Injection experiments performed with methane at 200 °C showed that the injection method used in the study is not proper for methane sensing. Injection period is too short either for the catalytic layer to sense methane or for methane to diffuse within the pores of the sensing layer. For methane studies the injection period should be increased, i.e., by increasing the reaction cell.
- The responses are temperature dependent and none of the sensors show a distinguishable response from the base line below 150 °C. The responses become more significant with the increasing temperature. The resistance response curves show that both types of the sensors achieve the best responses at the operating temperature of 200 °C.
- Alkali promotion enhances the oxygen adsorption on the surface. And, the increased number of the surface adsorbed oxygen species

causes a shorter response time and a larger resistance response in the case of oxygen free atmospheres. As an extension of this study the effect of other noble metals can be considered.

- In the case of Na promoted Pd/SnO₂ type of test sensor, addition of Na enhances the oxygen adsorption on the catalytic surface. Though in oxygen free atmospheres this provides better responses, in oxygen containing atmospheres addition of oxygen hinders the CO adsorption by the blockage of the active sites by oxygen. So, Na promotion is advantageous in oxygen free conditions and at relatively low temperatures.
- The sensor signal is not directly correlated with the CO₂ production. At lower temperatures than 200°C, CO adsorption may occur without the oxidation of the reducing gas and the subsequent release of electrons to the conduction band. In the presence of very small amount of oxygen and water, CO could adsorb on the surface of the sensitive layer and act as an electron donor. The released electron was inserted into the conduction band of the material and this resulted with an increase in the conductivity of the material. But in higher oxygen containing atmospheres the generation of CO₂ is the main reaction.
- In oxygen free atmospheres, in the possibility of adsorption and reaction, the direct adsorption results with a larger electrical effect.

REFERENCES

- [1] Baraton, M.I., Merhari, L., "Nanoparticles-based chemical gas sensors for outdoor air quality monitoring microstations", *Materials Science and Engineering B*, 112, 2004, p.206-213
- [2] Starke, T.K.H., Coles, G.S.V., "Laser-ablated nanocrystalline SnO₂ material for low-level CO detection", *Sensors and Actuators B*, 88, 2003, p. 227-233
- [3] Centi,G., Ciambelli,P., Perathoner,S., Russo,P., "Environmental catalysis: trends and outlook", *Catalysis Today*, 75, 2002, p.3-15
- [4] Mizsei, J., Voutilainen, J., Saukko, S., Lantto, V., "Structural transformations of ultra-thin sputtered Pd activator layers on glass and SnO₂ surfaces", *Thin Solid Films*, 391, 2001, p. 209-215
- [5] Tsang, S.C., Bulpitt, C.D.A., Mitchell, P.C.H., Ramirez-Cuesta A.J., "Some new insights into the sensing mechanism of palladium promoted tin (IV) oxide sensor", *J.Phys. Chem. B*, 105, 2001, p. 5737-5742
- [6] Korotcenkov, G., Brinzari, V., Boris,Y., Ivanov, M., Schwank, J., Morante,J., "Influence of surface Pd doping on gas sensing characteristics of SnO₂ thin films deposited by spray prolysis", *Thin Solid Films*, 436, 2003, p. 119-126
- [7] Sciliano, P., "Preparation, characterisation and applications of thin films for gas sensors prepared by cheap chemical method", *Sensors and Actuators B*, 70, 2000, p. 153-164
- [8] Yamazoe, N., Kurokawa, Y., Seiyama, T., "Effects of additives on semiconductor gas sensors", *Sensors and Actuators*, 4, 1983, p. 283-289
- [9] Wei, B., Hsu, M., Su, P., Lin, H., Wu, R., Lai, H., "A novel SnO₂ gas sensor doped with carbon nanotubes aperating at room temperature", *Sensors and Actuators B*, 101,2004, p. 81-89
- [10] Yamazoe, N., "New approaches for improving semiconductor gas sensors", *Sensors and Actuators*, 5, 1991, p. 7-19

- [11] Moseley, P., "Review Article: Solid state gas sensors", *Materials Science and Technology*, 8, 1997, p.224-237
- [12] Barsan, N., Schwizer-Barberich, M., Göpel, W., "Fundamental and practical aspects in the design of nanoscaled SnO₂ gas sensors: a status report", *Fresenius J. Anal Chem.*, 365, 1999, p. 287-304
- [13] Castro, M.S., Aldao, C.M., "Effects of thermal treatments on the conductance of tin oxide", *Journal of European Ceramic Society* 20, 2000, p. 303-307
- [14] Choi, S., Lee, D., "CH₄ sensing characteristics of K-, Ca-, Mg impregnated SnO₂ sensors", *Sensors and Actuators B*, 77, 2001, p. 335-338
- [15] Saukko, S., Lantto, V., "Influence of electrode material on properties of SnO₂-based gas sensor", *Thin Solid Films*, 436, 2003, p. 137-140
- [16] Montmeat, P., Lalauze, R., Viricelle, G., Pijolat, C., "Model of thickness effect of SnO₂ thick film on the detection properties", *Sensors and Actuators B*, 103, 2004, p. 84-90
- [17] Delabie, L., Honore, M., Lenaerts, S., Huyberegts, G., Roggen, J., Maes, G., "The effect of sintering and Pd-doping on the conversion of CO to CO₂ on SnO₂ gas sensor materials", *Sensors and Actuators B*, 44, 1997, p. 446-451
- [18] Hammond, J.W., Liu, C., "Silicon based microfabricated tin oxide gas sensor incorporating use of Hall effect measurement", *Sensors and Actuators B*, 81,2001, p. 25-31
- [19] Briand, D., Labeau, M., Currie, J.f., Delabouglise, G., "Pd-doped SnO₂ films deposited by assisted ultrasonic spraying CVD for gas sensing: selectivity and effect of annealing", *Sensors and Actuators B*, 48, 1998, p. 395-402
- [20] Harbeck, S., Szatvanyi, A., Barsan, N., Weimar, U., Hoffman, V., "DRIFT studies of thick film un-doped and Pd-doped SnO₂ sensors: temperature changes effect and CO detection mechanism in the presence of water vapour", *Thin Solid Films*, 436, 2003, p. 76-83
- [21] Göpel, W., Schierbaum, K.D., "SnO₂ sensors: current status and future prospects", *Sensors and Actuators B*, 26-27, 1995, p. 1-12
- [22] Heilig, A., Barsan, N., Weimar, U., Göpel, W., "Selectivity enhancement of SnO₂ gas sensors: simultaneous monitoring of resistances and temperatures", *Sensors and Actuators B*, 58, 1999, p. 302-309

- [23] Jin, Z., Zhou, H., Jin, Z., Savinell, R.F., Liu, C., “Application of nano-crystalline porous tin oxide thin film for CO sensing”, *Sensors and Actuators B*, 52, 1998, p. 188-194
- [24] Cobaniu, C., Savaniu, C., Buiu, O., Dascalu, D., Zaharescu, M., Parlog, C., Berg, A., Pecz, B., “Tin dioxide sol-gel derived thin films deposited on porous silicon”, *Sensors and Actuators B*, 43, 1997, p. 114-120
- [25] Fraden, J., “Handbook of modern sensors, physics, design and applications”, United Book Press. Inc., 1996, 2nd edition
- [26] Chau, J., “Hazardous Gas Monitors, “A Practical Guide to Selection, Operation and Applications”, Scitech Publishing, 2000
- [27] Barsan, N., Stetter, J.R., Findlay, M., Göpel, W., “High performance gas sensing CO: comparative tests for (SnO₂ based) semiconducting and for electrochemical sensors”, *Sensors and Actuators B*, 66, 2000, p. 31-33
- [28] Severcan, I., “Dynamic resistivity behavior of tin oxide based thick films under reducing and oxidizing conditions”, M.S. Thesis, 2002, Ankara
- [29] Dalin, C., “Fabrication and characterization of a novel MOSFET gas sensor”, Final Thesis, 2002, Freiburg
- [30] Niranjana, R.S., Mulla, I.S., “Spin coated tin oxide: a highly sensitive hydrocarbon sensor”, *Materials and Engineering B*, 103, 2003, p.103-107
- [31] Yoon, D.H., Choi, G.M., “Microstructure and CO gas sensing properties of porous ZnO produced by starch addition”, *Sensors and Actuators B*, 45, 1997, p. 251-257
- [32] Tiburcio-Silver, A., Sanchez-Juarez, A., “SnO₂: Ga films as oxygen gas sensor”, *Materials Science and Engineering B*, 101, 2004, p. 268-271
- [33] Tang, Y., “Synthesis and characterization of tin oxide for thin film gas sensor applications”, Ph.D. Thesis, 2004, Case Western Reserve University
- [34] Wang, Y., Wu, X., Li, Y., Zhou, Z., “Mesostructured SnO₂ as sensing material for gas sensors”, *Solid-State Electronics*, 48, 2004, p. 627-632
- [35] Cabot, A., Vila, A., Morante, J.R., “Analysis of the catalytic activity and electrical characteristics of different modified SnO₂ layers for gas sensors”, *Sensors and Actuators B*, 84, 2002, p. 12-20

- [36] Ertl, G., "Heterogeneous catalysis on the atomic scale", The Japan Chemical Journal Forum and John Wiley & Sons, Inc., 2001, Chem. Rec. 1:33-45
- [37] K.D. Schierbaum, U. Weimar and W. Göpel, "Multicomponent gas analysis: an analytical chemistry approach applied to modified SnO₂ sensors", Sensors and Actuators B, 2, 1990, p. 71-78
- [38] Schmid, W., Barsan, N., Weimar, U., "Sensing of hydrocarbons and CO in low oxygen conditions with tin dioxide sensors: possible conversion paths", Sensors and Actuators B, 103, 2004, p. 362-368
- [39] Wurzinger, O., Reinhardt, G., "CO sensing properties of doped SnO₂ sensors in H₂-rich gases", Sensors and Actuators B, 103, 2004, p. 104-110
- [40] Sermon, A.P., Self, V.A., Barrett, E.P.S., "Analysis of Pt/SnO_x during catalysis of CO oxidation", Journal of Molecular Catalysis, 65, 1991, p.377-384
- [41] Hahn, S.H., Barsan, N., Weimar, U., Ejakov, S.G., Visser, J.H., Soltis, R.E., "CO sensing with SnO₂ thick film sensors: role of oxygen and water vapour", Thin Solid Films, 436, 2003, p.17-24
- [42] Sze, S.M., "Semiconductor Devices Physics and Technology, John Willey & Sons, Inc., 2nd edition, 2002
- [43] Kapoor, A., Yang, R.T., Wong, C., "Surface Diffusion", Catal. Rev. – Science and Engineering, 31 (1&2), 1989, p.129-214
- [44] Cha, K.H., Park, H.C., Kim, K.H., "Effect of palladium doping and film thickness on the H₂- gas sensing characteristics of SnO₂", Sensors and Actuators B, 21, 1994, p. 91-96
- [45] Delgado, R.D., "Tin oxide gas sensors: an electrochemical approach" Ph.D. Thesis, 2002, Barcelona
- [46] Sanchez, J.B., Berger, F., Fromm, M., Nadal, M.H., Eyraud, V., "Tin dioxide-based gas sensors for detection of hydrogen fluoride in air", Thin Solid Films, 436, 2003, p. 132-136
- [47] Licnerski, B.W., Nitsch, K., Teterycz, H., Sobanski, T., Wisniewski, K., "Characterization of electrical parameters for multilayer SnO₂ gas sensors", Sensors and Actuators B, 103, 2004, p. 69-75

- [48] Wu, H.C., Liu, L.C., Yang, S.M., "Effects of additives on supported noble metal catalysts for oxidation of hydrocarbons and carbon monoxide", *Applied Catalysis A: General*, 211, 2003, p. 159-165
- [49] Su, P.G., Chen, I.C., "Laminating two-layer thick films structure tin-oxide based butane gas sensor operating at low temperature", *Sensors and Actuators B*, 99, 2004, p. 304-309
- [50] Schmid, W., Barsan, N., Weimar, U., "Sensing of hydrocarbons with tin oxide sensors: possible reaction path as revealed by consumption measurements", *Sensors and Actuators B*, 89, 2003, p. 232-236
- [51] Capone, S., Epifani, M., Quaranta, F., Siciliano, P., Vasanelli, L., "Application of a semiconductor sol-gel sensor array to the discrimination of pollutants in air", *Thin Solid Films*, 391, 2001, p. 314-319
- [52] Date, M., Haruta, M. "Moisture effect on CO oxidation over Au/TiO₂ catalyst", *Journal of Catalysis*, 201, 2001, p. 221-224
- [53] Mandayo, G.G., Castano, E., Gracia, A., Cornet, A., Morante, J.R., "Strategies to enhance the carbon monoxide sensitivity of tin oxide thin films", *Sensors and Actuators B*, 95, 2003, p. 90-96
- [54] Sakai, G., Baik, N.S., Miura, N., Yamazoe, N., "Gas sensing properties of tin oxide thin films fabricated from hydrothermally treated nanoparticles, Dependence of CO and H₂ response on film thickness", *Sensors and Actuators B*, 77, 2001, p. 116-121
- [55] Gulati, S., Mehan, N., Mansigh, A., "Electrical equivalent model for SnO₂ bulk sensors", *Sensors and Actuators B*, 87, 2002, p. 309-320
- [56] Blaustein, G., Castro, M.S., Aldao, C.M., "Influence of frozen distributions of oxygen vacancies on tin oxide conductance", *Sensors and Actuators B*, 55, 1999, p. 33-37
- [57] Manorama, S.V., Reddy G., C.V., Rao, V.J., "Tin dioxide nanoparticles prepared by sol-gel method for an improved hydrogen sulfide sensor", *Nanostructured Materials*, 11, 1999, p.643-649
- [58] Chung, W.Y., Lee, D.D., Sohn, B.K., "Effects of added TiO₂ on the characteristics of SnO₂ based thick film gas sensors", *Thin Solid Films*, 221, 1992, p.304-310

- [59] Mirkelamoglu, B., Karakas, G., "CO oxidation over palladium- and sodium- promoted tin dioxide: catalyst characterization and temperature-programmed studies", *Applied Catalysis A: General*, 281, 2005, p. 275,284
- [60] Samorjai, G., A., "The Catalytic Hydrogenation of CO: The Formation of Cl Hydrocarbons", *Catal. Rev. Sci. Eng.*, 23 (1/2), 1981, p. 189
- [61] Lambert, R.M., Williams, F., Palermo, A., Tikhov, M.S., "Modelling alkali promotion in heterogeneous catalysis: in situ electrochemical control of catalytic reactions", *Topics in Catalysis*, 13, 2000, 91-98
- [62] Mirkelamoglu, B., "Investigation of carbon monoxide oxidation over tin dioxide based catalysts by dynamic methods", M.S. Thesis, 2002, Ankara
- [63] Brinzari, V., Korotcenkov, G., Golovanov, V., "Factors influencing the gas sensing characteristics of tin dioxide films deposited by spray prolysis: understanding and possibilities of control", *Thin Solid Films*, 391, 2001, p. 167-175
- [64] Tomaev, V.V., Tikhonov, P.A., Galimov, Y.B., "Behavior of water and oxygen molecules on the surface of tin dioxide films", *Glass Physics Chemistry*, 29, 2003, p. 621-625
- [65] Martinelli, G., Carotta, M.C., "Influence of additives on the sensing properties of screen-printed SnO₂ gas sensors", *Sensors and Actuators B*, 15-16, 1993, p. 363-366
- [66] Rella, R., Serra, A., Siciliano, P., Vasanelli, L. De, G., Liccuilli, A., Quirini, A., "Tin oxide-based gas sensors prepared by the sol-gel process", *Sensors and Actuators B*, 44, 1997, p. 462-467
- [67] Yildirim, F.A., "PZT films on stainless steel by chemical solution deposition", M.S.Thesis, 2002, Ankara
- [68] Ponce, M.A., Aldao, C.M., Castro, M.S., "Influence of particle size on the conductance of SnO₂ thick films", *Journal of the European Ceramic Society*, 23, 2003, p. 2105-2111
- [69] Decher, G., Schlenof, J.B., "Multilayer Thin Films, Sequential Assembly of Nanocomposite Materials", Wiley-VCH Verlag GmbH & Co., 2002
- [70] Bornside, D.E., Macasko, C.W., Scriven, "Spin Coating: One-Dimensional. Model", *Journal of Applied Physics*, 66, 1989, p. 5185

- [71] İzgi, E., “Characterization of superconducting Bi-Sr-Ca-Cu-O system prepared by sol-gel processing”, M.S. Thesis, 1996, Ankara
- [72] Labeau, M., Gautheron, B., Deabouglise, G., Pena, J., Ragel, V., Varela, A., Roman, J., Martinez, J., Gonzalez-Calbet, M., Vallet-Regi, M., “Synthesis, structure and gas sensitivity properties of pure and doped SnO₂”, Sensors and Actuators B, 15-16, 1993, p. 379-383
- [73] Kappler, J., Tomescu, A., Barsan, N., Weimar, U., “CO consumption of Pd doped SnO₂ based sensors”, Thin Solid Films, 391, 2001, p.186-191
- [74] Bohle, G. Hofmeister, E., “Electronic Semiconductor Components”, Bestell
- [75] Mirkelamoğlu, B., Karakaş, G., Yürüm, A., “Li, Na, K Promotion of Pd/SnO₂ catalysts Part I: Catalyst Characterisation”
- [76] Doebelin, O., Ernest; “Measurement Systems Application and Design”, 4th Edd. Mc. Graw Hill International Edition, Mechanical Engineering Series, 1990

APPENDIX A

SAMPLE CALCULATIONS

A.1. SnO₂ Catalyst Preparation Calculations

For the preparation of the catalysts a weight percent based calculation procedure was followed, therefore the molecular weights of the used species are needed (Table A.1)

Table A.1. Molecular weights of the species used in the catalyst preparation

Compound	Molecular Weight (gr/mol)
Tin dioxide (SnO ₂)	150.689
Tin Tetrachloride Pentahydrate (SnCl ₄ .5H ₂ O)	350.551
Isopropyl alcohol (C ₃ H ₇ OH)	60.096
Water (H ₂ O)	18.015
Palladium Oxide (PdO)	122.394
Palladium Acetate (Pd(CH ₃ CO ₂) ₂)	224.490
Sodium Chloride (NaCl)	58.443

Basis: 5 gr product (SnO_2)

$$n_{\text{SnO}_2} = \frac{m_{\text{SnO}_2}}{MW_{\text{SnO}_2}} = \frac{5 \text{ gr}}{150.689 \text{ gr/mol}} = 0.0332 \text{ mol}$$

$$\begin{aligned} n_{\text{SnO}_2} = n_{\text{SnCl}_4 \cdot 5\text{H}_2\text{O}} &\Rightarrow m_{\text{SnCl}_4 \cdot 5\text{H}_2\text{O}} = 0.0332 \text{ mol} \times 350.551 \text{ gr/mol} \\ &= \mathbf{11.632 \text{ gr SnCl}_4 \cdot 5\text{H}_2\text{O}} \end{aligned}$$

The molar ratio of $\text{SnCl}_4 \cdot 5\text{H}_2\text{O}$: isopropyl alcohol is: 1 : 7

$$\begin{aligned} \Rightarrow n_{\text{C}_3\text{H}_7\text{OH}} &= 7 \times 0.0332 \text{ mol} \\ &= 0.232 \text{ mol C}_3\text{H}_7\text{OH} \\ m_{\text{C}_3\text{H}_7\text{OH}} &= 0.232 \text{ mol} \times 60.096 \text{ gr/mol} \\ &= \mathbf{13.966 \text{ gr C}_3\text{H}_7\text{OH}} \end{aligned}$$

For the hydrolysis reaction, water : $\text{SnCl}_4 \cdot 5\text{H}_2\text{O}$ is 5.38 : 1

$$\begin{aligned} \Rightarrow n_{\text{H}_2\text{O}} &= 5.38 \times 0.0332 \text{ mol} \\ &= 0.179 \text{ mol H}_2\text{O} \\ m_{\text{H}_2\text{O}} &= 0.179 \text{ mol} \times 18.015 \text{ gr/mol} \\ &= \mathbf{3.218 \text{ gr H}_2\text{O}} \end{aligned}$$

Again, for the hydrolysis reaction, water : isopropyl alcohol 1.14 : 1

$$\Rightarrow n_{\text{C}_3\text{H}_7\text{OH}} = 1.14 \times 0.179 \text{ mol} \\ = 0.204 \text{ mol C}_3\text{H}_7\text{OH}$$

$$m_{\text{C}_3\text{H}_7\text{OH}} = 0.204 \text{ mol} \times 60.096 \text{ gr/mol} \\ = \mathbf{12.260 \text{ gr C}_3\text{H}_7\text{OH}}$$

A.2. 1 wt. % Pd /SnO₂ Catalyst Preparation Calculations

Basis: 5 gr SnO₂

5 gr SnO₂ → 99% of the catalyst

X gr PdO ⇒ 1 % of the catalyst

$$\Rightarrow \mathbf{X} = \frac{5 \text{ gr SnO}_2 \times 1 \%}{99 \%}$$

$$= \mathbf{0.050 \text{ gr Pd}}$$

$$\Rightarrow n_{\text{PdO}} = \frac{m_{\text{PdO}}}{\text{MW}_{\text{PdO}}} = \frac{0.050 \text{ gr}}{122.394 \text{ gr/mol}} = 4.126 \text{ E- } 4 \text{ mol}$$

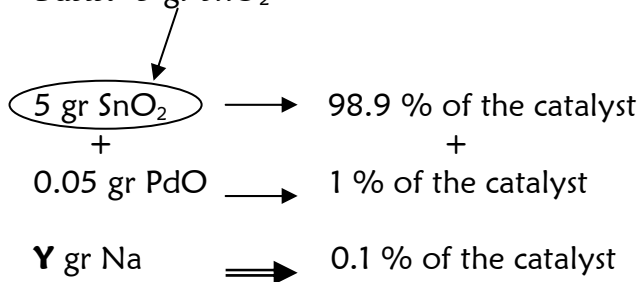
$$\Rightarrow n_{\text{PdO}} = n_{\text{Pd}(\text{CH}_3\text{CO}_2)_2} = 4.126 \text{ E- } 4 \text{ mol}$$

$$\Rightarrow m_{\text{Pd}(\text{CH}_3\text{CO}_2)_2} = 4.126 \text{ E- } 4 \text{ mol} \times 224.490 \text{ gr/mol} \\ = \mathbf{0.093 \text{ gr Pd}(\text{CH}_3\text{CO}_2)_2}$$

0.093 gr PdAc should be added to the calculated amounts of species in section A.1 for the synthesis of 1wt.% PdO/ SnO₂.

A.3. 0.1 wt. % Na, Pd / SnO₂ Catalyst Preparation Calculations

Basis: 5 gr SnO₂



$$\Rightarrow Y = \frac{(5 \text{ gr SnO}_2 + 0.05 \text{ gr PdO}) \times 0.1 \%}{(98.9 + 1) \%}$$

$$= 5.055 \text{ E} - 3 \text{ gr Na}$$

$$\Rightarrow n_{\text{Na}} = \frac{m_{\text{Na}}}{MW_{\text{Na}}} = \frac{5.055 \text{ E} - 3 \text{ gr}}{22.989 \text{ gr/mol}} = 2.199 \text{ E} - 4 \text{ mol}$$

$$\Rightarrow n_{\text{Na}} = n_{\text{NaCl}} = 2.199 \text{ E} - 4 \text{ mol}$$

$$\Rightarrow m_{\text{NaCl}} = 2.199 \text{ E} - 4 \text{ mol} \times 58.443 \text{ gr/mol}$$

$$= \mathbf{0.012 \text{ gr NaCl}}$$

0.012 gr NaCl should be added to the calculated amounts of species in section A.1 and A.2 for the synthesis of 0.1 wt. % Na-Pd/ SnO₂.

APPENDIX B

MASS FLOW CONTROLLER CALIBRATION CURVES

The mass flow controllers used in the experiments, have been calibrated by using a bubble flow meter and presented in the Figure B.1 and B.2.

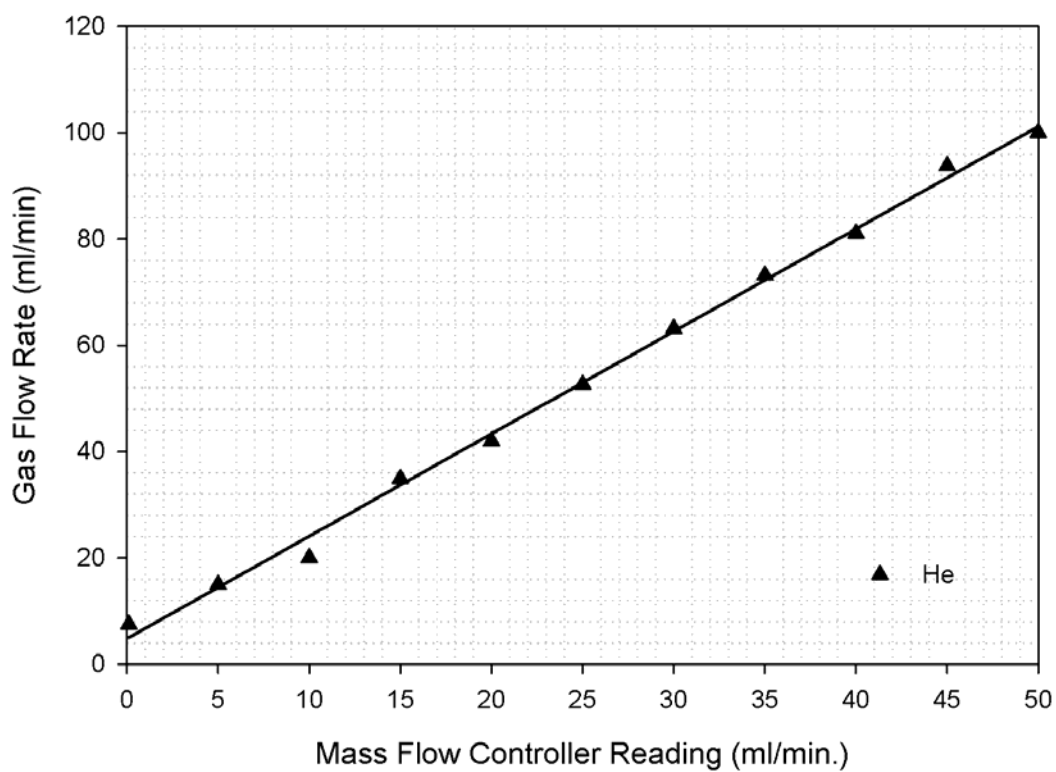


Figure B.1. Mass flow controller calibration curve for 99.99 % He gas

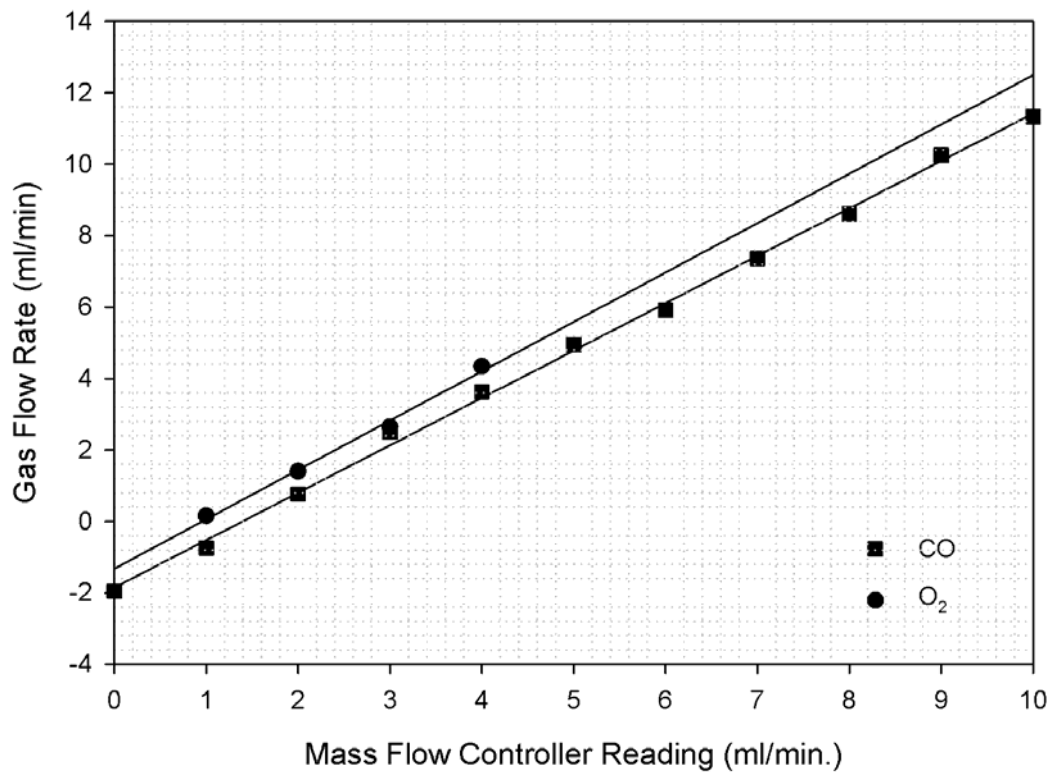


Figure B.2. Mass flow controller calibration curve for 1% CO and 5% O₂ gas in Helium

APPENDIX C

VOLUMETRIC FLOW RATE CALCULATIONS

In the current study the experiments have been conducted at different oxygen concentrations in He atmosphere. Therefore, the volumetric flow rate calculations have been done to keep the flow rate constant as increasing the oxygen content of the carrier gas.

- The carrier gas flow rate was kept constant at 20 ml/min. **(A)**
- The oxygen gas was introduced to system from the 5% O₂ in He **(B)** cylinder, which should be diluted to obtain a 1% O₂ in He by connecting another He line **(C)**.

Overall mass balance equation	⇒	$A = B + C$	┌──────────────────┐
Oxygen mass balance equation	⇒	$B \times 0.05 = (B+C) \times 0.01$	└──────────────────┘
A = 20 ml/min.	⇒	B = 4 ml/min.	←──────────────────┐
		C = 16 ml/min.	←──────────────────┘

APPENDIX D

EQUIVALENT RESISTANCE CALCULATIONS

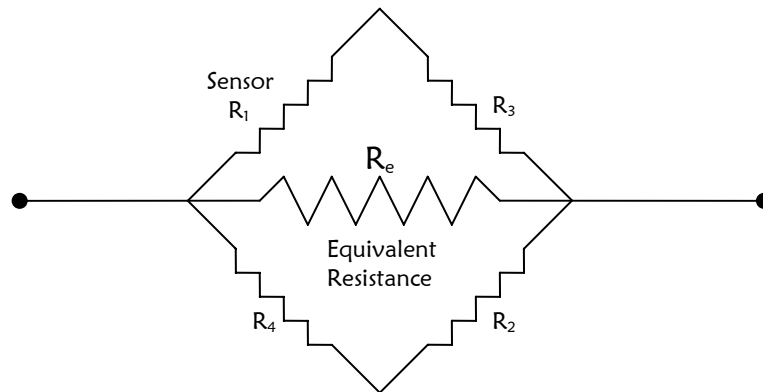


Figure D.1. Resistance configuration for the calculation of equivalent resistance value

$$R_e = \frac{R_1 \times R_2}{R_1 + R_2} + \frac{R_3 \times R_4}{R_3 + R_4}$$

For $R_e = 500$ ohm and $R_1 = 649.6$ ohm first R_2 should be calculated.

For an easy calculation R_3 and R_4 are assumed as 250 ohm.

$$\Rightarrow 500 = \frac{649,6 \times R_2}{649,6 + R_2} + \frac{250 \times 250}{250 + 250}$$

$$R_2 = 887,108 \text{ ohm}$$

